Stony Brook University

MECHANICAL ANALYSIS OF SMART RECEPTACLES AND INTELLIGENT FAULT DETECTION AND DIAGNOSIS FOR ARCING AND ENERGY MONITORING

A Dissertation Presented

by

Roosevelt Moreno Rodriguez

to

The Graduate School

in Partial Fulfillment of the

Requirements

for the Degree of

Doctor of Philosophy

in

Mechanical Engineering

Stony Brook University

May 2011

Stony Brook University

The Graduate School

Roosevelt Moreno Rodriguez

We, the dissertation committee for the above candidate for the

Doctor of Philosophy degree, hereby recommend

acceptance of this dissertation.

Dr. Imin Kao
Mechanical Engineering, SUNY at Stony Brook

Dr. Jon Longtin
Mechanical Engineering, SUNY at Stony Brook

Dr. Monica Fernandez Bugallo
Electrical and Computer Engineering, SUNY at Stony Brook

This dissertation is accepted by the Graduate School

Lawrence Martin
Dean of the Graduate School

Abstract of the Dissertation

MECHANICAL ANALYSIS OF SMART RECEPTACLES AND INTELLIGENT FAULT DETECTION AND DIAGNOSIS FOR ARCING AND ENERGY MONITORING

by

Roosevelt Moreno Rodriguez

Doctor of Philosophy

in

Mechanical Engineering

Stony Brook University

2011

Intelligent fault detection and diagnostic (iFDD) is a technology with growing interest and importance in engineering. The developments of several mathematical modeling and pragmatic techniques have facilitated the R/D with better approaches to improve the iFDD technology from biological to electronics fields. These techniques are applied from the component level to the system level. During the last years, many research efforts have been presented in the field of fault detection and diagnosis.

This dissertation presents the research in intelligent fault detection and diagnostic for low-power electrical systems, which are often found in household for daily use of electrical appliances. The research in iFDD utilizes data obtained from sensors and sensor network in a typical home electrical system to prevent hazardous conditions during abnormal operation. The diagnostic systems presented in this dissertation include the model-based and signal-based approaches. In the model-based approach, the physical model of the system is employed in the analysis of fault detection and diagnosis. In the signal-based approach, methodology of pattern recognition and fingerprint analysis is used to construct the iFDD model. Wavelet method has been employed to reduce the redundancy in a sensor network. The fingerprint of sampled signals under controlled faults of serial and parallel arcing are drawn fro m the coefficients of the wavelet decomposition to establish the relationship between the signature and the target faults. Experimental results and analysis are presented to illustrate the principle and applications of the iFDD technique

Contents

Chapter

1 INTRODUCTION 1

1.1 Background 1

1.2 Literature Survey 3

1.3 Glossary 4

1.4 Experimental Setup 6

1.5 Organization of This Dissertation 7

2 INTRODUCTION OF FAULT DETECTION AND DIAGNOSIS AND LITERATURE SURVEY 8

2.1 Introduction 8

2.2 Fault-Detection Methods 9

2.2.1 Fault models 10

2.2.2 Process models 11

2.3 Fault-Diagnosis Methods 12

2.4 Summary 14

3 MECHANICAL ANALYSIS AND EXPERIMENTAL STUDIES OF RECEPTACLES 16

3.1 Introduction 16

3.2 Causes of Electrical Fires and Injuries at Home 17

3.3 Arcing Fault 21

3.4 Experimental Study of a Serial Arcing Fault 22

3.5 FEM Simulation and Experimental Study 28

3.5.1 Heat transfer simulation 29

3.5.2 Thermal activated cut off mechanism of a BSafe receptacle 32

3.5.3 Discussions . . . 34
3.6 Experimental Study of Continuous Arcing and Degradation . . . 35
3.7 A new model for receptacles design . . . 38
3.8 Summary . . . 41

4 FDD OF SERIAL ARCING AND EXPERIMENTAL STUDY WITH MODELING 42
4.1 Introduction . . . 42
4.2 Arc Structure and Properties . . . 42
4.2.1 Formation of the electric arc . . . 44
4.2.2 Arc regions . . . 46
4.2.3 Arcing faults . . . 49
4.2.4 Parallel arcing . . . 50
4.2.5 Serial arcing . . . 51
4.3 Effects of Arcing Faults . . . 52
4.3.1 Mechanical forces . . . 52
4.3.2 Thermal stress . . . 52
4.3.3 System integrity . . . 53
4.4 Experimental Setup for FDD Study in Arcing . . . 53
4.4.1 Electrical setup . . . 54
4.4.2 Creation of arcing fault . . . 55
4.4.3 Real-time data acquisition system . . . 56
4.4.4 Sampling and data storage . . . 57
4.5 Modeling of Arcing Fault . . . 59
4.6 Fingerprint analysis . . . 63
4.7 Summary . . . 66

5 EXPERIMENTAL STUDY OF FDD FOR A SIMULATED POWER GRID DELIVERED SYSTEM 67
5.1 Introduction . . . 67
5.2 Description of the Simulated Power Grid Delivered System . . . 67
5.2.1 Experimental Setup . . . 69
5.3 Experimental Results . . . 69
5.4 Discussions . . . 75

5.5 Summary 76

6 CONCLUSIONS AND FUTURE WORK 77

6.1 Conclusions 77

6.2 Future Work 78

6.2.1 Sensor fusion and integration 78

6.2.2 Energy Monitoring 80

Bibliography 82

Appendix

A DATA FILE IDENTIFICATION 88

B THERMAL SIMULATION 90

C WAVELET TRANSFORM THEORY AND A LITERATURE SURVEY 101

C.1 Introduction 101

C.2 Background on Wavelet Transform 101

C.3 Multiresolution Analysis and Wavelet Construction 106

C.4 Time-Frequency Domain, Scale and Resolution 108

C.5 Improving The Wavelet Transform 109

C.6 Summary 112

List of Tables

Table

3.1 Devices used for temperature measurement during arcing fault 25
3.2 Configurations for FEM simulation of conduction heat transfer in blades of receptacles 32

4.1 Parameters required to form and sustain an arc. Source N.H. Wagar [58]. 47

5.1 Technical specifications of a 12 AWG copper wire. Source EncoreWire Corp. . . 70
5.2 Fault Location and error estimation using the Absolute Value of Impedance Method 73
5.3 Fault Location and error estimation using the modified Absolute Value of Impedance Method 75

6.1 Antenna and probes for various frequency ranges 80

List of Figures

Figure

1.1 Three main tasks of fault detection and diagnosis 2

2.1 General scheme of process model-based fault detection 9
2.2 Process configuration for model-based fault detection: (a) SISO (single-input single output); (b) Single-serial signal-input single output; (c) SIMO (single-input multi-output); (d) MIMO (multi-input multi-outpu) 10
2.3 Basic fault models for an output: (a) additive (b) multiplicative 11
2.4 Fault detection methods (Source : Isermann [32] 13
2.5 Basic fault diagnosis methods (Source Isermann [32]) 15

3.1 Causes of electric home fires between 2003 and 2006 (Source: NFPA) 18
3.2 Profile of residential fire causes (FEMA report 2003-2007) 18
3.3 Voltage overload due to open neutral 20
3.4 Outlet after 2 hours working under electric failure. (a) Glowing effect in wire, and (b) thermal distribution of the cords on service, some points are indicated . . 21
3.5 Basic topology of arcing fault. (a) Serial and (b) Parallel arcing fault 21
3.6 Basic types of residential grade receptacles: (a) Ungrounded, (b) Grounded, and (c) Grounded Fault Circuit Interrupter 23
3.7 Parts of a straight blade receptacle with connector types indicated 24
3.8 Duplex straight blade grounded receptacles available in the market 24
3.9 Creation of the electric arc fault on a loose connection 25
3.10 Back side of the receptacle under test: no damage over wire insulation can be seen as initial conditions 26

3.11 Front side (face plate) of the receptacle: hot spots are detected over the appliances cords. The electrical appliances employed are a water heater (upper side) and electric oven (lower side) . . . 26
3.12 Formation and progression of the glowing contact: temperature ranges from 24 °C to 280 °C . . . 27
3.13 Setup of temperature sensors over hot spots . . . 27
3.14 Infrared images of glowing contact in a conventional receptacle. with temperatures indicated . . . 28
3.15 A receptacle with thermal cut-off technology designed by BSafe Electrix . . . 29
3.16 Thermal simulation of BSafe receptacle with one terminal screw as heat source . 31
3.17 Schematic of a bimetallic blade receptacle designed by BSafe . . . 32
3.18 Spring loaded mechanism of the BSafe receptacle . . . 33
3.19 Components of the spring loaded mechanism of the BSafe receptacle . . . 33
3.20 Exploded views of BSafe receptacle with the contact point of this cut-off mechanism . . . 34
3.21 Progressive degradation of the insulation due to an overheated wire . . . 36
3.22 Cumulative degradation of wire reduce the time to reach higher values in temperature under the presence of an arcing fault . . . 37
3.23 Comparative of receptacle tests to reach a fixed value of temperature, (a) up to 100 °C and (b) up to 40 °C . . . 38
3.24 Experimental study of the deterioration of receptacle . . . 39
3.25 Conditions included in the proposed model, (a) normal operation and (b) time variation to reach a prescribed temperature after a continuous arcing fault in the system . . . 40

4.1 Different types of axisymmetric arcs. (a) Wall stabilized, (b) Ablation stabilized, (c) Vertical free burning and (d) Axial convection controlled arc [53]. . . . 44
4.2 Different types of non-axisymmetric arcs [53]. . . . 45
4.3 The opening sequence of an electric contact [57]. . . . 46
4.4 Electric Arc characterization [53]. . . . 47
4.5 Basic components of an U. S. electrical system [61]. . . . 49
4.6 Types of parallel faults. . . . 50

4.7 Types of arcing faults in single conductor circuits. 51
4.8 Schematic setup of the electrical system for experiments 53
4.9 A photo of the layout of the experimental setup 54
4.10 A photo of the platform used to move the wire. 55
4.11 Functional diagrama of a PC-base data acquisition system 57
4.12 Sampling of a Sine wave using a 3 bit digitizer. 58
4.13 Current waveform from an electrical load. Intermitted arcing can be present in less than one cycle. 60
4.14 Electric characteristics during a serial arcing fault. 61
4.15 Wavelet decomposition scheme using Daub5Coeffs. 63
4.16 Wavelet decomposition scheme using Daub6Coeffs. 64
4.17 Candidate feature generation 65

5.1 Faulted power system 68
5.2 Setup used to record data sensor from ground fault in an AC system 70
5.3 Voltage waveforms from points A and B during L-G fault at location X_1 71
5.4 Basic schematics to calculate the fault distance in an AC circuit 72
5.5 Esquematic of the simulated power grid deliver system. 72

6.1 Waveform from voltage sensor, receptacle under arcing fault 79
6.2 Waveform from current sensor, receptacle under arcing fault 79
6.3 Loop antennas use for detecting variations in the electromagnetic field. a) 8 inches diameter (7 turns), b) 0.75 inches diameter (10 turns) and c) 0.75 diameter (1 turn with isolation). 80

A.1 Parameters used to identification of data files 89

B.1 Thermal simulation of BSafe receptacle with one blade as heat source 91
B.2 Thermal simulation of regular receptacle with one blade as heat source 92
B.3 Thermal simulation of BSafe receptacle with one terminal screw as heat source . 93
B.4 Thermal simulation of regular receptacle with one terminal screw as heat source 94
B.5 Thermal simulation of BSafe receptacle with two blades as heat sources 95
B.6 Thermal simulation of regular receptacle with two blades as heat sources 96
B.7 Thermal simulation of BSafe receptacle with two terminal screw as heat sources 97

B.8 Thermal simulation of regular receptacle with two terminal screw as heat sources 98
B.9 Thermal simulation of BSafe receptacle with one terminal screw as heat source and considering yellow brass as one component of the bimetalic part 99
B.10 Thermal simulation of BSafe receptacle with one blade as heat source and considering yellow brass as one component of the bimetalic part 100

C.1 Basic representation and operations on wavelets. 103
C.2 Schematics of the Wavelet Transform procedure. 104
C.3 Schematic representation of nested spaces 107
C.4 Schematic representation of the decomposition algorithm 109
C.5 Schematic representation of the reconstruction algorithm 110
C.6 Lifting scheme forward wavelet transform 111

Chapter 1

INTRODUCTION

1.1 Background

In recent years, intellgent fault detection and intelligent diagnosis (iFDD) has gained a considerable amount of interests and business potential. The needs of efficient energy management and safety processes have stimulated research and development of real-time diagnostic tools and methods. Based on the great variety of processes as well as systems, different approaches have been introduced. These include dynamic model-based methods, multivariate statistical analysis, fuzzy logic-based methods, and neural networks [1].

The effectiveness of any intelligent diagnostic system is often based on a representative and reliable model of the overall system behavior in normal operation conditions. A malfunction behavior of a system is normally called a fault. Since a fault can prevent a system from working properly and sometimes even cause a fatality, it is very important to detect it in time. The objective of fault detection is to detect the signals of fault accurately whenever it appears [2]. Fault detection and diagnosis (FDD) implement three main tasks: (1) fault detection, (2) fault isolation, and (3) fault identification, as show in Figure 1.1 [3].

The isolation and identification tasks together are referred to as fault diagnosis. These tasks are designed to indicate that something is going wrong in the system (detection) and to determine the exact location and size of the fault (which component is faulty and where). The fault identification deals with the magnitude of the fault [3]. To implement a fault detection and diagnostic system, various computer-aided approaches have been developed. They covered a variety of techniques, from fault trees to knowledge-base and neural networks [4]. The most common method is model-based in which an on-line model of the system is running parallel to the system. The measured outputs of the system are compared with the simulated output of the model. In this case, an accurate model of the system is required. Furthermore, high computational processing

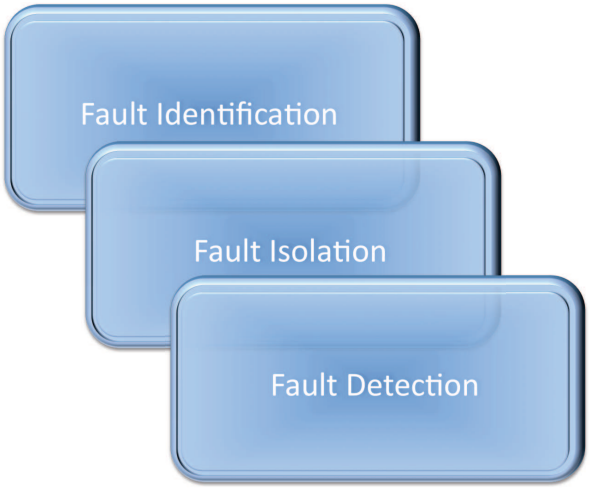

Figure 1.1: Three main tasks of fault detection and diagnosis

power is needed to run the on-line model, particularly for non-linear systems. Other important methods are based on the analysis of historical data of the system such as the Artificial Neural Networks (ANN). The ANN model uses nodes and layers to learn from functional mapping of inputs and outputs. The artificial neural network method can easily represents a complex system with a high accuracy in the pattern recognition of the failure; however, it requires long time to implement with high computational cost [5]. As we can realize, there is not a unique classification of a fault diagnostic system. Some researches uses the technique to detect the fault while others can use the method that represents the system to represent their models. According to Venkatasubramanian [4], the techniques can be classified as quantitative model-based, qualitative model-based and process-history-based approaches. Under the quantitative model-based approaches, some techniques use analytical redundancy to generate residuals that can be used for isolating process failures. The residual generation can be reached through diagnostic observers, parity relations, Kalman filters, and so on. Under the qualitative model-based approaches, the relationship between system variables can be described by the signed directed graph (SDG), Fault Trees, Qualitative Simulation (QSIM), and Qualitative Process Theory (QPT). Finally, under process- history-based approaches, some techniques with qualitative approaches (such as expert systems), qualitative trend analysis (QTA) techniques and some quantitative approaches (such as neural networks), PCA and statistical classifiers can be used in conjunction to detect the faults.

Most of the available literature is focused predominantly on model-based approaches. Ac-

cording to Kramer and Mah [6], the fault diagnostic problem is considered as a feature extraction and classification. Kramer [6], states that the classification stage can be considered in one of three main categories: (1) pattern recognition, where most of the process-history-based methods are discussed; (2) model-based reasoning, where qualitative model techniques are mostly used and (3) model matching , where symptomatic search techniques are mainly consider.

1.2 Literature Survey

Several mathematical methods for fault detection has been developed during the last 30 years [7]. Willsky examined some statistical techniques for fault detection, particularly in linear systems [8]. Gertler [3] described briefly the historical evolution in fault detection and explained in details the model-based approach. Korbicz *et al.* presented the status and likely development of fault diagnosis from a model-base perspective [9]. Chiang *et al.* presented the theoretical background in process monitoring and demonstrated the strengths and weaknesses of each approach in details [10]. Combastel used fuzzy logic for fault detection in electrical machines [11]. Kartalopoulus presented a very well organized work on the emerging field of fuzzy neural network as a result of his research experience [12].

Pattern recognition and its historical evolution were described by Kanal [13]. Cheng and Wazir compiled multiple pattern recognition models to create a useful knowledge base, which can integrate the available resources [14]. Jain *et al.* presented and summarized well-known methods in various stages of a pattern recognition system [15]. Xiaochun compared the fuzzy clustering method and the neural network method [16]. A new approach in pattern recognition to control a power system engineering was presented by Zhang [17]. Polycarpou and Vermuli presented a general methodology for fault detection using non-linear models in dynamical systems [18]. Application of fuzzy system theory to electrical power engineering field was presented by El-Hawari [19]. Fuzzy logic principles were used in a medical expert system to obtain a better realistic information for medical diagnosis purpose [20]. Quian *et al.* presented an overview on electric motor failures using neural networks, fuzzy logic and genetic algorithms [21]. Cheng developed a discrete wavelet algorithm to detect electrical failures on induced motor systems [22]. Korbicz and Kowai proposed an improved method to fault detection which combine the neural network with the structure fuzzy logic to achieve the fault detection system [23]. A predictive neural network was presented by Javadpour to diagnosis of faults in an automated manufacturing enviroment [24]. Capria and Kao combine intelligent Fault Detecttion and Diagnosis with

Fingerprint Analysis for intelligent systems [25]

Another approach for fault detection is signal processing. Mikelsons and Greitas presented a fault detection method for discrete signal samples. Gustafsson proposed a mixed model that included stochastic inputs and deterministic disturbances [26]. Cusido *et al.* presented a combination of wavelet and power spectral density to fault detection in motor current signature [27]. Widodo applied discrete wavelet transform method to build an intelligent fault detection system over induction motors [28]. Raffie *et al.* applied orthogonal wavelets for fault diagnosis of a complex gear box [29]. More applications using signal processing techniques in FDD can be found in various publications.

1.3 Glossary

Different approaches as well as terminologies have been used in this field, often not consistent with one another. This makes it difficult to compare methods, techniques and principles. Some of the basic definitions can be found in several publications and specialized dictionaries (such as the Reliability Availability and Maintainability dictionary) :

(1) States and Signals

- *Fault:* An unpermitted deviation of a least one characteristic property or parameter of the system from the acceptable, usual or standard condition.
- *Failure:* A permanent interruption of a systems ability to perform a required function under specified operating conditions.
- *Malfunction:* An intermittent irregularity in the fulfillment of a systems desired function.
- *Error:* A deviation between a measured irregularity or computed value of an output variable and its true or theoretically correct one.
- *Disturbance:* An unknown and uncontrolled input acting on a system.
- *Residual:* A fault indicator, based on a deviation between measurements and a model-equation-based computation.
- *Symptom:* A change of an observable quantity from normal behavior.

(2) Functions

- *Fault detection:* Determination of faults present in a system and the time of detection.
- *Fault isolation:* Determination of the kind, location and time of detection of a fault (follows fault detection).
- *Fault identification:* Determination of the size and time-varying behavior of a fault (follows fault isolation).
- *Fault diagnosis:* Determination of the kind,size,location and time of a fault (follows fault detection. Includes fault detection and identification).
- *Monitoring:* A continuous real-time task of determining the conditions of a physical system, by recording information, recognizing and indication in the behavior.
- *Supervision:* Monitoring a physical and taking appropriate actions to maintain the operation in the case of fault.

(3) Models

- *Quantitative model:* Use of static and dynamic relations among system variables and parameters in order to describe a systems behavior in quantitative mathematical terms.
- *Qualitative model:* Use of static and dynamic relations among system variables in order to describe a systems behavior in qualitative terms such as causalities and if-then rules.
- *Diagnostic model:* A set of static or dynamic relations which link specific input variables, the symptoms, to specific output variables, the fault.
- *Analytical redundancy:* Use of more (not necessarily identical) ways to determine a variable, where one way uses a mathematical process model in analytical form.

(4) System Properties

- *Reliability:* ability of a system to perform a required function under stated conditions, within a given scope, during a given period of time.
- *Safety:* Ability of a system not to cause danger to persons or equipment or the enviroment.
- *Availability:* Probability that a system or equipment will operate satisfactorily and effectevily at any point of time.

(5) Time Dependency of Faults

- *Abrupt fault:* Fault modeled as a stepwise function (it represents bias in the monitoring signal)
- *Incipient fault:* Fault modeled by using ramp signals (it represents drift of the monitored signal).
- *Intermittent fault:* Combination of impulses with different amplitudes.
- *Additive fault:* Influences a variable by an addition of the fault itself. They may represent, e.g. offsets of sensors.
- *Multiplicative fault:* Are represented by the product of a variable with the fault itself. They can appear as a parameter changes within a process.

1.4 Experimental Setup

One objective of this research is to study fault detection and diagnosis (FDD) of typical electrical systems at home. An electrical system is constructed and configured for this propose. A computer-based data acquisition system is established to obtain voltage, current, temperature, and other information of the system through sensors, as well as to control the conditions of faults in the system, such as arcing failure. The sensory data are saved in a file compatible with MATLAB for post-processing. The experimental system is presented in Chapters 4 and 5. The electrical system was built following the specifications of the National Fire Protection Association code 60 (NFPA 60), better known as National Electric Code (NEC). A replica of a residential indoor wall

with capabilities to connect to regular home appliances under a nominal current limit of 15 or 20 amperes has been conditioned in conjunction with 10 straight blade receptacles and a circuit breaker protection, as demanded by code for this type of applications [30]. Data are sampled at a sampling rate ranging from 100 to 250 kHz. Details of the system will be presented later. (See Section 4.4.2). In order to apply FDD, the faults must be detect and their effects over the system must be determined. Faults in this electrical system will be introduced and investigated using the experimental setup, which will be discuss in Section 5.2.1.

1.5 Organization of This Dissertation

The main objective of this dissertation is to study the algorithms and implementation of an intelligent fault detection diagnostic and prevention technology (iFDDP) for a residential electrical system. The dissertation consists of the following: Most of the terminology used in this dissertation is defined in Chapter 1 as well as the basic concept for Fault Detection and Diagnosis. Chapter 2 provides an introduction to Fault Detection and Diagnosis (FDD) methods. One of the models described in this chapter is selected to apply during the experimental stage. Chapter 3 presents a description of the thermal behavior of some straight blade receptacles based on experiments conducted under an arcing failure. Experimental results are presented and discussed. Arcing models and the selected feature detection algorithm are presented in Chapter 4. Finger print analysis through wavelet theory is presented as an innovative alternative to create an intelligent system in detecting arcing failures. Chapter 5 introduces a new technique for fault location based on a modified impedance method. Experimental results and comparative techniques are discussed.

Based on the ongoing research, conclusions and a future work are proposed in Chapter 6.

Chapter 2

INTRODUCTION OF FAULT DETECTION AND DIAGNOSIS AND LITERATURE SURVEY

2.1 Introduction

In general, Fault Detection and Diagnosis (FDD) are based on measured variables and states through instrumentation and observation. The automatic processing of measured variables for fault detection requires the heuristic knowledge of the analytical process and the evaluation of observed variables [31]. From this perspective, fault detection and diagnosis (FDD) can be considered within a knowledge-based approach.

The tasks of fault diagnosis consist of the determination of the type, size and location of the most possible fault, as well as its time of detection. To reach a successful FDD, Isermann describes the fundamental parameters and models to use from a knowledge-based approach [31]. Consequently, analytical information about the system must be acquired. First, this information can be obtained through direct measurements of the variables (signals) of interest. Secondly, data processing is needed to generate characteristic values. A characteristic value can be found by several methods such as comparison among signals measured with an accepted tolerances, correlation functions, frequency spectra, variances, and amplitude frequency parameters. Mathematical process models combine with parameter estimation, state estimation and parity equation methods are also used to determine the characteristic values of the system.

In some cases, additional information of the system is combined with qualitative information. Human observation is a valuable source in the knowledge-base approach. In this situation, the characteristic values can be obtained in different forms like colors, smells, special noise, taste, wear, etc. Maintenance reports as well as repairs from former faults are consider another type of qualitative information. Statistical data from experience with similar or same systems can be also included.

The first step in a fault diagnosis systems frequently is a physical and/or mathematical model of the system, its signals and expected faults. Here, simulation of the process behavior under normal conditions and with fault is included. The design of the FDD methods are created by considering these basic elements. Then, FDD method are combined with software simulation. A prototype is consequently developed. Prototyping generally is the combination of the real process with a real-time model in computer. The next step is the implementation of the final FDD system. The implementation includes testing and tuning the procedures. If the process is very complex, the implementation include software simulation with real process interaction; otherwise, this can be made directly with the real process. When a FDD system is implemented with other functions, for example, with automatic control, this is called system integration. The next step includes system test, verification and validation. In some cases, an additional certification stage may be required.

2.2 Fault-Detection Methods

The model-based method of fault detection deals with analytical relationship between variables or signals measured to obtain the information on possible changes caused by faults. A mathematical process model represents the relations between input and output signals. Thus, fault detection methods extract special features, such as residuals or sate variables. After comparing these features against their nominal values, the analytical information is generated. Figure 2.1 shows the basic structure of model-based fault detection methods.

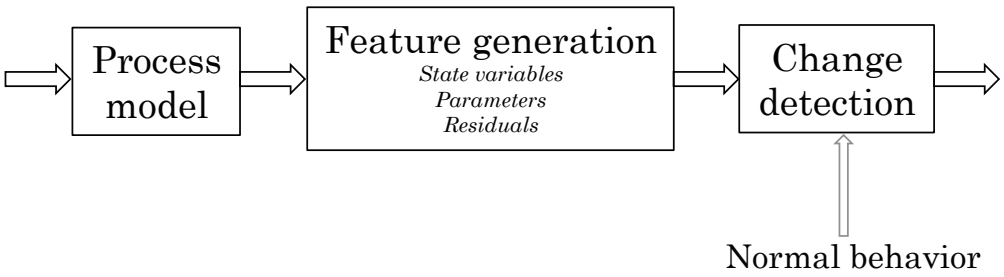

Figure 2.1: General scheme of process model-based fault detection

Process configuration (see Figure 2.2) has to be distinguished in order to apply the model-based methods. The process model can be classified as continuous models or discrete-event models. A continuous model is an equation-based model which may include linear, nonlinear

or time-variant relations. On the other hand, discrete-event models may be represented by finite state machines, functional diagrams or Petri-nets.

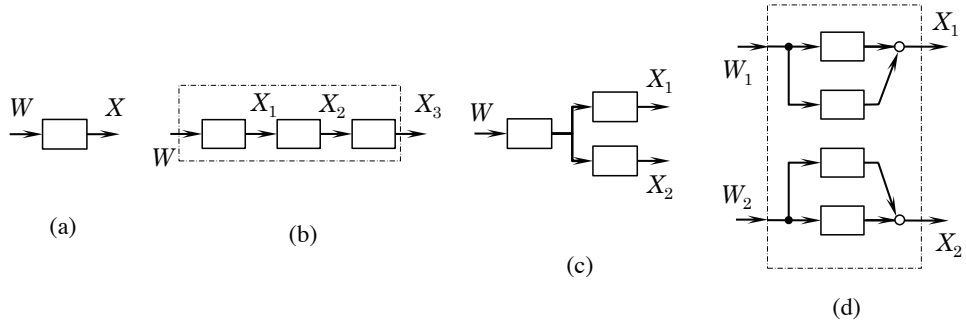

Figure 2.2: Process configuration for model-based fault detection: (a) SISO (single-input single output); (b) Single-serial signal-input single output; (c) SIMO (single-input multi-output); (d) MIMO (multi-input multi-outpu)

2.2.1 Fault models

Fault detection methods depend on the choice of modeling of fault. A better understanding of the real physical faults and their effects on the mathematical process model is a more realistic approach. A fault can be present for many reasons, such as corrosion, wrong operation, wrong design, missing mantineance, wear, wrong assembling, etc. A fault may appear during any phase (step) of a process or may appear suddenly with small or large size in frequency or gradually. Faults can be considered as deterministic fault or stochastic (intermittent) faults.

Two basic models can be considered as a basic fault models [31]. In any case a fault is an unpermitted change of one characteristic of the system (see Section 1.3). When this characteristic is a part of a physical law, then the fault may appear as a change of signals or parameters involved in that law. Hence, we can have additive faults or multiplicative faults.

For instance, let us consider a variable $W_u(t)$ which is changed by an adition of $f(t)$, as shown in Figure 2.3. Here, the detectable change $\Delta W(t)$ of the variable is independent of any other signal. In contrast, if $W(t)$ is changed because another variable $V(t)$ is multiplied by $f(t)$, then the detectable change of the output $\Delta W(t)$ will depend on the input signal as shown in Figure 2.3.

Some faults can be represented for the stochastic character of the output. In that case, the mean value and variance of the output are applied in the model of fault

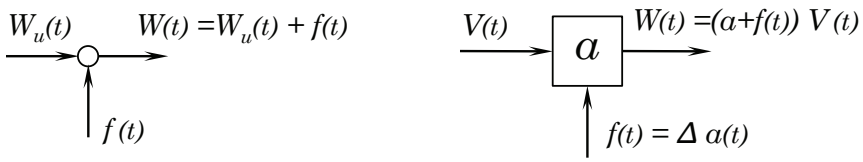

(a) (b)

Figure 2.3: Basic fault models for an output: (a) additive (b) multiplicative

$$E = \{Y(t)\} \qquad \text{and} \qquad \sigma_y^2 = E\{[Y(t) - \bar{Y}]\}^2$$

2.2.2 Process models

2.2.2.1 Theoretical and experimental modeling

Theoretical modeling and analysis represent the process from the basis mathematical relationship between variables of the system; in other words, formulated laws of nature are used. Several type of basic equations can be found, e.g. energy balance, mass conservation, state equations, and thermal transfer laws. A system of ordinary or partial differential equations represent the process. The system usually must be simplified due to the complexity of some equations. The simplification is made using linearization, reduction of parameters (lumped analysis), or reduction of order.

In the experimental modeling, sometimes called identification, the mathematical model is obtained from measurements. Input and output signals are compared in order to find a mathematical relation. Several techniques for signal identification can be found in [32], [33], [34].

2.2.2.2 Static process models

In static process models, the steady state of the process is generally described by graphical representation of characteristic curves. Must of them are polynomials (or quasi polinomials) curve types.

2.2.2.3 Linear dynamic process models

Dynamic models bring additional information to the process directly related to faults. The time dependent signals provide information on changes caused by faults. A continuous time dynamic model generally is nonlinear. However, if small deviations are considered, the model can be linearized. A similar situation can be used in the case of discrete time dynamic models.

2.2.2.4 Nonlinear process models

Most of the process are nonlinear due to the nature of mathematical description of the relation between signals and variables. According to Isermann [31], the most suitable methods for fault identification are frequently based on polynomial approximators, for example, Volterra-series, Kolmogorov-Gabor polynomials, Hammerstein model, Wiener model, bilinear systems and artificial neural networks.

There are several descriptions for a variety of models. The description of each one of them is beyond the objective of this dissertation. A summary of the fault detection methods is listed in Figure 2.4

2.3 Fault-Diagnosis Methods

According to Fussel [35] , the main challenges of fault diagnosis are:

- The knowledge representations
- The introduction of prior knowledge
- The typical symptom distribution
- Data size and representation

Knowledge representation can be analytical or heuristic. The first one comes from physical laws or quantitative measurements and observations. The second is the result of learning by experimental methods (especially trial-and-error methods). Prior knowledge includes general information that can be use to structure the diagnosis system. Prior knowledge usually comes form experience or physical understanding of the process. When experimental data is used to build

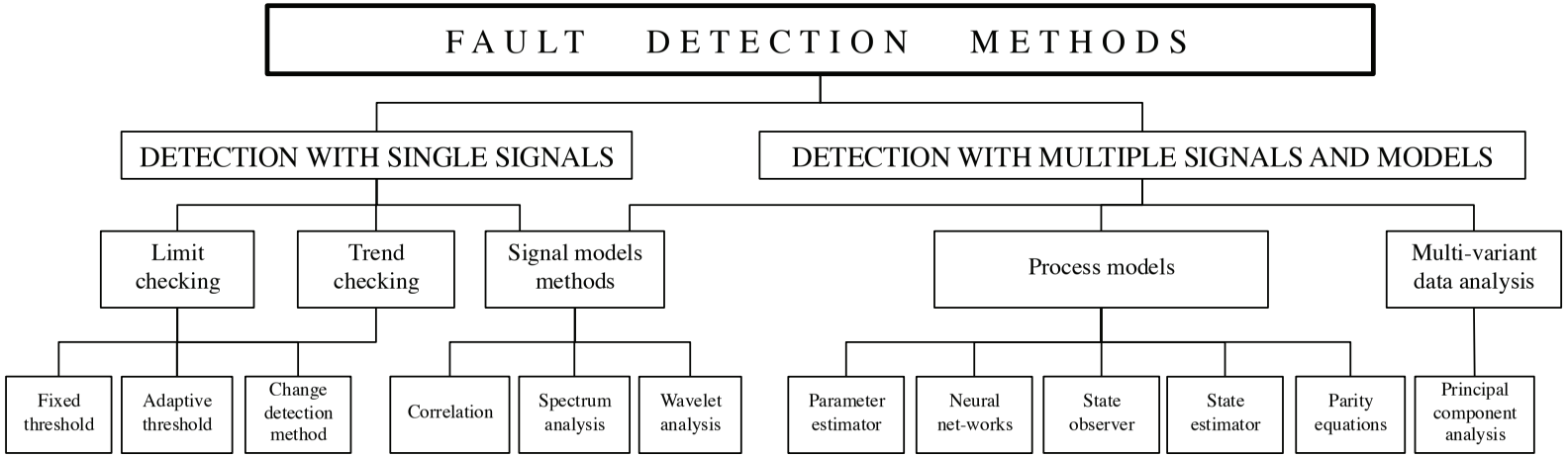

Figure 2.4: Fault detection methods (Source : Isermann [32]

a diagnosis system, the typical statistical distribution of such information must be considered. Experimental data systems relies on changes of the estimated model parameter or on deviation of the outputs and signals known as residuals.

Data size represents a typical problem of the experimental fault diagnosis. Several factors are related with data size and depend on the process. For instance, the system can be too expensive to implement or too dangerous to operate. Finally, symptom representation is a capability of a diagnosis system to deal with different problems. System representation is based on how data will be classified [35]. Four different type of data can be utilized:

(1) Binary variables in which only two values are allowed;

(2) Multi value variables, where different states can be named;

(3) Metric scale variables when a number represents a value, and

(4) Interval scaled variables in which a fraction of the unit is generally consider.

Figure 2.5 represents a summary of the most common models used in fault diagnosis [35].

2.4 Summary

In this chapter, a concise literature review about Fault Detection and Location methods are presented. Relevant differences between methods are shown. Based on the experimental results, the pattern recognition method is used as a Fault Diagnosis technique and wavelet analysis is selected as a Fault Detection method.

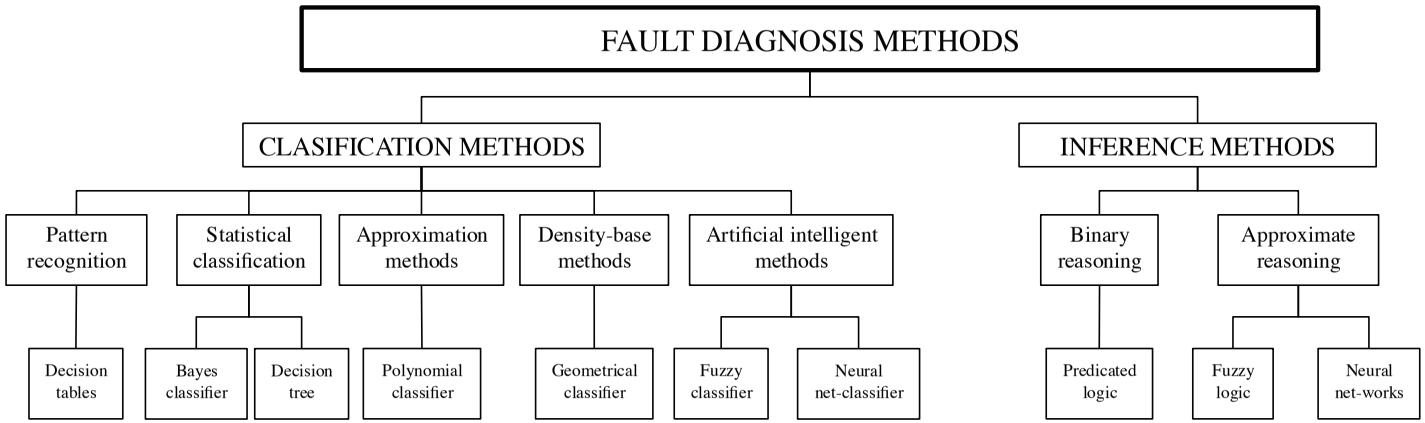

Figure 2.5: Basic fault diagnosis methods (Source Isermann [32])

Chapter 3

MECHANICAL ANALYSIS AND EXPERIMENTAL STUDIES OF RECEPTACLES

3.1 Introduction

Electrical receptacle outlets in walls and floors of household may present shock and electrical fire hazards to consumers. The U.S. Consumer Product Safety Commission (CPSC) estimates that 3,900 injuries associated with electrical receptacle outlets are treated in hospital emergency rooms each year. Approximately a third of these injuries occur when young children insert metal objects, such as hair pins and keys, into the outlet, resulting in electric shock or burn injuries to the hand or fingers. CPSC also estimates that electric receptacles are involved in 5,300 fires annually which claim 40 lives and injured 110 consumers [36].

Electrical systems can pose a serious fire and safety hazard. Under certain conditions (generally unexpected and unusual) electrical connections can initiate a fire. In a controlled environment, researchers try to re-create conditions based on data from failures reported by several agencies or sources, such as fire investigators, National Fire Protection Association (NFPA), engineers, and electrical product manufacturers. Most of the hazardous conditions found in the field may take many years and even decades to form [37]. An appropriate experimental set up must be used to study failure conditions.

Electrical faults can be either serial, parallel, or a combination of both. A serial fault happens as a result of a break in one branch of a circuit, either line or neutral. A parallel fault occurs when two different branches of the circuit (line-neutral, line-ground) get in contact (see Figure 3.5 for illustration). Each class can have its own set of circumstances that can lead to potentially hazardous conditions, including damage, misapplication, loose connections, harsh conditions, and wire aging. The National Electric Code classify the wires used in a residential system in two groups: (1) behind the wall (fixed wiring) and (2) portable wiring (appliances cords, extension cords, etc.) [30]. Some examples for fixed wiring failures may include loose

connections at an outlet, a staple or drywall screw bridging conductors, and excessive self-heating by current flow leading to wire insulation degradation and failure. Examples of portable wiring faults include cut wires, broken strands, abraded wire insulation, loose connections, and self-heating. All these conditions can occur for old as well as new wiring. Aged wiring and in particular fixed wiring, since it is much more costly to replace than portable wiring, may fail due to insulation degradation, especially if rework or retrofitting has disturbed the wiring. Moving and bending old wiring that has become embrittled from age, can crack the insulation and expose conductors possibly leading to an electric fault [37].

In this chapter, we will describe the electrical fault of a typical residential system. The study will focus on serial arcing fault in a straight blade receptacle due to a loose connection. A thermal test over a new type of receptacle will be performed. Thermal simulation for comparison between regular receptacles and new type will be presented.

3.2 Causes of Electrical Fires and Injuries at Home

The U.S. Fire Administration (USFA) reports that in year 2007 alone there were 1.6 million fires, resulting in 3,430 death, 17,675 injuries, and $14.6 billion direct property loss [38]. USFA also states that "fire killed more Americans than all natural disasters combined, and 84 percent of all fire deaths occurred in a home environment ".

The Federal Emergency Management Agency (FEMA) reports that electrical distribution and lighting equipment account for 46% of the electrical home fires between 2003 and 2006, and the rest is associated with other equipment such as electric stove, electric space heater, fan, clothes dryer, air conditioner, etc. Figure 3.1 shows the causes of electric fire and death reported by National Fire Protection Association (NFPA) [39]. Both agencies have reported that the electrical wiring, including fixed wiring, outlets, and switches, are the main causes of electrical home hazards [37].

The lamps and lighting are the second causes of fires, but cords and plugs are the second causes of death. FEMA reported that bedroom, attics, and kitchen are the top three areas of fire hazards, and they also reported that the insulation around electrical wires or cables building, wood structural framing, and acoustical insulation materials are the top three objects that are first ignited, with rates of 30%, 17%, and 7%, respectively. Figure 3.2 shows the fire cause profiles for residential structures. At 40%, cooking is by far the leading cause of fires. The second leading cause of fires is heating, accounting for 14% of fires.

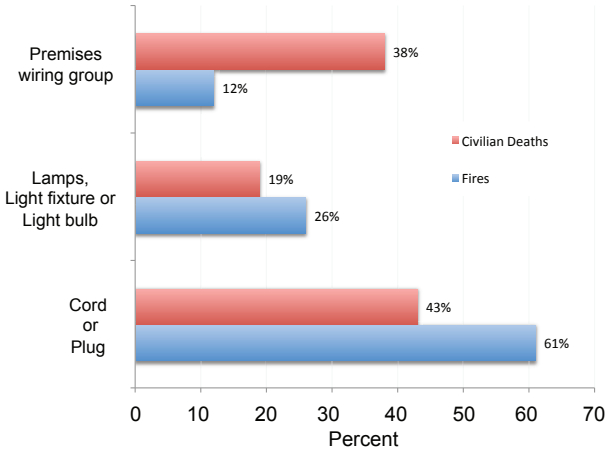

Figure 3.1: Causes of electric home fires between 2003 and 2006 (Source: NFPA)

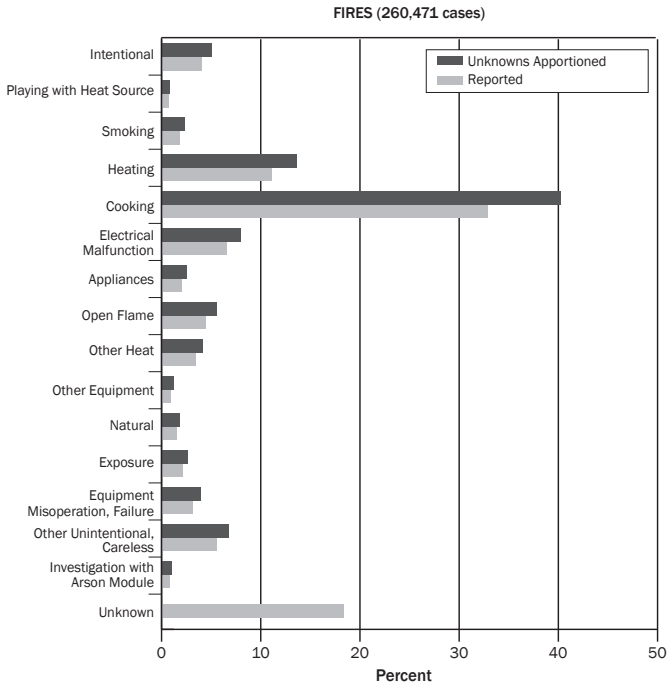

Figure 3.2: Profile of residential fire causes (FEMA report 2003-2007)

These percentages (and those that follow) are adjusted, which proportionally spreads the incidents with unknown causes over the other 15 cause categories. The two leading causes of fatal

fires (fires that result in civilian deaths) are smoking at 18% and other unintentional or careless actions at 14% [38].

In additional to home fires, the electrical injury is another main home hazard. According to the US Department of Health and Human Services, electrical injuries consist of four main types: electrocution (fatal), electric shock, burns, and falls caused as a result of contact with electrical energy. CPSC estimated that on average there are about 200 electrocutions in the US homes. It has been recognized that electrical injury is a major home injury of children [36]. By examining the data of large hospitals over 15 years, Rabban *et al.* and Zubair *et al.* reported independently that the electrical cords and wall outlets are the leading causes of electrical injuries to children at home [40] - [41]. The former one is a result of young children biting electrical cords, and the second one is because children insert objects into electrical sockets. Currently, plastic plug covers and tamper resistant receptacles with shutter are used in the homes to protect the electrical injury from outlets.

There are many data about the causes of electrical fires, but there is little systematically research examining the electrical fire mechanisms [38]. However, understanding the physics of electric fires is critical for the electrical hazard detection and prevention. Fire ignition needs sufficient heat or temperature in addition to combustibles and oxygen. Based on the limited literature, we classify the mechanisms as the following four:

- Electrical overload in current or voltage
- Brownout, or electrical underload
- Poor connection or junction
- Electrical arcing

Electrical wiring systems are not designed to have the same life as the house. According to Underwrite Laboratories (UL), one-third of the homes in US are over 50 years. Consider the rapid development of electrical appliance and the expansion of the numbers in the past half century, it is quickly obvious that current overload is likely on the electrical wiring under aged insulation. The heat will continuously built up in the overloaded wiring behind the house structure, and the fire danger could not be seen until the fire starts. The gross overloaded is usually protected by fuses or breakers rated 15 or 20 amperes. However, many cords or extensions are rated at 10A.

Voltage overload can also happen, frequently caused by open neutral, as seen in Figure 3.3. When the neutral wire of 120V system is disconnected, the voltage on the electric appliance can be up to 240V, and power can be four times larger. This overvoltage can result in excessive heating in the wiring or appliance and cause fires [42].

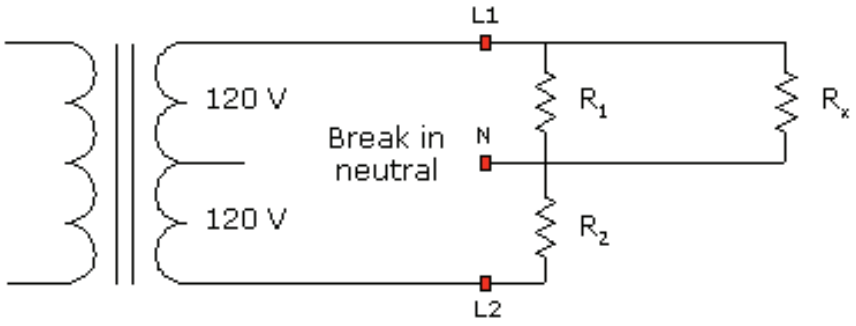

Figure 3.3: Voltage overload due to open neutral

In addition to the overload, another fire mechanism is under load due to low electrical voltage, which often happens in holiday seasons. It sometime is called brownout. At abnormal low voltage, the motors in the appliance may not operate, and the current flow will be high and cause overheating or fires.

Another important fire ignition mechanism is local ohmic heating at the poor connections. The insufficiently tightened wire terminals, contaminated or corrosive outlet contacts, damaged areas of wiring, or loose splicing wire connections can yield a progressive failure with an unstable positive feedback loop. Poor connection creates high resistance and localized heating, heating increases oxidation and creep, and the connection become worse and further heating more, until very high temperature occurs such as glowing [43]. The glowing connection of copper-copper contacts can be close to the melting point 1230 °C. It has been identified using x-ray that the high-resistance of copper-copper connection is due to the progressive formulation of Cu_2O. Since the glowing heating is localized at the connection, it only has very small voltage drop (1-2 V), and thus hazard may not be noticed at early stage [44]. Figure 3.4 shows the glowing connection inside the outlet and an infrared picture over a poor connection at the front side of an outlet. The ohmic heating due to poor connection can set the home structure or the wire insulation in fire, or degree the wire insulation's properties can cause fires later.

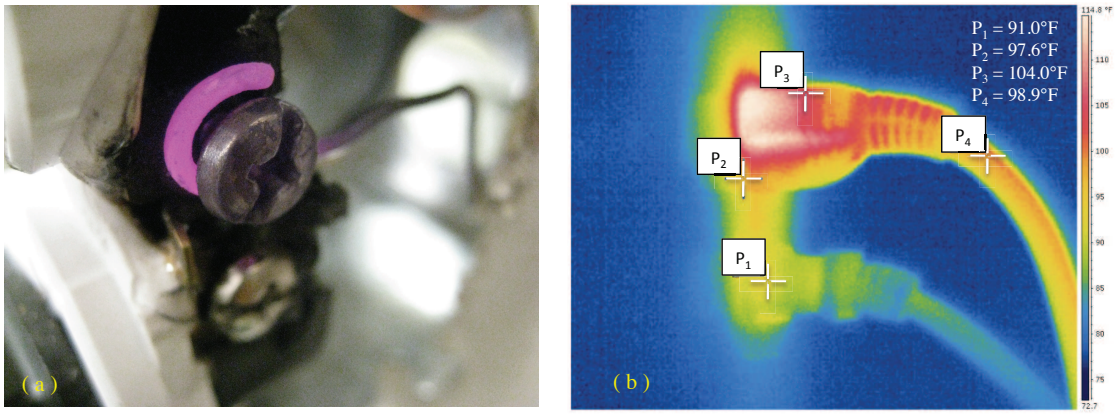

Figure 3.4: Outlet after 2 hours working under electric failure. (a) Glowing effect in wire, and (b) thermal distribution of the cords on service, some points are indicated

3.3 Arcing Fault

Arcing is defined as a luminous discharge of electricity across an insulating medium, usually accompanied by partial volatilization of the electrodes. Consequently, an arcing fault is an unintentional arcing condition in a circuit [45]. Topologically, the arcing fault can happen in serial or in parallel with the electrical load, as shown in Figure 3.5. The instant current peaks of the parallel arc can be several hundred amps, and the instant current of serial arc is usually less than 20A due to the resistance of the electrical load. Because of their intermittent nature, the average current is usually small and can not trip a common thermal-magnetic circuit breaker before fires start. Arcing type faults are the most difficult to locate due to their non-continuous nature and conductor concealment in conduit, or inside of walls or outlets.

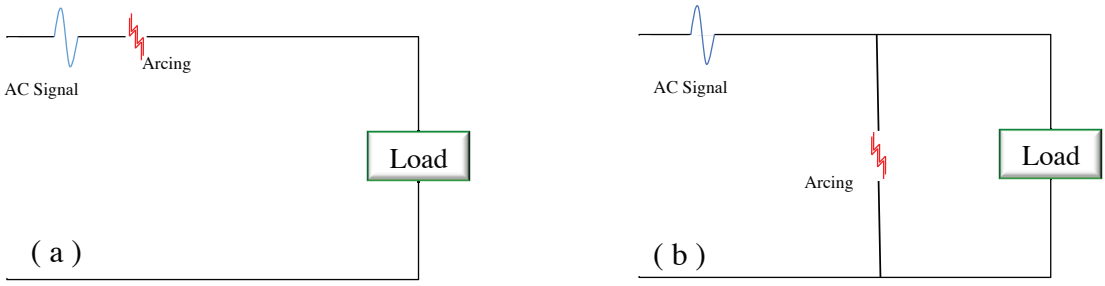

Figure 3.5: Basic topology of arcing fault. (a) Serial and (b) Parallel arcing fault

Electrical arcs can ignite fires, create glowing connection, or cause burn injury. Actually, one-third of home fires are caused by electrical arcs [43]. However, arcs have not been identified as electrical hazard until very recently. In 1982, Lee drew attention of arc hazard in his paper [46]. The National Electric Code (NEC) for arc prevention only came out in 2002. The low-voltage (around $120V_{rms}$) electric arcs are still not well understood. Babrauskas pointed out the three primary causes of arcs: carbonization of insulation, induced ionization of air, or short circuits [42]. PVC, which comprises two-thirds of the insulation used in the building wiring in the US, is susceptible to becoming charred semiconductor at 160 °C and at 110 °C during short or longer period of exposures. When combined with moisture or preheat, PVC carbonization can happen at mild temperatures such as 40 °C or even room temperature [47]. Therefore, initial current flow through the carbonized layer can ionize the air, cause local arc, melt the metal and generate sparkles. The intrinsic dielectric strength of air is about 3V/m, so it generally requires a gap less than 50μm between contacts to break down the air insulation or ionize the air. The electrical breakdown happens more often if there are flames, ionization, or pre-existing arcs. Sometimes, defective appliances and damaged extension cords can create a firm contact (bolted short) with large current to trip the breaker. The arc current lasts only for a very short time (sub second or sub millisecond), and the current stops when the melted metal is push away as sparkles, or it heats up and generates new arcs with current flowing through the ionized air gap again [44].

3.4 Experimental Study of a Serial Arcing Fault

The National Electric Code (NEC) first mandated the use of Arc-Fault Circuit Interrupter (AFCI) in 1999 for the protection of branch circuits supplying bedroom receptacle outlets. According to NEC, an AFCI is a device intended to provide protection from the effects of arcs faults by recognizing the characteristics unique to arcing and by functioning to de-energize the circuit when an arc fault is detected.

This set of experiments is intended to show that it is possible to produce hazardous fire conditions when an arcing fault is presented as a result of a loose connection in a straight blade receptacle (outlet). The arcing we are reproducing is a serial type. The arcing leads to the glowing contact and/or charred insulation, a precursor to continuous serial arcing and ashes from ignitable gases. A repeatable, yet realistic, method was needed to reproduce an intermittent electric fault that can result from real-life long term in service or from an inappropriate circuit installation. Wire damage especially can easily be observed near the arcing location.

Other component of interest besides wire, is the straight blade receptacle. According to the NEC, a receptacle is defined as an electrical outlet. An electrical outlet is a point on the wiring system where current is taken to supply utilization equipment and it includes receptacles, power strips, wall sockets and other similar elements [30]. Home electrical systems include at least one type of the receptacles shown in Figure 3.6. Electrical receptacles in walls and floors may present shock and electrical fire hazards to consumers. Older homes may have receptacles which are damaged or which, otherwise, may have deteriorated over the years. According to CPSC, outlets also deteriorate from repeated use when plugging-in and unplugging appliances as is often done in kitchens and bathrooms. As a result, when plugs fit loosely into receptacles, especially the two-prong ungrounded type, they may slip partially or completely out of the receptacle with only slight movement of the attached cord. Receptacles in this condition may overheat and pose a serious fire hazard [36].

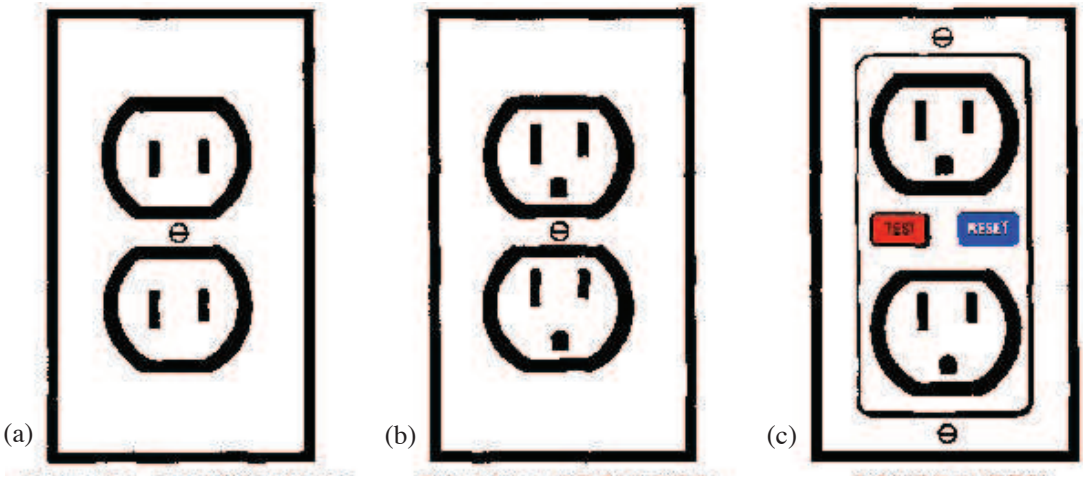

Figure 3.6: Basic types of residential grade receptacles: (a) Ungrounded, (b) Grounded, and (c) Grounded Fault Circuit Interrupter

The general design of an electrical receptacle can vary in details, but must meet or exceed the UL 498 standard. The UL 498 covers attachment plugs, receptacles, cord connectors, inlets, current taps provided with wiring terminals for flexible cord, and flatiron and appliance plugs - all intended for connection to a branch circuit for use in accordance with the National Electrical Code, ANSI/NFPA 70 [48]. All receptacles used in this research are grounded duplex type NEMA 5-15R or 5-20R (2 poles 3 wire grounded) and their basic characteristics are shown in Figure 3.7.

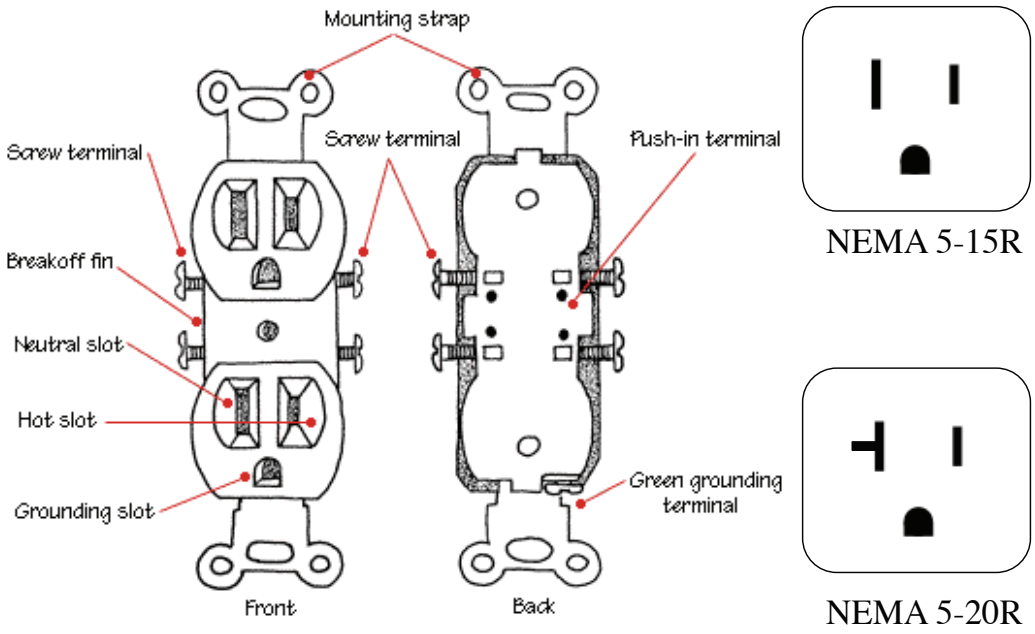

Figure 3.7: Parts of a straight blade receptacle with connector types indicated

Ten different types of grounded receptacles manufactured by United States companies are available for this test, some of them are shown in Figure 3.8. A complete information about each receptacle can be found at the manufacturers webpage.

Figure 3.8: Duplex straight blade grounded receptacles available in the market

Arcing creates high intensity heating at the point of the arc, resulting in burning particles that may over time ignite surrounding material [49]. Sensor measuring electrical current and temperature are configured for real-time measurement and data acquisition. A list of devices used for thermal and current measurements is shown in Table 3.1

Device	**Manufacturer**	**Range of operation**
Hall effect current sensor	Functional Devices	$0\,A_{rms} \sim 50\,A_{rms}$
Digital thermometer (dual input)	Fluke	$-200\,^{\circ}\text{C} \sim 1372\,^{\circ}\text{C}$
Infrared thermometer	Fluke	$-35\,^{\circ}\text{C} \sim 275\,^{\circ}\text{C}$
Current clamp meter	Fluke	$0\,A_{rms} \sim 50\,A_{rms}$
Thermocouples (K type)	Omega wires	$-270\,^{\circ}\text{C} \sim 1250\,^{\circ}\text{C}$
Infrared camera	Flir Systems	$-10\,^{\circ}\text{C} \sim 350\,^{\circ}\text{C}$

Table 3.1: Devices used for temperature measurement during arcing fault

Serial arcing was created deliberately during the experiments in order to understand the cause of damages and subsequent failure. Snapshots of arcing creation are illustrated in Figure 3.9.

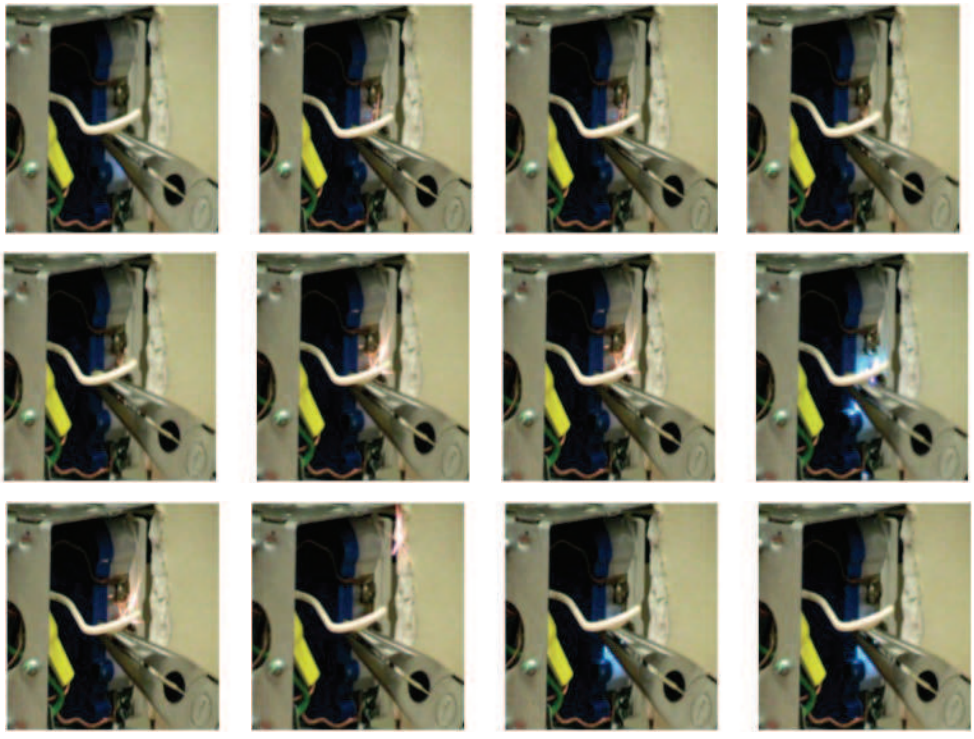

Figure 3.9: Creation of the electric arc fault on a loose connection

Infrared (IR) thermal images were taken to identify hot spots in some of the receptacles available. Figure 3.10 and Figure 3.11 give us non-contact information about changes in temperature during this test.

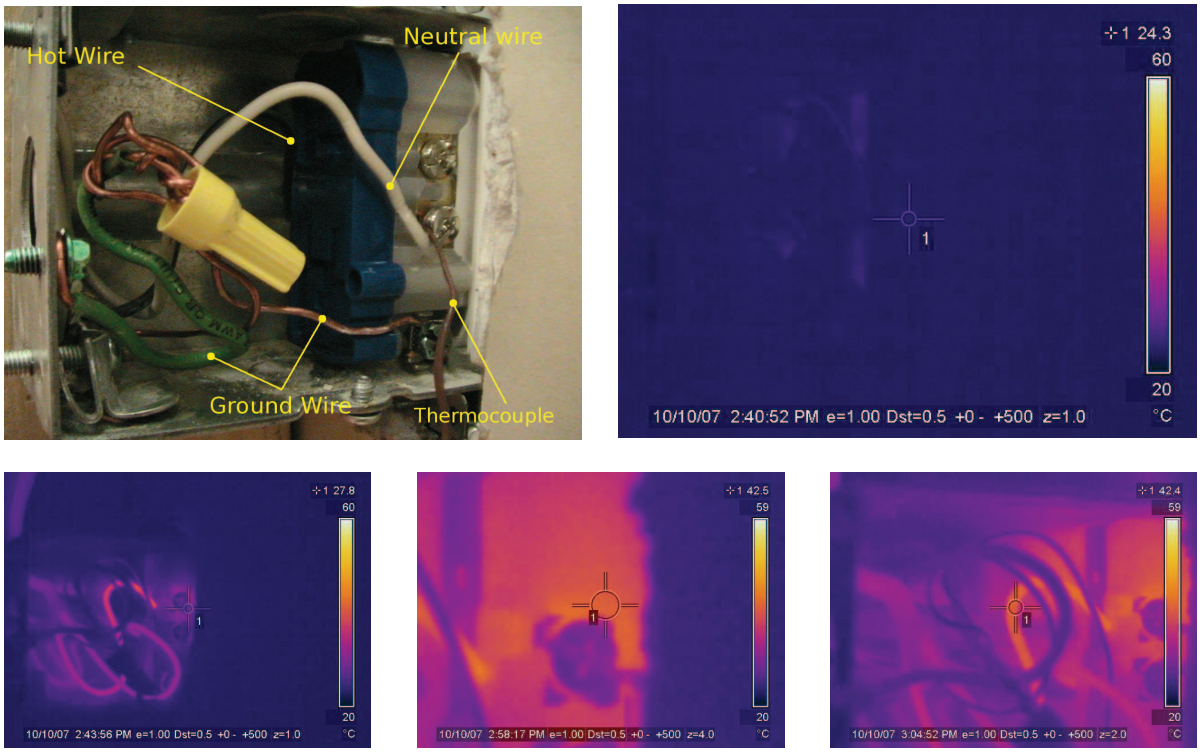

Figure 3.10: Back side of the receptacle under test: no damage over wire insulation can be seen as initial conditions

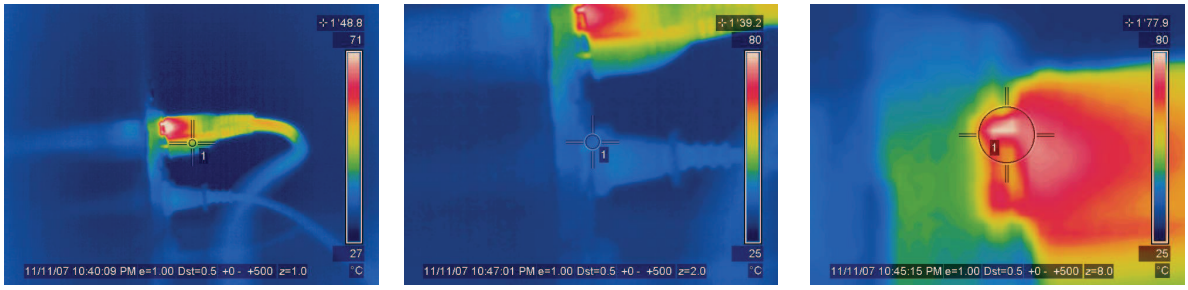

Figure 3.11: Front side (face plate) of the receptacle: hot spots are detected over the appliances cords. The electrical appliances employed are a water heater (upper side) and electric oven (lower side)

Another way in which insulation can become overheated and ignite or burn is from over-surface arcing. During this test a current of 11 A at 115 V are used. According to Slade, this arc will extinguish at the next current zero in the AC waveform and not continue because the breakdown strength between contact points will follow the Paschen's minimum for air. This serial arcing results in a plasma hot enough to char insulation located in close proximity of the arc. Carbon on the wire heated by an arc, continues to arc because of the thermionic emission properties of the carbon [50]. This intermittent arc leads to the glowing effect as illustrated Figure 3.12.

Figure 3.12: Formation and progression of the glowing contact: temperature ranges from 24 °C to 280 °C

A set of thermocouples and thermistors were used to obtain real time data. These sensor were labeled and installed as shows in Figure 3.13.

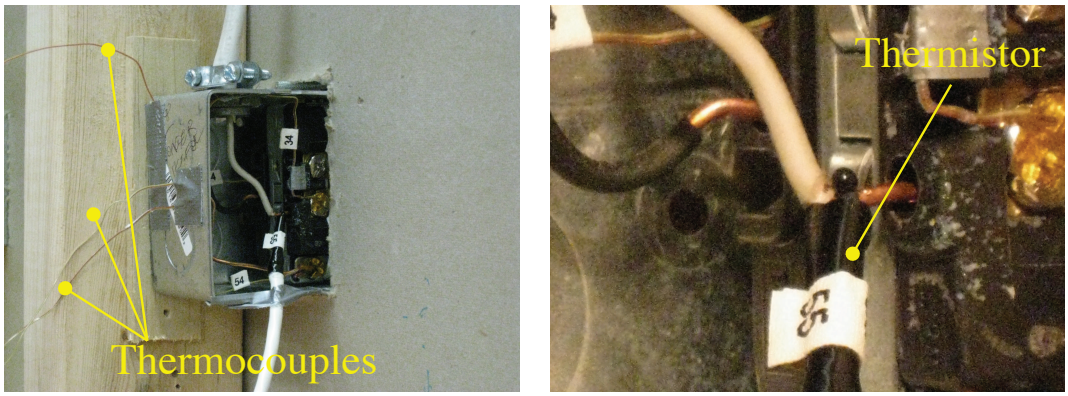

Figure 3.13: Setup of temperature sensors over hot spots

Data taken directly from the thermocouples and thermistors were corrupted due to the electromagnetic field generated when arcing fault was in progress. In the most extreme case, the

PC-based system was damage due to this phenomena. In an attempt to use an isolated instrument to detect change of the wire's temperature, arcing fault currents are capable of harming the equipment, resulting in wrong calibration, erroneous data or permanent damage of equipment. A non-direct contact approach can be used to obtain thermal information when arcing appears. Figure 3.14 shows change in temperature near to the arcing points. In some cases, the temperature can exceed the limits of the IR equipment.

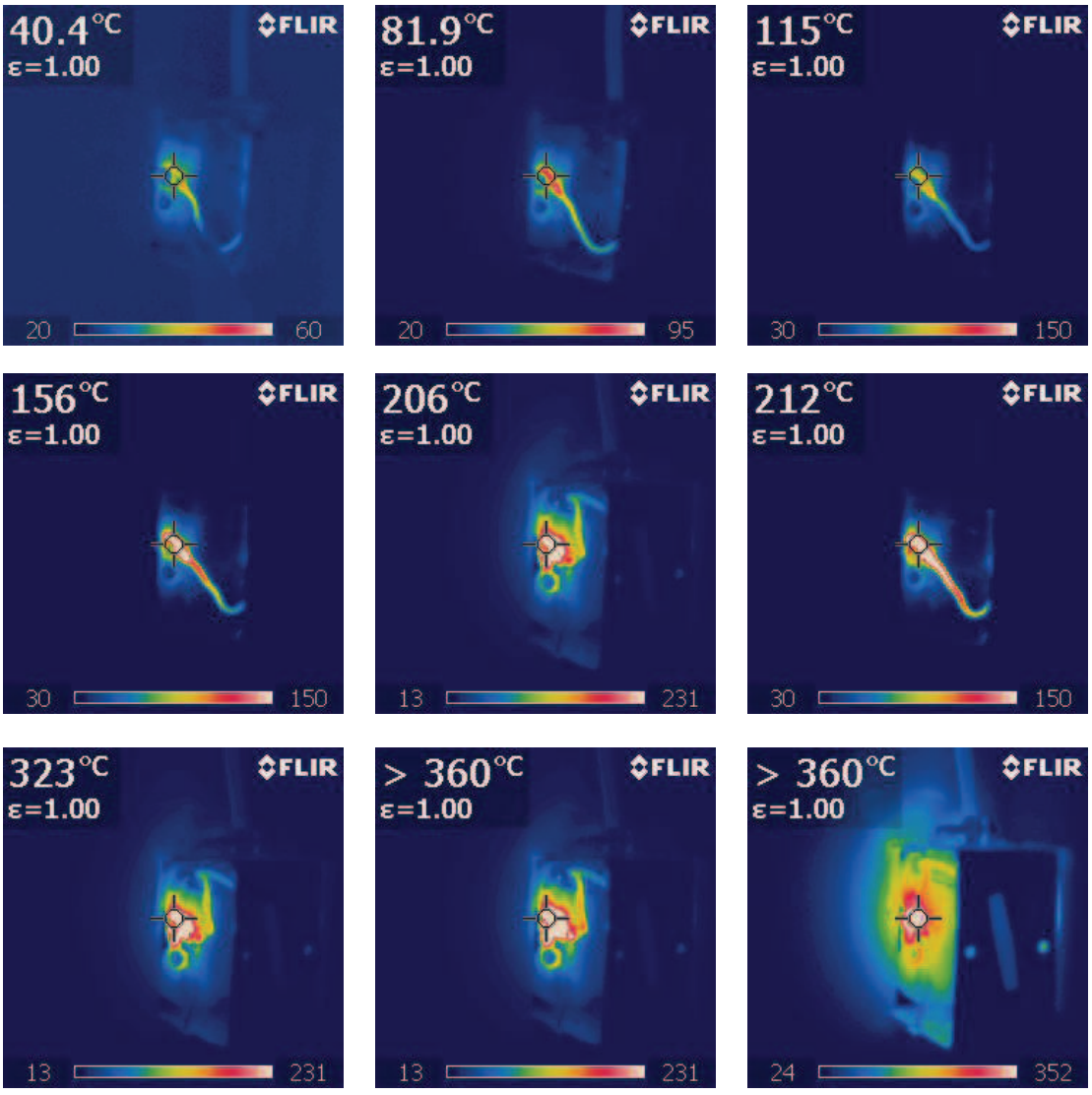

Figure 3.14: Infrared images of glowing contact in a conventional receptacle. with temperatures indicated

3.5 FEM Simulation and Experimental Study

In 2007, NEMA published a white paper analyzing the impact of home electrical fires. Through the Low Voltage Equipment Section (LVDE), this paper reviews the potential effect that arc fault circuit interrupters (AFCIs) may have on reducing the risk of an electrical fire. Manufactures are designing and developing breaker devices under the AFCI program; however, this is the only component in the home electrical system considered by them. In contrast, a New York based company (BSafe Electrix) created in 2008 an innovative electrical receptacle. This new BSafe device is shown in Figure 3.15 and was designed based on NEMA, NEC and UL standards [48]. The BSafe receptacle includes a thermal switch which measures temperatures in the vicinity of the binding head screw terminals and cuts off power supply when certain temperature threshold is exceeded due to abnormal heat generation that may cause fire hazards.

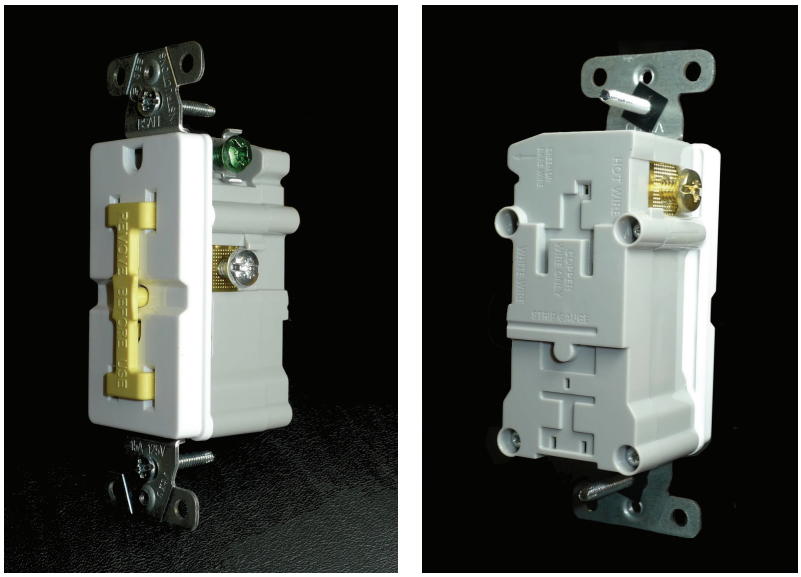

Figure 3.15: A receptacle with thermal cut-off technology designed by BSafe Electrix

The design and operation of BSafe's mechanism are analyzed with FEM simulation in the lab at Stony Brook. They are presented and discussed as follows.

3.5.1 Heat transfer simulation

In order to understand the heat transfer in the BSafe receptacle and to compare with the regular ones, ANSYS software is used to perform the simulation. The finite element model (FEM)

analysis is built based on "*shell* " element because the metallic component of the receptacles is thin and does not require a 3D geometry model. Characteristics to perform the FEM simulation are:

(1) Heat sources and initial conditions

The terminal screws and blades were identified as the candidates of heat sources based on the thermal in the previous section. As a result, four different settings of heat sources are configured in simulation for each BSafe and regular receptacle and they are:

- one blade (e.g., one load plugged into one set of blade),
- one terminal screw,
- two blades, and
- two terminal screws.

(2) Material properties

For the straight blade in both models we consider copper; therefore,

- The heat conductivity is 401 W/(m $^{\circ}$K).
- The heat capacity is 0.38 kJ/(kg $^{\circ}$K).
- The density is 8920 kg/m^3.
- The thickness of the metallic blade is 0.76 mm.

For the revised design as a result of the study, BSafe includes yellow brass materials. From Olin Copper Alloy guide, the yellow brass (brass 268) has the following properties:

- The heat conductivity is 116 W/(m $^{\circ}$K).
- The heat capacity is 0.38 kJ/(kg $^{\circ}$K).
- The density is 8470 kg/m^3.
- The thickness of the metallic blade is 0.76 mm.

Various modeling and simulation of heat transfer for the Bsafe and regular receptacles using different heat sources were performed. Temperature of the heat source was assumed at 180 °C, and the initial conditions for the metallic part at 15 °C. Figure 3.16 shows a typical result of FEM analysis with conduction heat transfer. More results are shown in Appendix B.

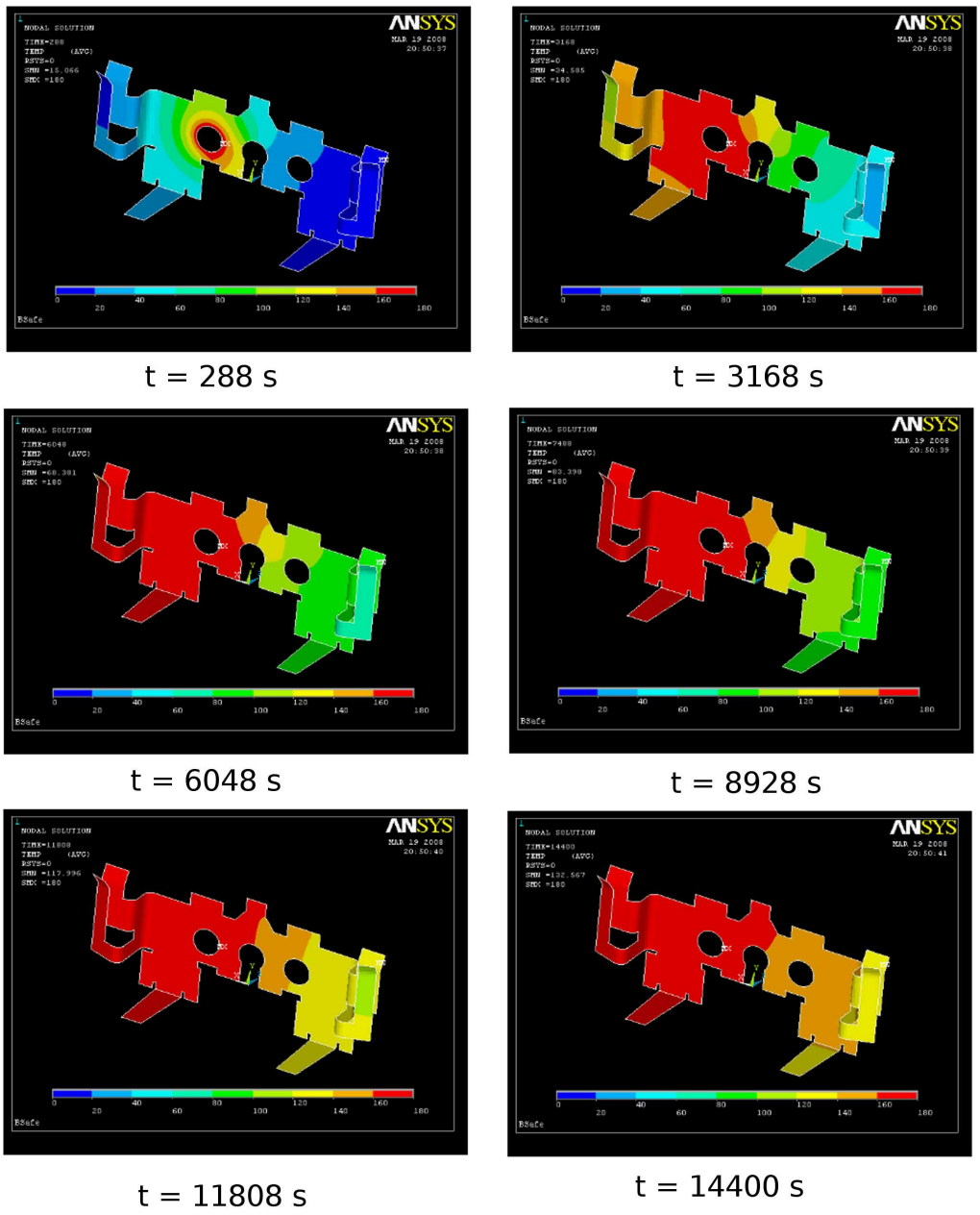

Figure 3.16: Thermal simulation of BSafe receptacle with one terminal screw as heat source

Combination of parameters and conditions for FEM simulation are presented in Table 3.2

Figure	Model Type		Heat Source				Observations
	BSafe	Regular	1 blade	2 blades	1 screw	2 screw	
Fig. B.1	√		√				
Fig. B.2		√	√				
Fig. B.3	√				√		
Fig. B.4		√			√		
Fig. B.5	√			√			
Fig. B.6		√		√			
Fig. B.7	√					√	
Fig. B.8		√				√	
Fig. B.9	√				√		yellow brass
Fig. B.10	√		√				yellow brass

Table 3.2: Configurations for FEM simulation of conduction heat transfer in blades of receptacles

3.5.2 Thermal activated cut off mechanism of a BSafe receptacle

BSafe's design detects excessive heat and employs a thermo-mechanical cut off mechanism. The main part of the mechanism is composed by a bimetallic transducer. Based on the innovation, the metallic blade of a conventional receptacle has been replaced by two different metallic plates. A schematic of the bimetallic transducer is presented in Figure 3.17.

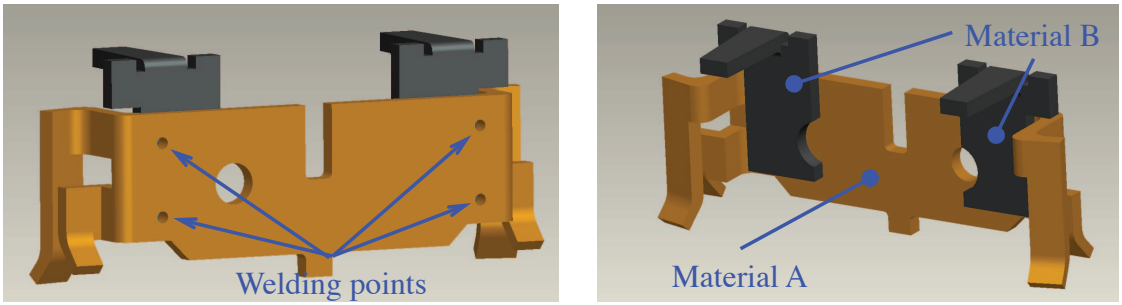

Figure 3.17: Schematic of a bimetallic blade receptacle designed by BSafe

The metallic part made from Material B is designed to deflect after reaching a prescribed temperature. Tests performed in our lab has established an average value of 130°C with an error of 5%. The bimetallic part is assembled as a trigger of a spring loaded mechanism. Once the

temperature in the blade reaches the set point, the bending action of the bimetallic transducer releases the spring loaded mechanism which will open the circuit and consequently cut off the current flowing through the system. The spring loaded mechanism is shown in Figure 3.18, a layout of the components is shown in Figure 3.19 and an exploded view of the BSafe receptacle is presented in Figure 3.20.

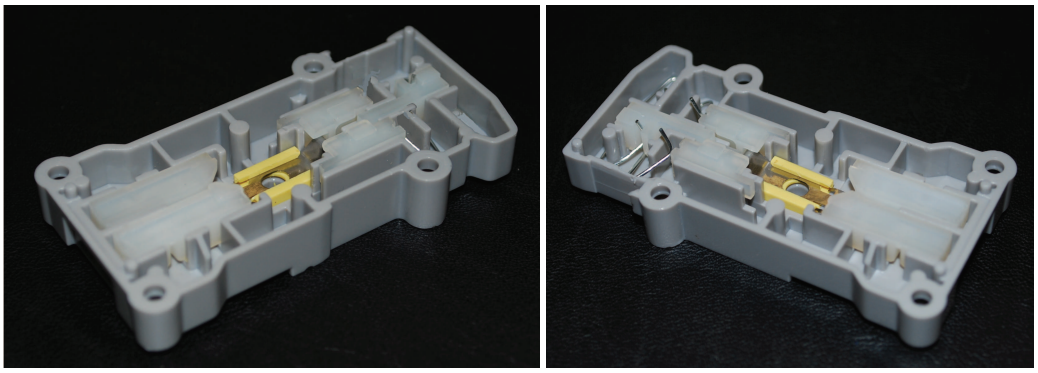

Figure 3.18: Spring loaded mechanism of the BSafe receptacle

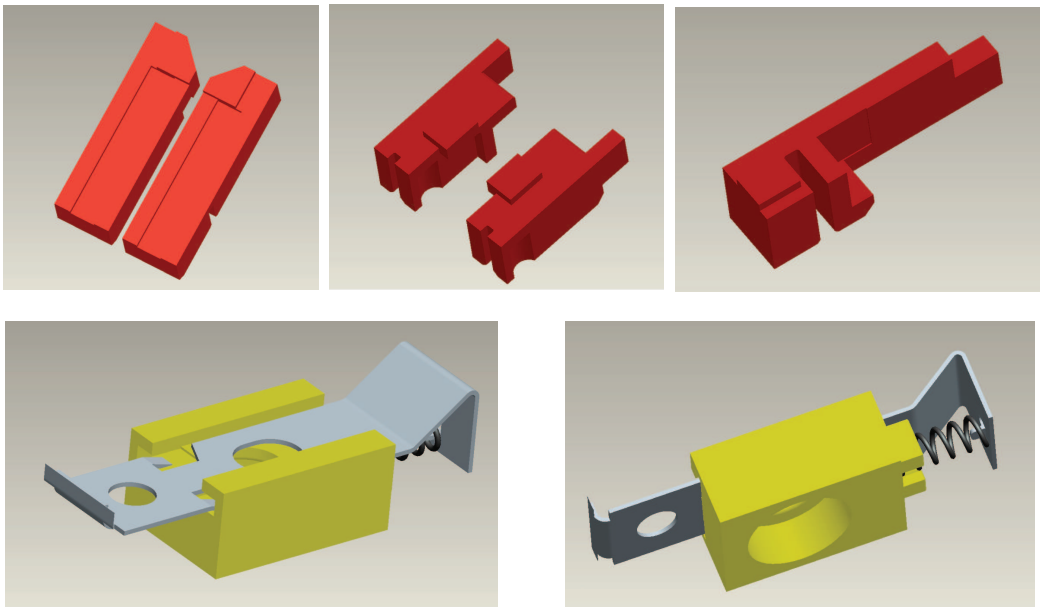

Figure 3.19: Components of the spring loaded mechanism of the BSafe receptacle

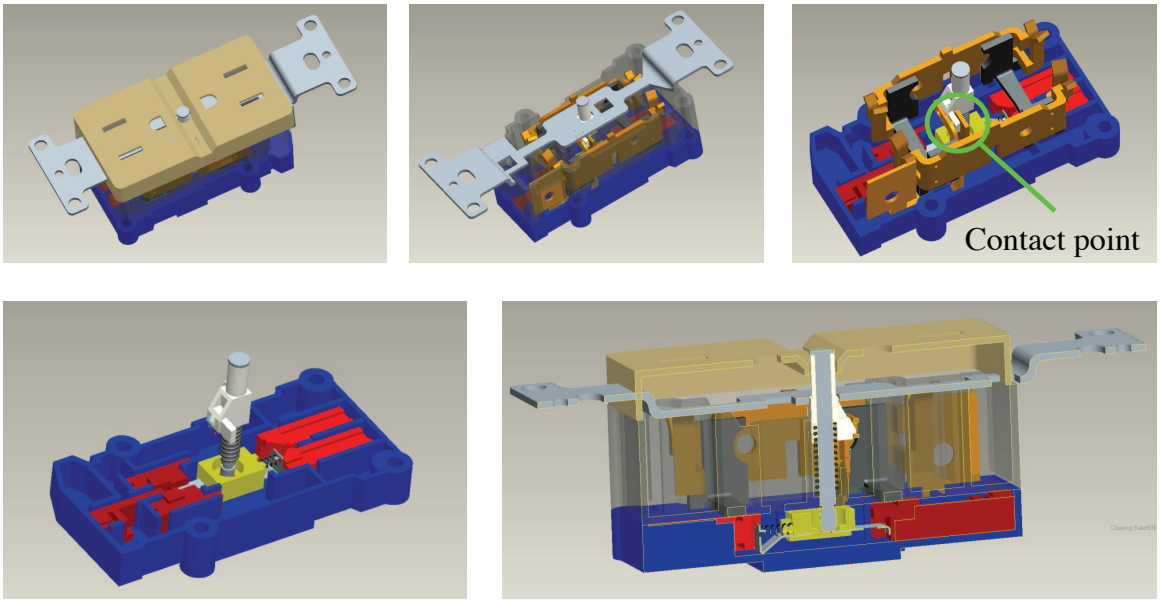

Figure 3.20: Exploded views of BSafe receptacle with the contact point of this cut-off mechanism

3.5.3 Discussions

The FEM simulation provides us a better understanding of conduction heat transfer within a receptacle, and provides insights into the design of such smart and automatic cut-off outlets. The key of this design is the bimetallic transducer which acts as a sensor of temperature (deflect when temperature changes because of the different coefficients of thermal expansion for the two metals) and an actuator to disengage the contact to cut off electricity flow.

Comparing Figure B.1 to Figure B.4, we find that it is easier for the BSafe receptacle to transfer heat from one side of the metallic component to the other. On the other hand, it takes longer for the regular receptacles to transfer heat to one extreme of the straight blade to the other. The main reason for such difference is because of the wider bridge which connects two sides of the BSafe receptacles; while the thinner interconnect for regular receptacle works as a bottleneck for heat transfer.

By comparing Figure B.1 and Figure B.3, it is observed that if the terminal screw is the heat source, the bimetallic component will be heated up faster due to the central location of the heat source. However, it is noted that this is only true when the heat sources are given the same temperature.

When the heat source involves two blades or two terminal screws, as shown in Figure B.5

to Figure B.8, it becomes obvious that the receptacles will reach higher and more homogeneous temperature distribution much quicker than those with one blade or terminal screw as heat source.

When the yellow brass (brasses 268) material is employed in simulation, the heat transfer is slower due to the significantly lower heat conductivity as compared to copper. Figure B.9 and Figure B.10 show the simulation of the BSafe receptacles with yellow brass under different heat sources. It can be readily seen that the heat transfer rate is much slower compared to Figure B.3 and Figure B.4. Nevertheless, the trend of the heat transfer and temperature distribution remains similar.

The designed mechanism prevents to reach temperatures over 110°C. Same situation was presented when BSafe's receptacle was installed in a deteriorated wire. In contrast, using conventional receptacles under serial arcing fault condition always allows to reach higher temperatures. The FEM simulation and experimental study helped us to gain in-depth understanding of the mechanism and facilitated the revisions of the design of this outlet.

3.6 Experimental Study of Continuous Arcing and Degradation

A new study was performed for the analysis of serial arcing and the resulting degradation of extended period of sustained arcing. This new research result presents a degradation of receptacles under serial arcing condition which resembles exponentially decaying characteristics. In this section, we present quantitative results from experimental study.

Important findings on the changes in temperature, when an arc fault is presented, suggest that the concept and analytical tools have high potential and are very promising towards the development of an intelligent and integrated diagnostic tool for grounded electrical receptacles. Serial arcing faults typically can not be detected by the existing breaker system,such as a breaker panel rated at 15A or 20A. Such serial arc produced overheating of the insulation and ambient can produce ignitable gases if the wire insulation is made of plasticized PVC as well as the receptacle. A sequence of the degradation of the insulation in wires is illustrated in Figure 3.21.

Generally, it takes longer for a serial arc to generate the same volume of gases from wire insulation due to the lower arc energy compared to a parallel arcing fault [37]. Flammable gases from a degraded wire insulation can ignite, this increases the chances of igniting a secondary ignitable material, in the vicinity of the fault, or igniting the wire insulation itself. As mentioned previously, an arcing fault may take several months or years to develop a fire hazard condition; however, once established in the system, it will take a few minutes to reach higher temperatures

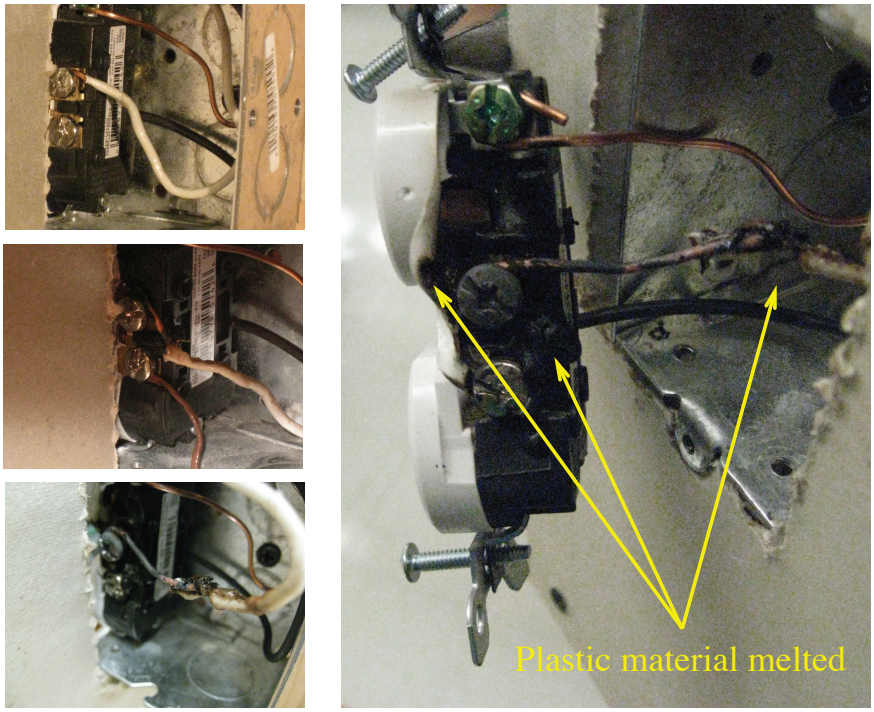

Figure 3.21: Progressive degradation of the insulation due to an overheated wire

as shown in Figure 3.22. Such cumulative degradation of wire and connection in an outlet is of critical importance.

In the experiment presented in Figure 3.22, a deliberate serial arcing fault was manually create. The initial condition is a brand new receptacle. Wire and receptacle degradation is a cumulative process. The more number of tests performed over the same receptacle, the less time it takes to reach the same level of temperature as shown in Figure 3.23. During the initial tests higher values of temperature were no easily achieved. Due to the self extinction nature of arcing, the system tries to return to its own thermal balance. As a result, a stabilized temperature can be achieved and measured.

In Figure 3.22 is shown that room temperature (23 °C) is the initial condition stablished for the cumulative degradation experiments. Once the electric load is activated, the arcing fault is introducing in the system. The changes in temperature are recorded as a function of time. When the arcing fault disappears, a constant or decreasing temperature is observed. In this situation the test is conclude and the system is cooling down to reach the initial condition after which the next test is performed.

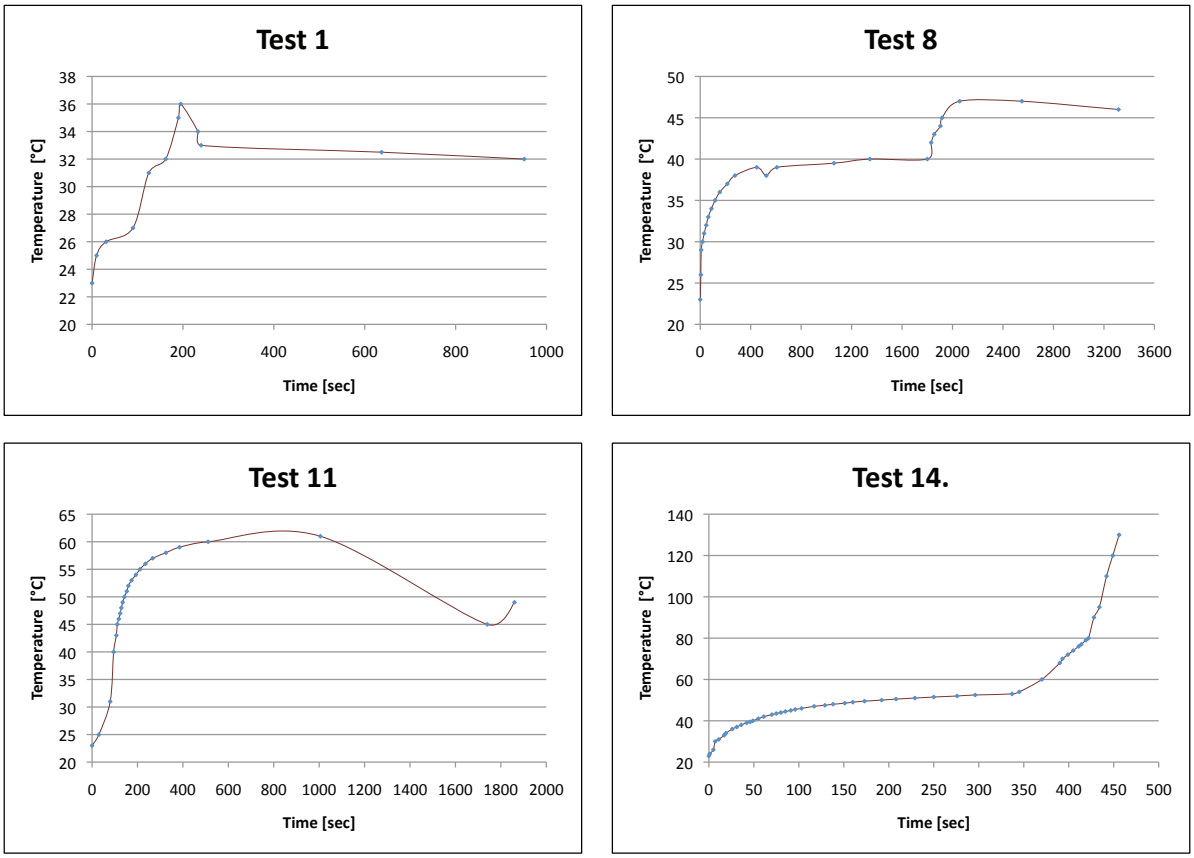

Figure 3.22: Cumulative degradation of wire reduce the time to reach higher values in temperature under the presence of an arcing fault

As we can observe, after 4 minutes, the maximum temperature reached in Test 1 was 36 °C. A similar time is observed in Test 8 for the same temperature; however, the presence of arcing fault allows to reach a maximum temperature of 47 °C. In the case of Test 11, the cumulative degradation and the induced arcing fault reduced the time to get 36 °C up to 50% less (2 minutes) and a higher level of temperature was achieved (62 °C). In contrast, Test 14 reveals a dramatic damage degradation, taken less than 20 seconds to reach 36 °C.

The presence of an arcing fault changes drastically the thermal profile of the system. In Test 8, a smooth increasing temperature gradient is observed after 10 minutes. The arcing fault re-strikes 20 minutes later to reach the maximum temperature in less than 5 minutes. A similar behavior is observed in Test 11, when arcing is introduced around the minute 30; however, before the re-strike, we had a decreasing constant gradient. Finally, after 5 minutes, in Test 14 the

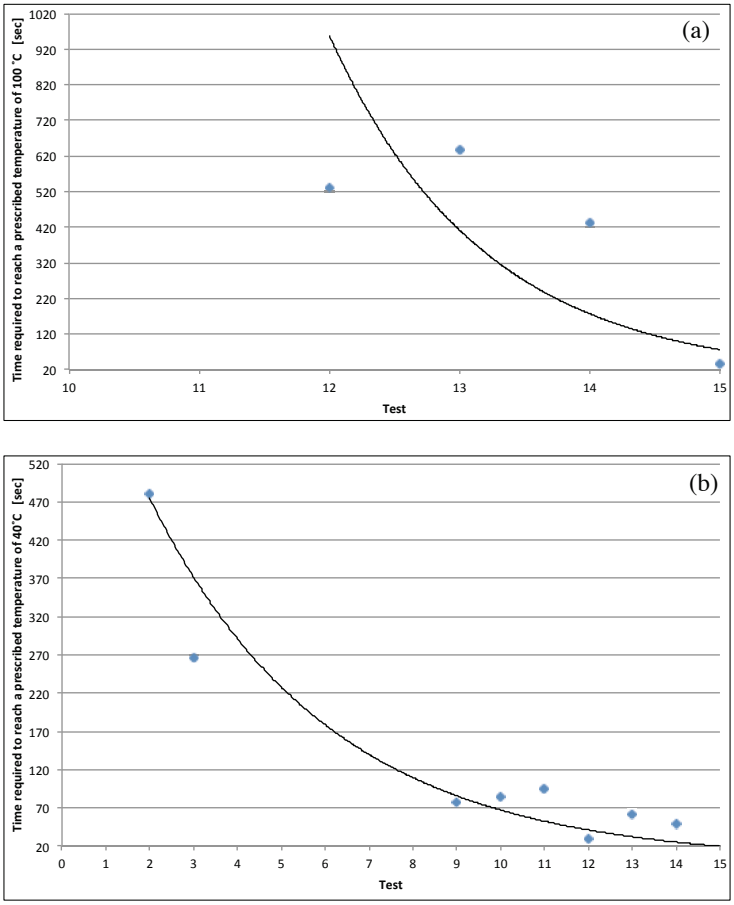

Figure 3.23: Comparative of receptacle tests to reach a fixed value of temperature, (a) up to 100 °C and (b) up to 40 °C

temperature rises faster than the other tests due to a permanent arcing fault allowing the wire to heat up considerably (beyond 120 °C) to cause fire hazard.

3.7 A new model for receptacles design

Based on the recorded data, a new approach for the design of receptacles can be created. Figure 3.23 represents the evolution of the wire's degradation through each test. For a prescribed temperature, the time to reach the specific value decreases as the amount of test (under serial arcing fault) were performed. For instance, prescribing the temperature to 40 °C took 4 minutes in Test 3; meanwhile, took 40 seconds in Test 14.

An exponential decay (curve fitting) can be used to represent this relationship as shown

in Figure 3.24. First, we must consider the receptacle under normal conditions. According to NEMA [51], receptacle wire terminals are permanent static contacts. Once installed they must be capable of operating safely as part of the wiring system for an indefinite time. The receptacle blade contacts are separable. They must be capable of safe operation when plugging in or disconnecting a large variety of electrical prongs, for a wide range of plug insertion frequency and sustained current loading. Experimental data from receptacles without arcing fault change between manufacturers as well as internal design. However, following the UL498 standard, the limiting temperature for a receptacle must be below 70 °C [48] . Our experiments registered up to 45 °C.

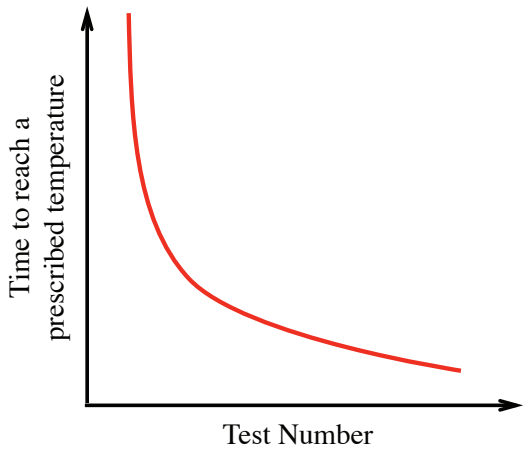

Figure 3.24: Experimental study of the deterioration of receptacle

As a result, the proposed model represents the normal operation, after reaching the steady state condition, as showing in Figure 3.25. With no arcing fault, the prescribed value will be the the normal temperature T_N. Therefore, there is no change in this value through the number of test performed. A particular test was performed using a receptacle with more than 10 years of service and the results demonstrated a very good performance of the device. Second, when a serial arcing fault is included, all receptacles had overheated to hazardous levels at the attachment plug contacts, after the seventh test. Removed from the outlet, the attachment plug shows obvious damage from the overheating plug blade contacts. With the attachment plug inserted, however, there is no visible sign of the developing hazard. Experiments show that utilization of electrical appliances would operate properly in spite of the abnormally high contact resistance. This type of failure is not likely to be detected at this stage by any of the conventional electrical protection

devices (breakers). The cumulative degradation of the wire connected to the receptacle can be used as a protective mechanism against this fault. Here, we consider the amount of test N as an independent variable and t our time indicator parameter. When the same receptacle is tested under a serial arcing fault, the degradation increases and consequently, the time to reach a defined value of temperature decreases.

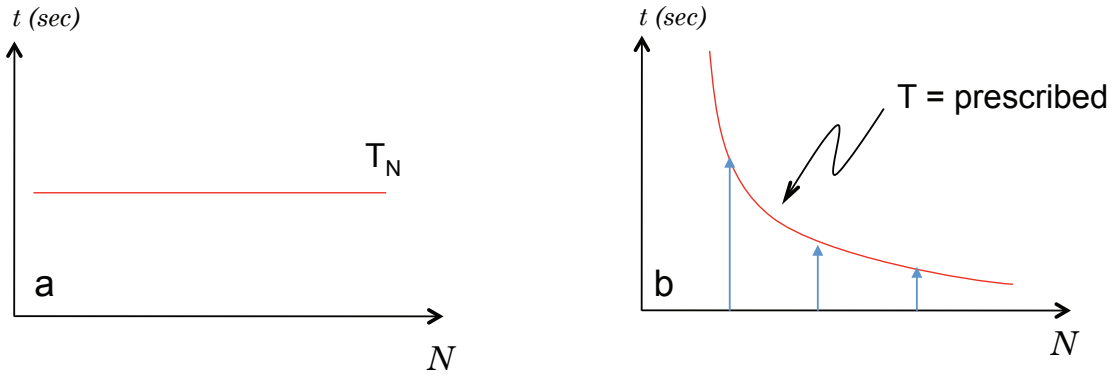

Figure 3.25: Conditions included in the proposed model, (a) normal operation and (b) time variation to reach a prescribed temperature after a continuous arcing fault in the system

Our exponential model can be presented by the next equation:

$$t = T_N e^{-kN} \tag{3.1}$$

In this basic model, T_N represents the nominal value of the temperature under normal operation. T_N is different for every receptacle device. A measured temperature in our experiments ranged from 30°C to 50°C considering an average load of 10 amperes. In this case, the value of the parameter k must be equal to zero. With no fault, the time needed to reach the temperature of operation depend of the load managed by the system, however it will no change with the number of test performed. In contrast, if an intermittent connection is presented, the value of k is related with the amount of disconnections (or connections) happening during a particular test. The k parameter must included the amount of electric energy transformed into heat and light due to the arcing fault during each test. This cumulative damage can be use as an innovative approach for the design of protective methods again serial arcing fault.

3.8 Summary

In this chapter, we consider the temperature as an important variable in the system. Through experiments, we found that appropriate fault isolation and sensors condition are required. FEM analysis of conductive heat transfer and experimental studies are conducted to understanding fundamental thermal behavior within a receptacle and the results are utilized in design and revision of a receptacle design.

A new contribution of the experimental study of the degradation of electrical outlets under the presence of serial arcing is presented. We have found a model to describe such degradation by plotting the time it takes to reach a prescribed temperature versus the cumulative time of sustained arcing. The curve of degradation resembles an exponential decay curve. This new model will contribute to the fundamental understanding and facilitate the design of future receptacles.

Chapter 4

FDD OF SERIAL ARCING AND EXPERIMENTAL STUDY WITH MODELING

4.1 Introduction

Although the dangers associated with arcing faults are widely understood, no single method of quantifying the hazard has received overwhelming approval. Most of the attention has been dedicated to electric high voltage transmission systems (greater than 1KV). From electrical equipment perspective, several procedures were established in IEEE Standar 1584 [52]. Furthermore, the standard has led to the establishment of an IEEE and National Fire Protection Agency (NFPA) joint task force to investigate the hazards associated with arcing.

According to the IEEE Committee for Industrial Applications, there is still wide-spread discussion on the best method of modeling arcing faults. Some believe that the equations should be derived from physics and that the equations in IEEE Standard 1584-2002, based on statistical analysis, are not representative of the arcing phenomenon. Some engineers think that both IEEE Standard 1584-2002 and physics-based equations are too complicated for the average user. Some support modeling the arc as a simple circuit element. However, because a nonlinear circuit element better represents the arcing phenomenon, some engineers argue that a nonlinear model would yield the most accurate results.

In this chapter , we will introduce a new model for the case of serial arcing in low voltage electric systems. Feature extraction will be discuss in Section 4.6 . At the end of the chapter, application of the technique to the experimental data will be presented.

4.2 Arc Structure and Properties

There are several mechanisms to initiate an electric arc, some of them are: by the separation of current carrying contacts, the melting and vaporization of thin wires and, transition from a glow

discharge, or transition and follow through of an impulse or high-frequency spark breakdown.

For all arcs the conducting gas between the electrodes has a high temperature ($> 4000\,^{\circ}$K) and high luminosity. The arc may be distinguished from other electrical discharges by its ability to conduct relatively high currents (extending from a fraction of an ampere to hundreds of kiloamperes) while being sustained by a relatively low electric field strength [53]. Because of its gaseous nature, the arc is easily influenced by gas flow. However, the spatial stability of arcs is greatly dependent on the nature of the cathode material. Thus with typically refractory cathodes, e.g. carbon, molybdenum and tungsten, the cathode temperature is high and the arc is relatively stable. With low melting point cathodes, e.g. copper and mercury, the cathode termination is a highly mobile and concentrated spot which moves constantly over the cathode surface in an irregular fashion. These visual differences are the result of different cathode mechanisms and lead to the classification of arcs into two main types —refractory and non-refractory or cold-cathode arcs. Both arc types, however, have essentially the same column properties [54].

The relation between Voltage and Current (V/I) or Voltage and Arcing Length (V/l) is used to obtain considerable information on arc structure and properties. Once a steady-state is achieved, some generalizations can be made. According to Jones, most of the studies had been done in high pressure arcs ($>$ 1bar). Nonetheless many of the diagnostic techniques are also applicable to low pressure and vacuum arcs [53]. High pressure arcs are subdivided into two main categories which are axisymmetric and non-axisymmetric arcs. The axisymmetric arc column burns symmetrically along the inter-electrode axis so providing good cylindrical symmetry, as shown in Figure 4.1.

Most of these arcs, are relatively easier to control or modified because they are been used in practical applications as welding or furnace induction ovens. Beside the difficulty to model, the symmetry reduce the amount of variables during the analysis. On the other hand, non-axisymmetric arc columns are less amenable to diagnosis not only on account of the reduced cylindrical symmetry but also because they are either in a state of dynamic equilibrium or continuous motion. Lateral movement of such arcs may be caused by an imbalance between aerodynamic and magnetic forces so further complicating the use of highly localized diagnostic techniques [53]. A number of practical forms of non-axisymmetric arcs are shown on Figure 4.2.

In this case, (a) Horizontal arc with or without crossflow, (b) Arc between linear rail electrodes with or without crossflow with or without an external B field. (c) Arc driven between deionizing plates, (d) Rotating arc between ring electrodes. (e) Helical arc in coaxial geometry with or

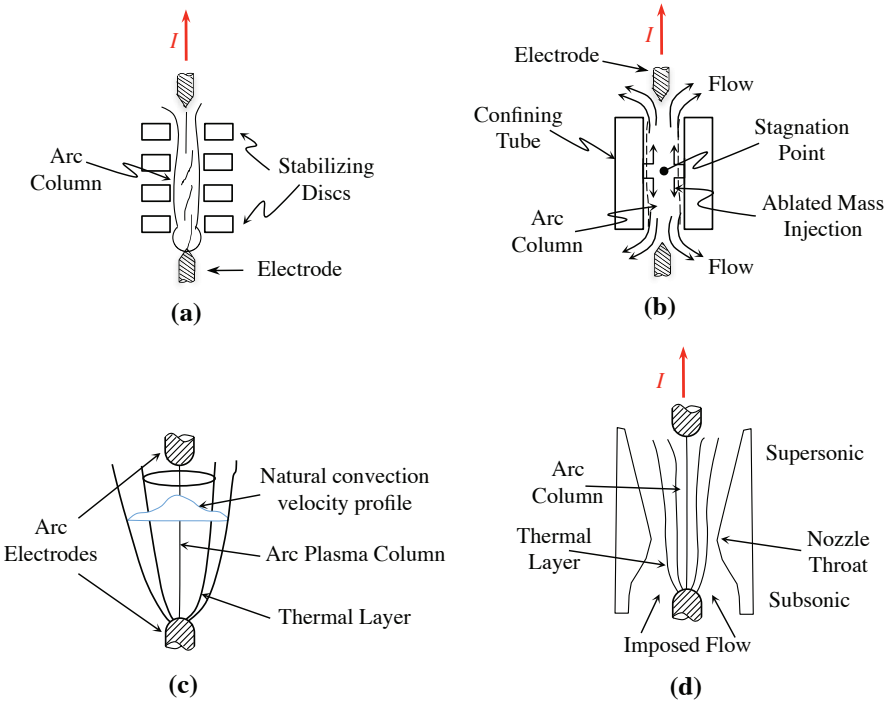

Figure 4.1: Different types of axisymmetric arcs. (a) Wall stabilized, (b) Ablation stabilized, (c) Vertical free burning and (d) Axial convection controlled arc [53].

without imposed flow, and (f) Spiral arc with part wall ablation stabilization. Non-axisymmetric arcs can also be found in several applications, and sometimes they are only a consequence of the required effect, such in discharging rods or current pick-up in the case of electric traction vehicles.

4.2.1 Formation of the electric arc

4.2.1.1 Electric arc during contact closing

According to Slade, once a voltage is impressed across and open contact gap, there are two important time periods [50]. The first is the statistical time lag t_{st}, in which the first electron becomes available to begin the breakdown process. The second is the formative time lag t_f, which is defined as the time required for the discharge to become establish. The t_f depends upon the over-voltage, the gas, the contact geometry, and the number of initiating electrons [55].

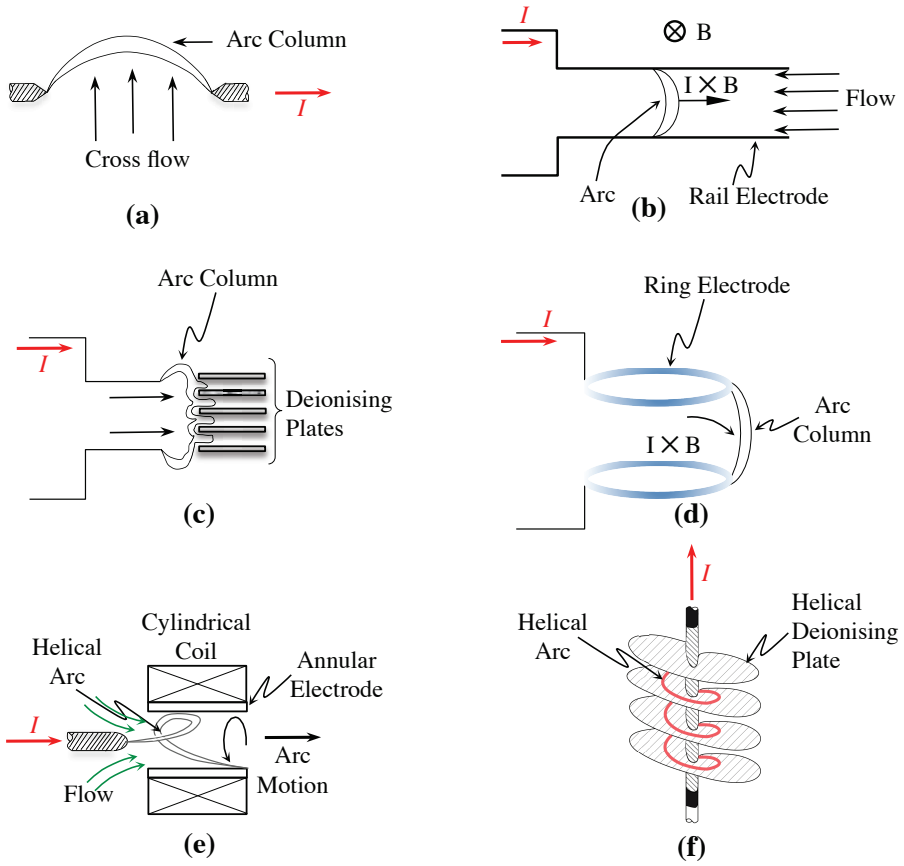

Figure 4.2: Different types of non-axisymmetric arcs [53].

4.2.1.2 Electric arc during contact opening

The arc formation depends entirely upon the properties of the contact material and the arc always initiates in metal vapor from the contacts themselves. The contact resistance R_c is given by:

$$R_c = \frac{\rho}{2} + \sqrt{\frac{\pi H}{F}}$$

where H is material hardness, ρ is resistivity and F the holding force. As the contact begin to open $F \rightarrow 0$ and so R_c will increases, consequently the voltage drop across the contacts also increases, thus:

$$V_c = IR_c$$

Once the contact spot has melted and the contacts continue to part, they draw a molten metal bridge between them. This molten metal bridge always forms between the contacts even at low currents [56], even when the contacts open with a very high acceleration, and even when they open in vacuum [57]. The more gap between contacts the more instability of the arc.

There are a number of physical reasons for this instability, including surface tension effects, boiling of the highest temperature region, convective flows of molten metal resulting from the temperature variation between the bridge roots and the high-temperature region. The bridge will eventually rupture, releasing metal vapor into the contact gap. The hot metal gas release into the space between the contacts establishes a condition where thermal ionization can take place. Here ionization is not only produced by electron-atom collisions, but it can also be caused by atom-atom collisions and even by radiation. Under these conditions, a proportion of the metal vapor atoms will have high velocities because of the high temperature that occurs just after the rupture of the molten metal bridge. The sequence of the arcing during the contact opening can be seen in Figure 4.3.

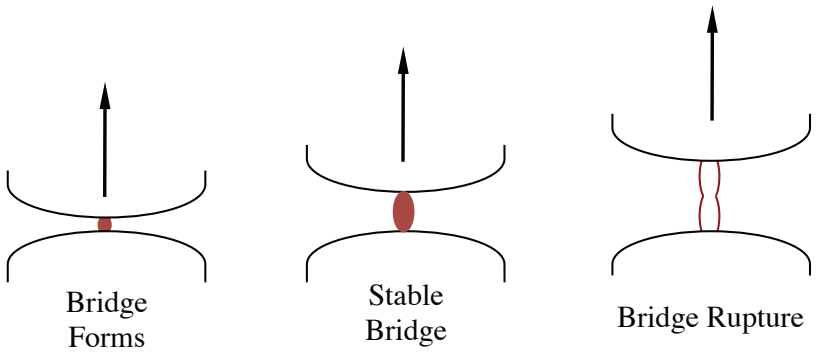

Figure 4.3: The opening sequence of an electric contact [57].

Table 4.1 summarized some of the observations made by Wagar. Here, d repesents the distance between contacts (in mm), V_B is the voltage for breakdown, and E_c represents the critical breakdown field which is a material property dependent.

4.2.2 Arc regions

In general, electric arcs consist of three physically distinct regions which correspond to two electrode regions and an interconnecting plasma column as showing in Figure 4.4.

Condition			V (across contacts)	I (in the circuit)
To initiate breakdown	Gas breakdown	non conduction to glow	V_B gas $> 329 + 7 \times 10^6 d$	$I \approx 0.01 - 0.6$ A
		non conduction to arc	V_B gas $> 329 + 7 \times 10^6 d$	$I > 0.01 - 1.0$ A
	Small gap or vacuum breakdown	non conduction to arc	$V_{B_{VAC}} > E_c d$ $0.5 \lesssim E_c \lesssim 30.0$ $E_c \times 10^8 [V/m]$	$I > 0.05 - 1.0$ A
To sustain breakdown	Glow	gas dependent	$V_G = 280 + 10^3 d$	$I_{G_{min}}$ $0.01 - 0.6$ A
	Arc	material dependent	$U_A = U_{min} + 10^4 d$	$I_{min} \approx 0.05 - 1.0$ A

Table 4.1: Parameters required to form and sustain an arc. Source N.H. Wagar [58].

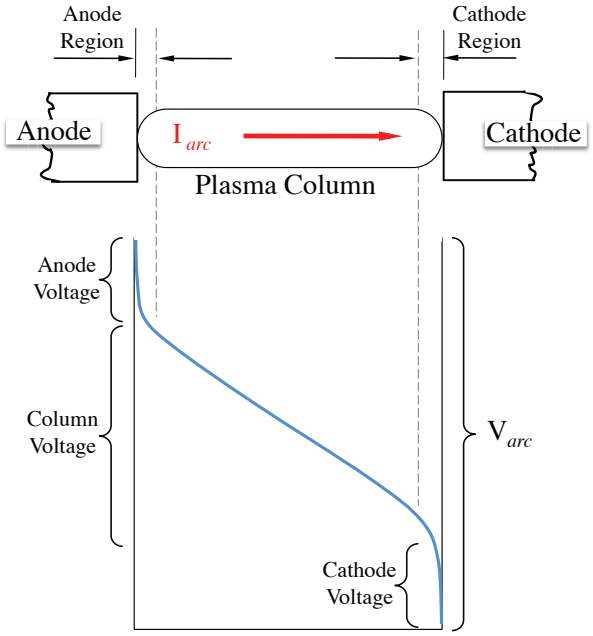

Figure 4.4: Electric Arc characterization [53].

There are of course exceptions such as high frequency induction arcs, which have no electrodes, and unipolar arcs, which possess only a single electrode. The relative importance of the three arc regions in governing the overall behaviour of the arc gap depends upon a number of factors, which include the length of the arc gap, the type of arc and the electric power dissipated in the discharge. Thus short arcs (few *mm* in length) are generally dominated by electrode effects; long arcs at high pressures and low power are governed by plasma column effects [59].

The theoretical behaviour of an arc plasma may be described by the Maxwell equations and the fluid conservation equations [60]. In cylindrical coordinates, assuming thermal equilibrium and neglecting azimuthal variations, the conservation equations for plasma arc column are:

- Mass

$$\frac{\partial \rho}{\partial t} + \frac{1}{r}\frac{\partial}{\partial r}(\rho r v) + \frac{\partial}{\partial z}(\rho u) = 0$$

- Momentum

$$\rho\left(\frac{\partial v}{\partial t} + v\frac{\partial v}{\partial r} + u\frac{\partial v}{\partial z}\right) = \rho f_r - \frac{\partial \rho}{\partial r} + \left(2\mu\frac{\partial v}{\partial r} - \frac{2}{3}\mu\Delta\right) + \frac{\partial}{\partial z}\left[\mu\left(\frac{\partial v}{\partial z} + \frac{\partial u}{\partial r}\right) + \frac{2\mu}{r}\left(\frac{\partial v}{\partial r} - \frac{v}{r}\right)\right]$$

- Energy

$$\rho\frac{\partial h}{\partial t} + \rho\left(v\frac{\partial h}{\partial r} + u\frac{\partial h}{\partial z}\right) + \rho u v\left(\frac{\partial u}{\partial r} + \frac{\partial v}{\partial z}\right) + \rho\left(v^2\frac{\partial v}{\partial r} + u^2\frac{\partial u}{\partial z}\right) + \rho v\frac{\partial v}{\partial t} - \frac{\partial p}{\partial t} = \frac{1}{r}\frac{\partial}{\partial r}\left[r(k+k_1)\frac{\partial T}{\partial r}\right] + \frac{\partial}{\partial z}\left[(k+k_1)\frac{\partial T}{\partial r}\right] + Q_R + \sigma E^2 + \chi\Delta^2 + 2\mu\sum_{\alpha,\beta} e_{\alpha\beta}^2$$

where:

$$\begin{aligned}
\Delta &= \frac{\partial v}{\partial r} + \frac{v}{r} + \frac{\partial v}{\partial z} \\
\rho\frac{\partial h}{\partial t} &= \text{thermal storage} \\
\rho\left(v\frac{\partial h}{\partial r} + u\frac{\partial h}{\partial z}\right) &= \text{entalphy convection} \\
\rho u v\left(\frac{\partial u}{\partial r} + \frac{\partial v}{\partial z}\right) + \rho\left(v^2\frac{\partial v}{\partial r} + u^2\frac{\partial u}{\partial z}\right) &= \text{flow kinetic energy} \\
\frac{1}{r}\frac{\partial}{\partial r}\left[r(k+k_1)\frac{\partial T}{\partial r}\right] + \frac{\partial}{\partial z}\left[(k+k_1)\frac{\partial T}{\partial r}\right] &= \text{thermal and turbulence conduction} \\
Q_R &= \text{radiation} \\
\chi\Delta^2 + 2\mu\sum_{\alpha,\beta} e_{\alpha\beta}^2 &= \text{viscous dissipation}
\end{aligned}$$

4.2.3 Arcing faults

In U.S.A the electrical system is composed by five principal elements, Generation Stations, Bulk Transmission, Subtransmition, Primary Distribution, and Secondary Distribution, as shown in Figure 4.5.

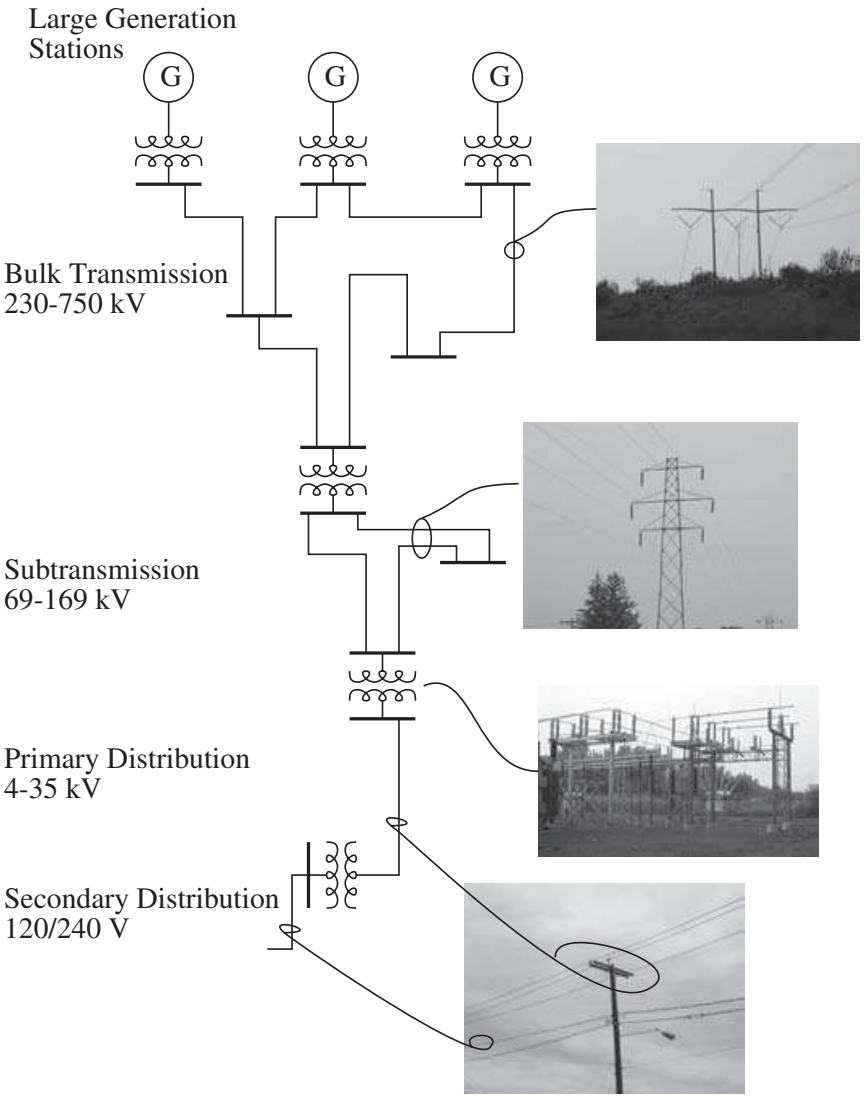

Figure 4.5: Basic components of an U. S. electrical system [61].

The consequences caused by electrical faults strongly depend on the magnitude of the fault current, which in turn depends on the type of fault, the location of the fault, the system earthing, the source impedance, and the impedance of the fault [59], [60]. In most cases, electrical faults can

cause damage or potential hazard to humans and property. The duration of the fault is also of considerable importance when estimating the consequences of a fault.

One way to characterize the types of faults is to describe them as parallel (shunt) or series faults. Parallel faults are faults in which one or more of the phases are short-circuited (possibly to earth). Parallel faults are in general more severe than series faults, which could be described as an interruption in one or more of the phases.

4.2.4 Parallel arcing

Parallel Arcing is a fault that is characterized by the ow of current between two or more phases or between phase(s) and earth at the frequency of the associated power system. It is important to realize that fault currents are mainly of power frequency character but that they also can contain high frequency components. Such high-frequency components can consist of the discharge current of a capacitor bank or stray capacitances in cables and bushings. The different types of parallel faults are illustrated in Figure 4.6.

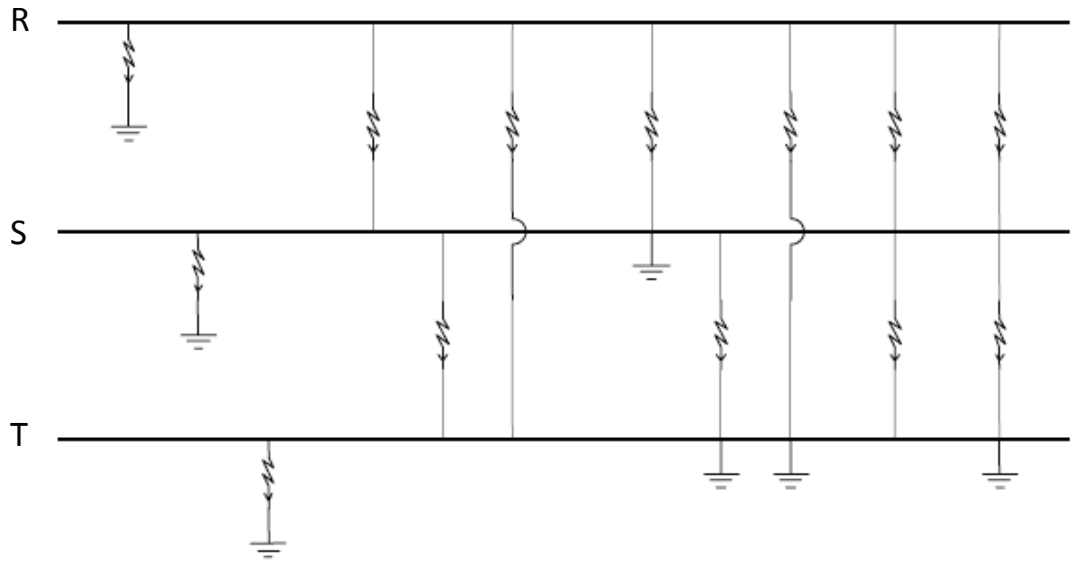

Figure 4.6: Types of parallel faults.

Fault currents due to parallel faults depend on the system impedance as seen from the fault location, and of the fault impedance. In general, fault currents are much larger than load currents. However, the magnitude of single-phase fault currents is largely dependent on the

system grounding and can be large in magnitude (of the same order as three-phase fault currents in solidly grounded systems) or small (a few Amperes in high-impedance grounded systems).

4.2.5 Serial arcing

Serial Arcing is defined as a fault for which the impedances of each of the three phases are not equal, usually caused by the interruption of one or two phases. Series faults give rise to fault currents proportional to the load currents. Series faults can be due to a broken conductor, a fuse operation in one or two phases, a circuit breaker malfunction in one or several phases, or a loosen connection between components over the same line.

Arcing faults can be easily represented in a single conductor circuits. Most of literature review, presents three types of arc faults: series; line-to-line (neutral); line-to-ground. The series arc depicted in Figure 4.7.(a) occurs in a single conductor. Examples might be a frayed conductor in a cord that has pulled apart or a loose connection to a receptacle or in a splice. A series arc is load limited, such that arc current cannot be greater than the load the conductor serves. The line-to-ground arc depicted in Figure 4.7.(b) can occur only when a ground path is present. For example, it will not occur in a two-wire appliance or extension cord or within an ungrounded appliance. However, when there is a grounded conductor or enclosure present, other types of arc faults will frequently also include a line-to-ground fault. The line-to-line arc depicted in Figure 4.7.(c) is a short circuit. Examples might be wire insulation cut by a staple or a cord cut by a metal table placed on it. However the las two are considered as parallel faults. More details can be found in [62].

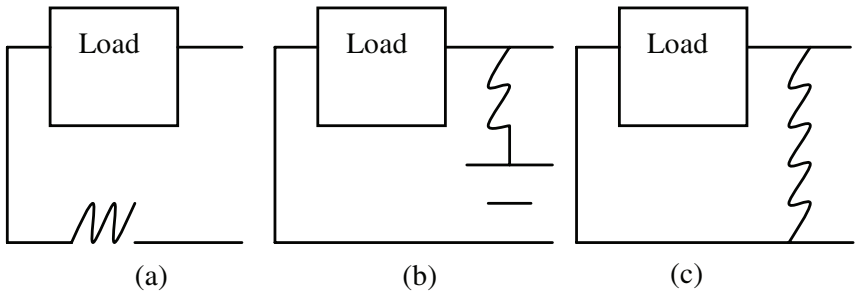

Figure 4.7: Types of arcing faults in single conductor circuits.

4.3 Effects of Arcing Faults

Generally, effects of faults can be classified into two big groups. The first one, includes all about the initiation of the fault (e.g. insulation breakdown, aged process, chemical reactions), and the second one, which is dependent on the duration of the fault. The initiation of the fault cannot be reduced by faster fault detection whereas the part dependent on the duration of the fault can.

4.3.1 Mechanical forces

According to Christopoulos [63], for parallell conductors in a single-phase or a three-phase system, the maximal force imposed on one of the conductors can be calculated by using the next equation:

$$F_{max} = \frac{2\,k\,k_r\,i_s^2}{d}$$

where F_{max} is the largest force imposed on the conductors, i_s is the peak current (in kA), d is the distance between neighboring conductors (in cm), and k and k_r are constants. Since k, k_r , and d are design parameters, it can be concluded that for a given power system component, the maximal force imposed upon it is proportional to the square of the peak-current. Thus, when a short-circuit current is carried by the phase conductors, there will be a mechanical force upon them and that force will grow rapidly with increasing short-circuit currents since it depends on the square of the current. Therefore, the largest mechanical force imposed on the power system components is caused by the largest peak current.

4.3.2 Thermal stress

The heat losses in any electrical conductor can be calculated by:

$$P = R\,I^2$$

where, P denotes the heat losses for a conductor caused by the current I (rms value), when passing through the resistance R. Depending on the size and material of the conductor, the heating will eventually lead to meltdown and destruction of the conductor. If the fault current is lower than the rated value, the time before meltdown occurs is increased.

4.3.3 System integrity

A short-circuit normally gives rise to high fault currents in the faulted current path and consequences associated therewith. At the same time, the voltage will drop, giving rise to a voltage dip that can be noted throughout large parts of the power system and disturb sensitive processes. Transient stability conditions is generally not considered for distribution systems. However, the increasing amount of distributed generation, might lead to such considerations even for distribution systems.

4.4 Experimental Setup for FDD Study in Arcing

The schematic of the configuration of the computer-based data acquisition system for experimental study of FDD in arcing is shown in Figure 4.8. The computer-based data acquisition system connects hardware and software to capture the sensory information of the system and experimental setup. This integrated system performs the task of real-time data acquisition and monitoring of sensory devices of the system, as well as post-process data analysis.

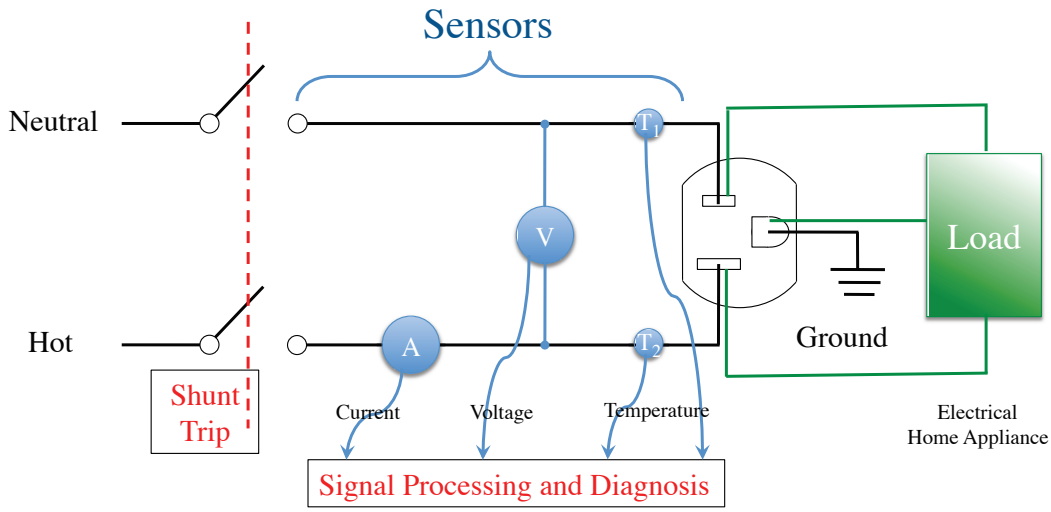

Figure 4.8: Schematic setup of the electrical system for experiments

4.4.1 Electrical setup

The experimental setup is established and shown by the photos in Figure 4.9, corresponding to the schematic in Figure 4.8.

Figure 4.9: A photo of the layout of the experimental setup

The National Electric Code (ANSI/NFPA 70) is a standard in the United States for the safe installation of electrical wire and equipment. Under this code, the electrical power is composed of (i) A circuit breaker box (Rock Solid Load Center) rated 100 amperes maximum, (ii) 12 plug-in circuit breakers type BR rated 15 amperes maximum, (iii) solid copper wire conductor 14 AWG Romex Type NM-B (nonmetallic-sheathed cable) rated 600 volts, manufactured as 2 conductor cable with a ground wire, the conductor insulation is 90°C rated made of polyvinyl chloride (PVC), nylon jacketed, and (iv) the service points, are represented by residential grade straight blade grounded receptacle, duplex type 15 amperes rated. Home electrical appliances are using to represent the load of the system. An electrical oven (1200 watts), a single ranger plate (800 watts), a water heater (1000 watts) and a halogen lamp (250 watts) are employed to perform the experiments. An electric fault can be located in the appliance, over the wires, in a receptacle or in a connection point. During normal operation a nominal value of 120 AC voltage remains constant, and the power consumption depends on the load used in the system. On the other hand, if there is an electrical failure, part of the energy supplied by the distribution system will be transformed principally into heat that can cause a hazard condition. To simulate a failure in our system, a micro-positioner device has been adapted. The micropositioner device holds one of

the systems wires and can move back and forward to simulate a loosen connection between wire and receptacle. Sensory information is obtained and recorded using the host computer during the experiments.

4.4.2 Creation of arcing fault

Whenever a fault diagnosis and detection system is created, simulation of the fault is critical to ensure that the system meet the criteria and the objective proposed. No FDD system will be adopted without extensive simulation studies about the fault of interests. As defined previously, fault diagnosis deals with the determination of the kind, size, location and time of detection of a fault; therefore, the change in the signal of reference when a fault is in progress must be required. In this research, we are concerned about a specific fault called *arcing*.

An arcing fault is an unintended arc created by current flowing through an unplanned path [45]. Arcing creates high intensity heating at the point of the arc, resulting in burning particles that may over time ignite surrounding material [51]. During the experiments, the connection between the white wire (neutral) connector and the receptacle is abruptly interrupted while the black wire (hot) and grounded (bare or green) connectors remains attached to their required points as demanded in NEC (section 250-50b). The physical interruption of the connection is achieved by using a micro positional system . The micro positional system is a platform formed by three stepping pulse motors model DSI-200-1, and is shown in Figure 4.10. The planar displacement is controlled by two of the motors meanwhile a rotational displacement over one of the planar axes can be performed by the third one.

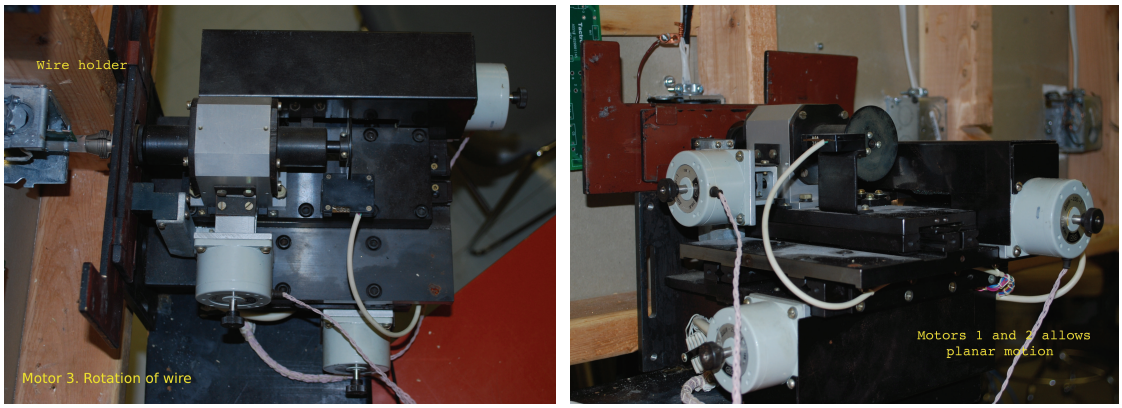

Figure 4.10: A photo of the platform used to move the wire.

4.4.3 Real-time data acquisition system

A data acquisition (DAQ) system, built around the power and flexibility of a PC, consists of a wide variety of diverse hardware and equipment, from different manufacturers. The basic elements of a DAQ system are: Sensors and transducers, field wiring, signal condition, data acquisition hardware, operating system (PC) and data acquisition software. Each element of a DAQ system is important for accurate measurement and collection of data from the process or physical phenomena being monitored.

The components are described as follows: (i) Transducers and sensors are devices capable of converting a physical phenomenon into electrical signals that the signal conditioning and/or data acquisition unit can accept. In this experimental setup, current, voltage, temperature, audio, light and electromagnetic field sensors are used. Three different current sensors (Hall effect type) are using to obtain the current flowing through the system during the test. A small resistor value is used to mirror the instantaneous voltage. Photodiodes located near to the failure point are used to detect sparks when the intermittent connection is taking place. A small diameter loop antenna is also used to measure changes in the electromagnetic field due to the abrupt current variation. A small microphone (electret type) can register some acoustic variations near to the vicinities of the electrical failure. (ii) Field wiring represent the physical connection from the transducer and sensors to the signal condition and/or data acquisition software. To reduce the effect of noise during the test, 3-conductor wire, 22 AWG (0.32 mm2) shielded communication and instrumentation cable is used. (iii) Signal condition is the stage in which sensors and transducers can communicate with the DAQ hardware. Most of the task performed by signal condition includes: filtering, amplification, linearization, isolation or excitation. Most of the sensor used in this research requires external excitation; therefore, the signals are conditioned with electronic circuits before they are sent to the DAQ board for sampling. (iv) Data acquisition hardware can be defined as the component of the complete data acquisition and control system. A DAQ system can perform several functions and is selected according to the need. Some of the functions of a typical DAQ may include: processing and conversion of analog inputs to digital format measured from a system, processing of digitals inputs which contain information from a system, analog output to be use for the control option, digital output , timing input or output (frequency ,counters or pulsing generation). In this experiment, a national instruments PCI-6143 data acquisition board is used for data sampling. The NI-PCI-6143 has 8 channels for analog data input when connected in ref-

erenced/no referenced single ended or in differential mode. This board has a sample rate of 250 KS/s by channel and a resolution of 16 bits. Furthermore, it can perform simultaneous sampling tasks. In addition, the DAQ has 8 digital I/O and 2 on board timer and counter, which are not used and will not be discussed here.

The acquired data are sent to the host computer for processing. The computer can also provide system clock. The interface between DAQ board and the computer is offered by the data acquisition software. In this experimental setup, the LabView signal express is used in conjunction with a windows PC platform. The component in a data acquisition system, along with their relationship, are shown in Figure 4.11

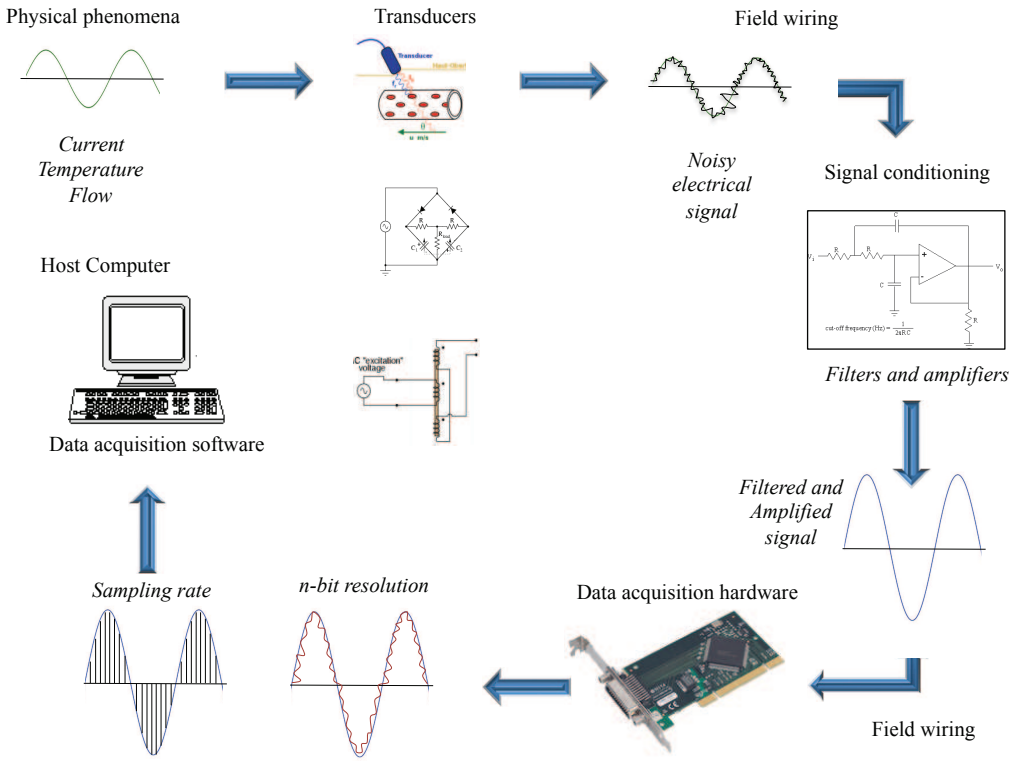

Figure 4.11: Functional diagrama of a PC-base data acquisition system

4.4.4 Sampling and data storage

Sampling rate is the rate at which data is sampled. Sampling rate is not directly related to the bandwidth specifications of a high-speed digitizer. Sampling rate is the speed at which the digitizers ADC converts the input signal, after the signal has passed through the analog input

path to digital values. Hence, the digitizer samples the signal after any attenuation, gain, and/or filtering has been applied by the analog input path, and converts the resulting waveform to digital representation. There are several products available in the market and the choice of the most appropriate device for any application will depend on the signal of interest. PCI-6143 DAQ board has a 16-bit resolution and up to 250 kS/s per channel sampling capabilities. The sampling rate of a high-speed digitizer is based on the sample clock that controls when the ADC converts the instantaneous analog voltage to digital values. The higher sampling rate results in more sampling points as noted in Figure 4.12.

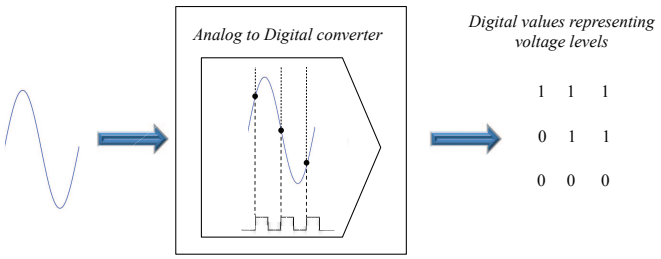

Figure 4.12: Sampling of a Sine wave using a 3 bit digitizer.

DAQ hardware can be divided into two main categories based on signal sampling method: scanning hardware and simultaneous sample and hold (SSH) hardware. Scanning hardware samples input signals sequentially. SSH hardware samples input signals simultaneously. PCI-6143 is a SHH hardware with multi-ADC architecture which delivers higher sample rates per channel, better dynamic accuracy, and less complexity. This architecture does not require a multiplexer to route all incoming signal [64]. Sample rate used in the experiment has been setting on 250kHz. In a DAQ system the buffer size must be consider any time. Record length refers to the amount of memory dedicated to storing digitized samples for post processing or display for a single acquisition. In a digitizer, record length limits the maximum duration of a single-shot acquisition. In the present experimental setup, with a 25,000-sample record and a sample rate of 250 kHz, the duration of the acquisition is 100 ms (the number of points multiplied by the acquisition time per sample, or 25,000 x 4μs). LabView signal express is used as a DAQ software, with which we can control the executing time, synchronize signal and external conditions to capture data. National Instruments LabVIEW SignalExpress is interactive measurement software for quickly acquiring, analyzing, and presenting data from hundreds of data acquisition devices and instruments, with

no programming required. During the experiments data obtained for a duration of 3 seconds at each sampling rate will be saved to hard disk. Data information will be saved in the LabView native format (data logging) as well as exported to an ASCII format or text format. During the post-processing stage MATLAB will be used.

Home appliances are used to represent the load in the electrical system under consideration. While in use, the connection is interrupted by using the micro positional system. Sensors are located in the system to measure changes in signals during the test. The sampled data are saved in files with identification based on the following name convention. For example, a typical file name can be VO1S06CT03T15AROL. The identification convention is describe as follows:

- "VO1" means voltage sensor number 1
- "S06C" means identification of the receptacle used
- "T03" means the amount of tests (experiments) perform over the receptacle
- "T15" represents the amount of tries achieved during the same test
- "AR" means test perform under arcing fault
- "O" represent the type of load used, in this case the electric oven
- "L" means the external condition when the test was performed

A detailed combination and possibilities of file identification can be found in the Appendix A. Data of the system under failure condition with different sensory information are sampled and saved. The saved files will be used in later chapters for data analysis.

4.5 Modeling of Arcing Fault

The physics of arc phenomena is complex, and the physical constants are particularly hard to clearly define for real world arcing faults in electrical systems. Most of the knowledge has been largely developed based on the observation and analysis of electrical measurements. The volt−ampere ($V-I$) characteristics are fundamentals to understand the arcing fault. According to Ammerman, early researchers often failed to specify test conditions, the configuration type, and if AC or DC arcs had been initiated. Since the $V-I$ characteristic is dependent on test conditions, it can be difficult to assess the early published work for accuracy and coherence [65].

An arcing fault is a short circuit formed by a hot gaseous conducting medium with a low nonlinear resistance, roughly inversely proportional to the instantaneous value of the current. Its inductance is negligible, so that the voltage drop in an AC arc can be considered in phase with the current and its waveform will be generally flattened. A fault arc develops in a random fashion, depending on various factors with the result that, in general, it is difficult to evaluate its key parameters. Furthermore, most of the studies have been performed in lab environment in a form that is not easily applicable to real systems.

In Low Voltage (LV) systems (< 300 V) , the arc resistance is relatively high compared to the total circuit impedance. Consequently, the arc current is lower than the short-circuit current and its shape is somewhat deformed, notably near zero crossings. For this reason, the development of an LV fault is sometimes intermittent, in other words, short periods of arcing alternating with shorter or longer periods without any arcs (without fault current) as shown in Figure 4.13.

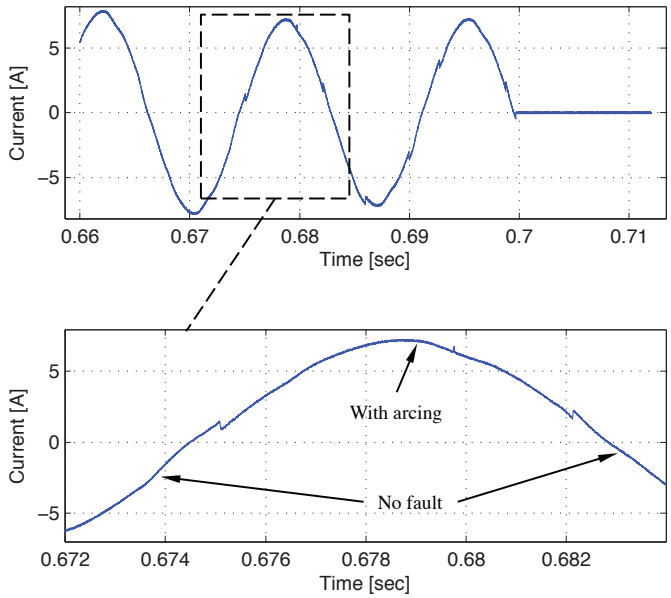

Figure 4.13: Current waveform from an electrical load. Intermitted arcing can be present in less than one cycle.

Serial arcing fault is particularly dangerous because conventional overcurrent protection systems may take a long time, or even prove unable, to detect it so that a large amount of energy is released. It is almost impossible to determine the parameters of an intermittent fault because of its highly random development [66]. Electrical companies at present continue developing the AFCI techniques to improve arcing fault detection to a certain extent, however the huge challenge for

detecting series arcing faults is the difficulty in reliable discrimination between undesired series arcs and normal arcs that is designed or occurs in distribution equipment, and the arcing-like load current may also contain the features mentioned in previous paragraphs.

It is extremely difficult to accurately simulate a complete arc circumstance due to its irregularity. The arc behavior changes from one half-cycle (power frequency) to the other as revealed by the experimental arc characteristics shown in Figure 4.14. This constitutes one cycle specific to an arc and it is characterized by unsymmetrical half-cycles. So, the arc model parameters extracted using the positive half-cycle are inappropriate for the others. Additionally, the self extinguished probability increases the complexity for modeling.

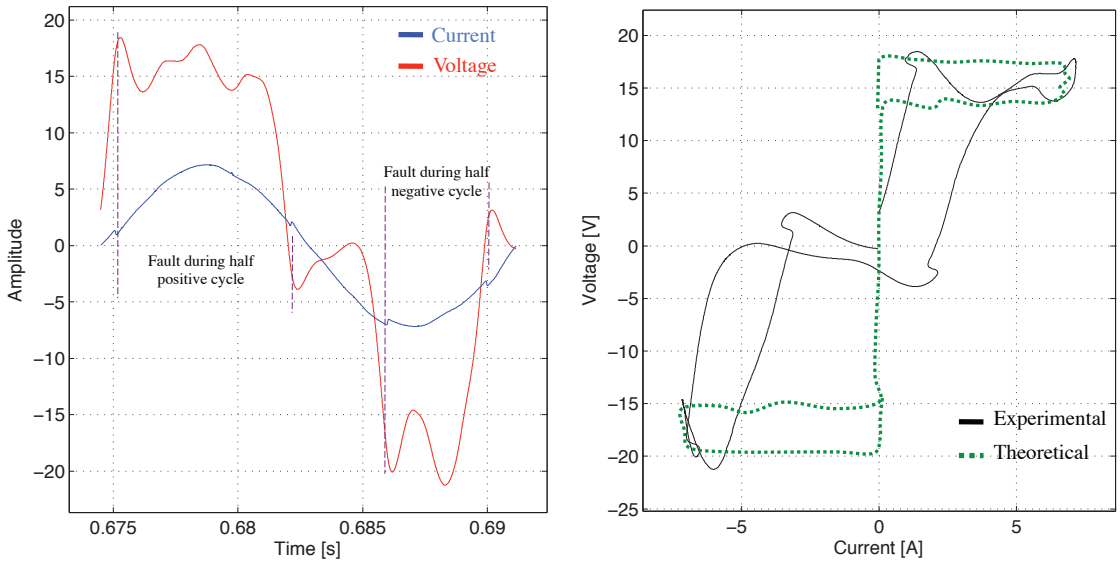

(a) Current and voltage waveforms

(b) Arc dynamic *V-I* characteristic

Figure 4.14: Electric characteristics during a serial arcing fault.

As we can observe in Figure 4.14 (b), the theoretical $V-I$ characteristic (shown in green) has been mentioned as a cyclogram in previous work, specially for High Voltage and Parallel Arcing since 1950's [67]. However, in real cases and for Low Voltage systems, intermittent arc is more likelihood rather than a complete cycle of an arcing fault situation.

Series arcing faults are in series with the load, which means that the fault current is the same as the input and load current, therefore:

$$i_{arc} = i_{sys} = i_{load}$$

for this reason, conventional protective devices are not suitable to detect serial arcing since its magnitude is less than that of normal operating current of the system being protected, in other words:

$$i_{arc} = \frac{V_{sys} - V_{arc}}{Z_{sys}} < i_{load}$$

There are various concepts for arc modeling. Most of them are based on thermal equilibrium and have the longest history since Cassie and Mayr models [68]. Cassie model has been used in the case of high current arcing fault, original stated as:

$$\frac{1}{R} \cdot \frac{dR}{dt} = \frac{1}{\tau}\left(1 - \frac{V^2}{E_0^2}\right)$$

It can be shown that the original Cassie equation can be transformed to

$$G = \frac{V \cdot I}{P_0^2} - \tau \cdot \frac{dG}{dt} \tag{4.1}$$

Mayr developed a model based in Cassie equation. In the steady state condition, when currents and voltage are changing very slowly, this Mayr's model has a better representation when low current range are considered. The Mayr equation is:

$$\frac{1}{R} \cdot \frac{dR}{dt} = \frac{1}{\tau}\left(1 - \frac{V \cdot I}{P_0}\right)$$

similarly as an equation 4.1, using the dynamical of arc conductivity, the Mayr's equation ca be rewrite by:

$$\frac{1}{G} \cdot \frac{dG}{dt} = \frac{1}{\tau}\left(\frac{V \cdot I}{P_0} - 1\right) \tag{4.2}$$

where: V and I are the instant values of the arc voltage and current, G is the dynamic conductance of the electric arc column, P_0 is the dissipate power at current crossing by zero, E_0 is the constant steady-state arc voltage and τ is the time constant of the electric arc, which is defined by:

$$\tau = \frac{dG}{dt} \cdot \frac{G}{P}$$

here P represents the dissipate power by the column arc to the environment.

4.6 Fingerprint analysis

In this dissertation, wavelet transform is used in feature extraction. A survey review of wavelet transform concepts can be found in Appendix C. The principal characteristics of wavelet can be reduce to two fundamental concepts: (1) The wavelet decomposition coefficients include all information in the original signal, and (2) the large-scale and the fine scale information in the original signal is separated into the wavelet detail and approximation coefficients. In this dissertation, sensor information were segmented and 10 different wavelets are selected to perform the wavelet transform. The signal was decomposed up to six levels. Figures 4.15 and 4.16 shows an example of that differences.

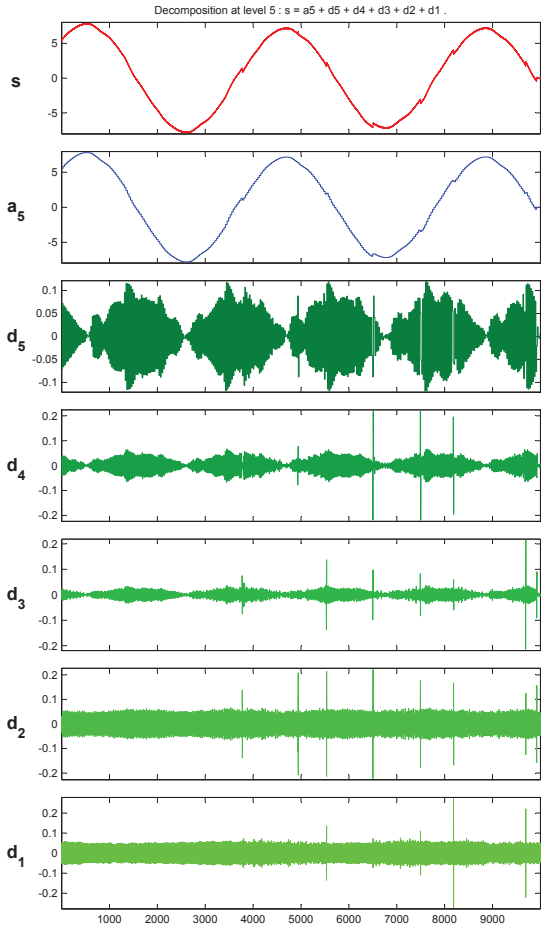

Figure 4.15: Wavelet decomposition scheme using Daub5Coeffs.

Current and voltage signals were subjected to wavelet analysis. The essence of this processing is that any signal is investigated at each point with the help of the function called mother wavelet. The result of the wavelet analysis is the time spectrum, which represents the power corresponding to the breaking contact effect with duration t. According to the figures, **s** represents the segmented original signal, $\mathbf{a}_5$ and $\mathbf{a}_6$ are the wavelet approximation (reconstruction) which in both cases are a good one; however, the selected wavelet function as well as the respective decomposition in Figure 4.15 can not be used due to the excess of information on each stage. On the other hand Figure 4.16 shows more details of the arcing signature, creating a well identified feature when arcing is presented in the signal.

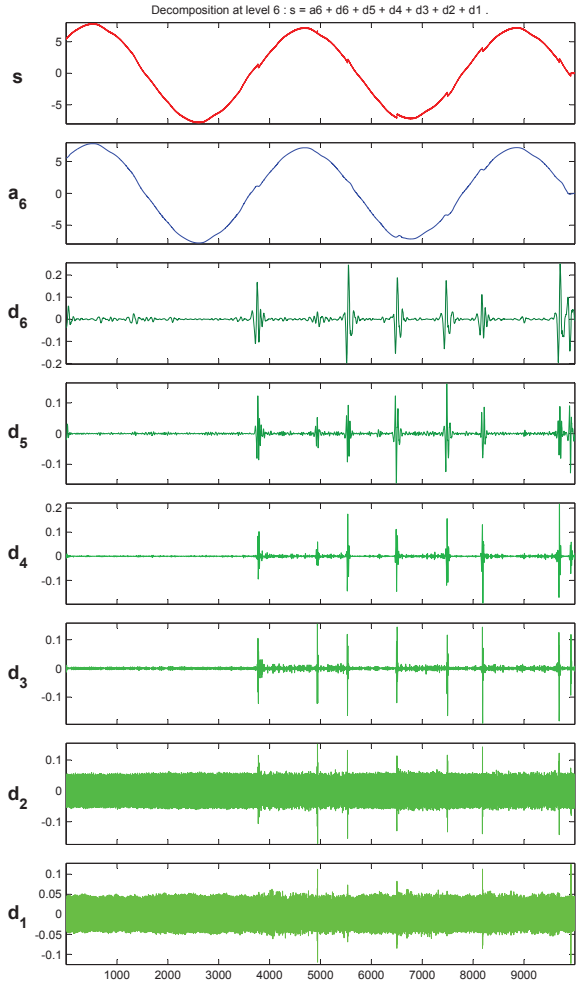

Figure 4.16: Wavelet decomposition scheme using Daub6Coeffs.

Each combination of a wavelet transform, a signal, a part selected from a signal, and a statistical property defines a possible feature as showing in figure 4.17. After comparing more than 1000 of segmented data and apply the respective decompositions, for this particular application of serial arcing the Daubechies mother wavelet 6 (db6) with six levels of decomposition (D6 and D5) are the most suitable. We have chosen " db6 " as our mother wavelet, because it is a popular basis wavelet and is compactly supported and orthogonal . It can give good mapping of the input waveform for our application.

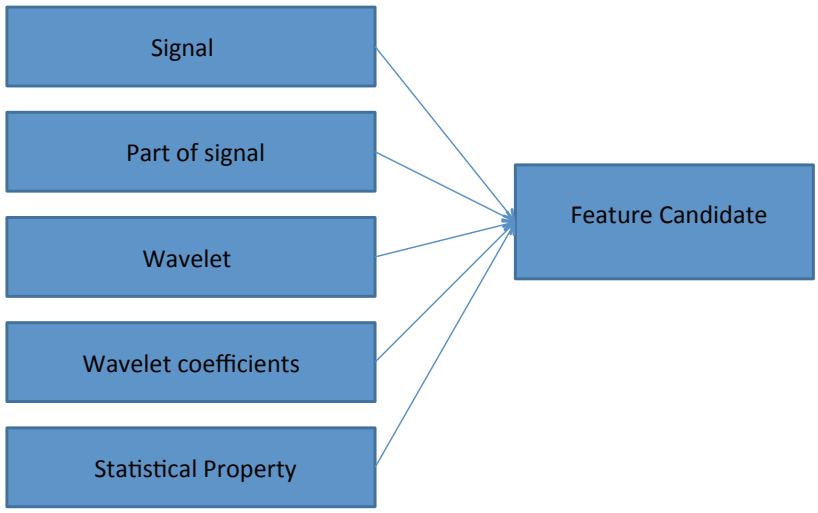

Figure 4.17: Candidate feature generation

The choice of mother wavelet is an issue that may affect the feature selection. One of the advantages of wavelet transform is that it is adaptive, i.e., we can select a mother wavelet that can best approximate the input waveform. We experimented with a number of mother wavelets, e.g., db2, morlet, Haar, etc. and observed how the arcing feature differs for different wavelets for a particular point of fault initiation. In any case, we can empirically determine the best basis wavelet, which can give the best resolution for the set of selected data. The option of choosing an appropriate basis function involves some extra work, but it needs to be done only once for each test. Among the mother wavelets we have examined, orthogonal wavelets with compact support usually give very good mean square error since they closely match the supply current waveform.

4.7 Summary

In this chapter, some arcing models were presented. Through experiments, we found that the complexity of serial arcing is a non-linear system time dependent. Further studies are required in order to create a model which consider the variations of the parameter described. We have demonstrated that multiresolution analysis of the waveform using the wavelet transform can be effective for fault detection. During this random phenomena, the optimal set of mother wavelets is necessary to make the testing process more accurate.

Chapter 5

EXPERIMENTAL STUDY OF FDD FOR A SIMULATED POWER GRID DELIVERED SYSTEM

5.1 Introduction

In an electric system distribution, electrical faults create voltage sags and in some cases force interruptions. Total elimination of a fault is impossible, however, a proper practice of maintenance and control is required to reduce the impact of the damages over the system. According to the IEEE, a fault is physical condition that causes a device, a component, or an element to fail to perform in a required manner; for example, a short circuit or a broken wire. A fault almost always involves a short circuit between energized phase conductors or between a phase and ground [67]. Distribution faults occur on one phase, on two phases, or on all three phases. Single-phase faults are the most common. Almost 80% of the faults measured involved only one phase either in contact with the neutral or with ground [69]. Based on those informations, most faults are single phase because most of the overall length of distribution lines is single phase, so any fault on single-phase sections would only involve one phase.

5.2 Description of the Simulated Power Grid Delivered System

Ground fault protection devices fall into one of two categories, personnel protection and equipment protection. The personnel protection devices do protect equipment to an extent and the equipment protection devices do protect personal to an extent. Since 1920, circuits breaker appears as an equipment protection devices. However, fault location is an important topic of research, particularly in transmission lines because in practice it is often not possible to provide all of the data necessary for exact determination of the fault location. According to Christopoulos [63] several locations methods (algorithms) have already been proposed and utilized.

Fault location algorithms can be classified in two categories. The first category is founded on the data from only one terminal of a transmission line. The second one includes the data measured at both terminals of a transmission line, but in some cases is not an option due to the long-distance data transfer required. Most of these methods are developed for the transmission lines with power sources at both terminals. Using two power sources, generates a fault current from one of the terminals that is unknown, but contributes to the fault current through the fault place. In order to overcome this situation, some researches creates approximations and assumptions which may include the impedance value of the opposite side of the line or phase difference between line extremes. However, those considerations depending on the characteristic of the power network connected to the line.

The present experiment is focused on a single phase-to-ground, a type of fault that is the same observed over 90% of all transmission line faults . For a single phase-to-ground occurring anywhere along the line, the electrical circuits established during the fault can be presented as in Figure5.1

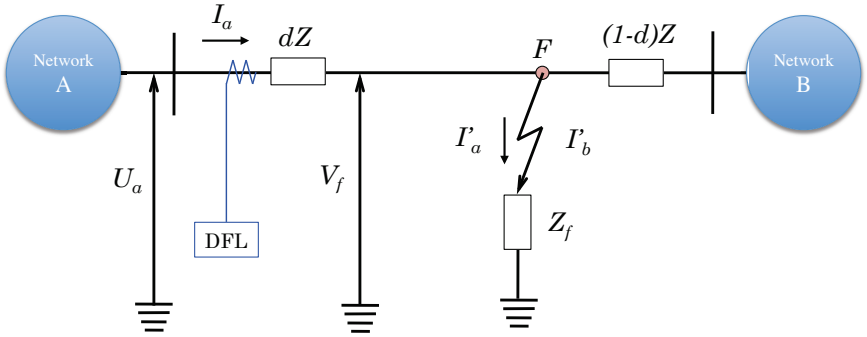

Figure 5.1: Faulted power system

On the basis of the quantities measurable on the left line terminal (voltage U_a and current I_a), it is necessary to determine the fault point F or in other words to find out the distance to the fault point (d). If we assume for a moment that the fault impedance Z_f is negligible, the line impedance to the fault point dZ will be very easy to determine. As this impedance is proportional to the distance d, the determination of the fault position will be also easy. But fault impedance is not negligible,therefore at the fault place a potential V_f appears with a value proportional to the total fault current $(I_a + I_b)$ for a certain value of the impedance Z_f. Since the fault current from the opposite end of the line I_b contributes to the creation of this potential, the sensor (DFL)

sees an apparent impedance that is somewhat larger than the real impedance ($dZ + Z_f$). This increment introduces a deviation in the measurement data (U_a and I_a) that we will use for the fault distance determination.

Consequently, for a more accurate estimation of the fault location, it is necessary to eliminate the influence of the unknown (not available by measurement) quantities on the data obtained by measurement. In the circuit shown in Figure5.1, the fault impedance represents only one part of the loop impedance measured at the selected location (DFL), or in the local station. However, in practice, this is an equivalent impedance of a very complex and spontaneously formed electrical circuit. Because of that, it is certain that more information about the fault impedance can be obtained only through a detailed investigation of this circuit.

Our simulated power grid consider only one network service at one extreme of the service line, the other extreme will be the user side. The network service is represented by a variable transformer which can delivered a controllable voltage from 0 to of 10 volts without compromise the integrity of the system itself.

5.2.1 Experimental Setup

The fault generation is performed in an electrical home system with no electric load. This fault was created by making direct contact between ground and hot line. Two sensing points (A and B) where established in order to measure the voltage between lines at different locations. Three contact points where selected over the hot line, labeled X_1, X_2 and X_3 all of them located between points A and B as shown in Figure 5.2.

70 meters of copper wire were used between points A and B, from which 60 meters were wrapped around a PVC plastic tube of 11.5 mm of diameter, forming an air core solenoid of 185 turns. The wire is a thermoplastic insulated, soft-drawn copper conductor with a Nylon jacket that is high heat-resistant and rated 90°C in dry and wet locations (THHN type). The specifications of the wire are shown in Table 5.1. Voltage across the points were digital recorded in a DAQ system at a sample rate of 250 kHz in order to perform data analysis.

5.3 Experimental Results

The nonlinear variations of the fault causes the voltage and current waveform distortion, distorting it into a near square wave with fault voltage amplitude V_f, what is given in Figure 5.3. it

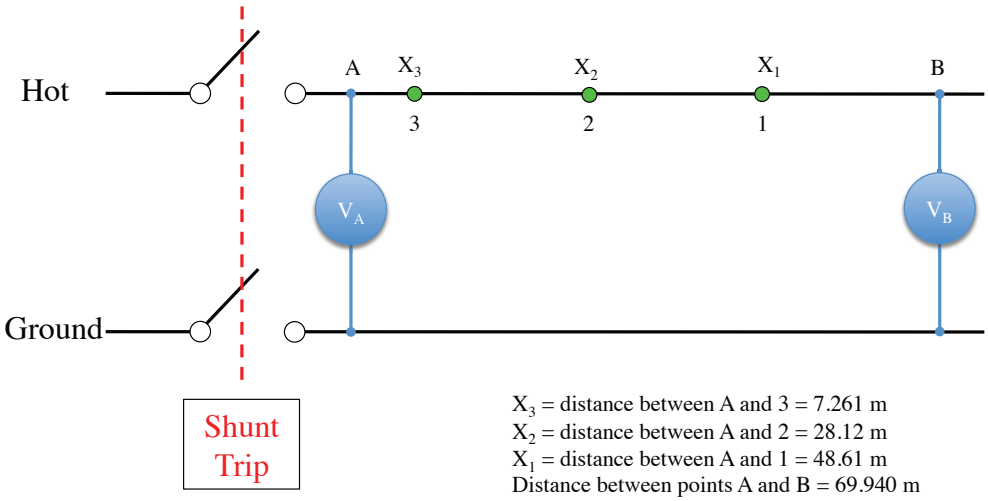

Figure 5.2: Setup used to record data sensor from ground fault in an AC system

Property	**Value**	**Units**
Material	Copper	Type T90
Size	12 AWG	Solid
Cross Sect. Area	3.31	mm^2
Nylon Jacket Thicness	0.100	mm
PVC Insulation Thickness	0.015	mm
Outside Diameter	3.017	mm
Allowable Ampacity	20	Amps
Resistivity	5.21	Ω/Km

Table 5.1: Technical specifications of a 12 AWG copper wire. Source EncoreWire Corp.

is obvious that the voltage sensed after this fault is equal to zero due to the system protection. The breaker (or fuse) had been trip off and there is no current flowing through the lines. Consequently, no relevant information can be extracted in order to calculate the estimate distance where the fault is taken place. If any power system reach this stage, the system is classified as out of service and a fault location is not possible to establish accurately.

To overcome this situation, we must guarantee a continuous operation of the system during the fault. After severals adjustments to our system, the simulated grid was stabilized and typical fault characteristics were achieved. Our main goal is to formulate a better Fault Detection algorithm, reducing the error founded in current models. The magnitude of fault current is limited

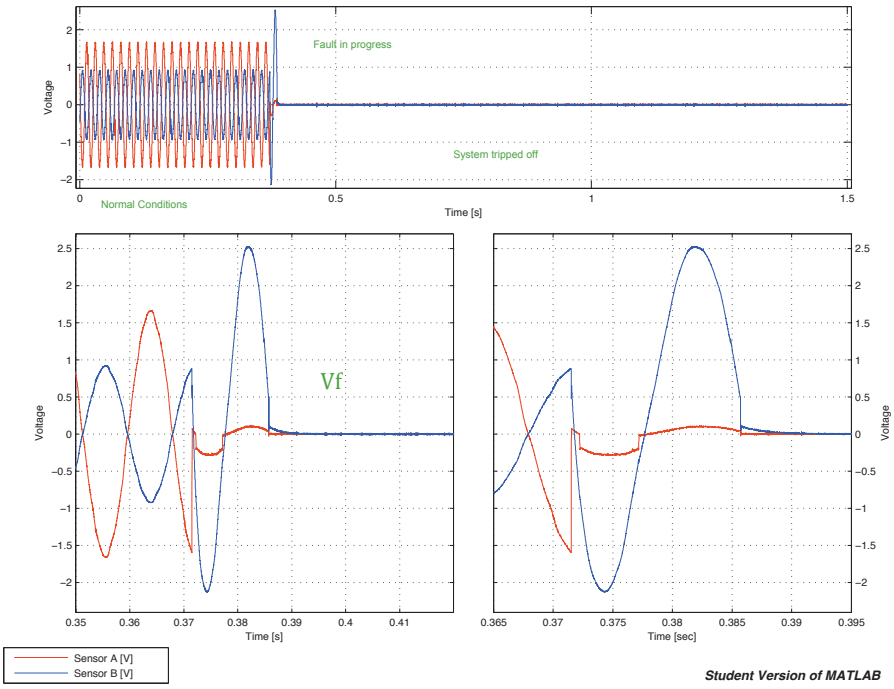

Figure 5.3: Voltage waveforms from points A and B during L-G fault at location X_1

only by the system impedance and any fault impedance. The system impedance includes the impedances of wires, cables, and transformers back to the source. For faults involving ground, the impedance includes paths through the earth and through the neutral wire. The impedance of the fault depends on the type of fault.

The absolute value of impedance method uses the voltage and current information during a fault as a way to estimate the distance to the fault. In this case, Ohm's Law is used as basic equation, as shown in Figure 5.4 we can write:

$$d = \frac{V}{I \cdot Z_L} \tag{5.1}$$

expressing the distance to the fault d in terms of the voltage during the fault V, the current during the fault I an the line impedance per unit length Z_L. In the case of AC systems, complex values entered for the voltages, impedances and currents, produces a distance estimation as a complex number. Because distance is an scalar magnitude, the real component should be a realistic estimate of the distance to the fault; the imaginary component should be close to zero.

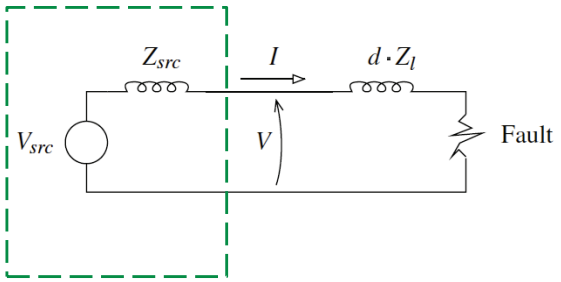

Figure 5.4: Basic schematics to calculate the fault distance in an AC circuit

This approach can be simplified using the reactance to the fault by:

$$d = \frac{\mathrm{Im}(\frac{V}{I})}{\mathrm{Im}(Z_L)} \tag{5.2}$$

Using the reactance has the advantage of avoiding the arc impedance which is mainly resistive. The Absolute Value of Impedance Method is the simplest method. This method requires only one side information, the fault resistance is neglected and absolute values of voltage and current are used. Figure 5.4 represents the schematic used in our experiments.

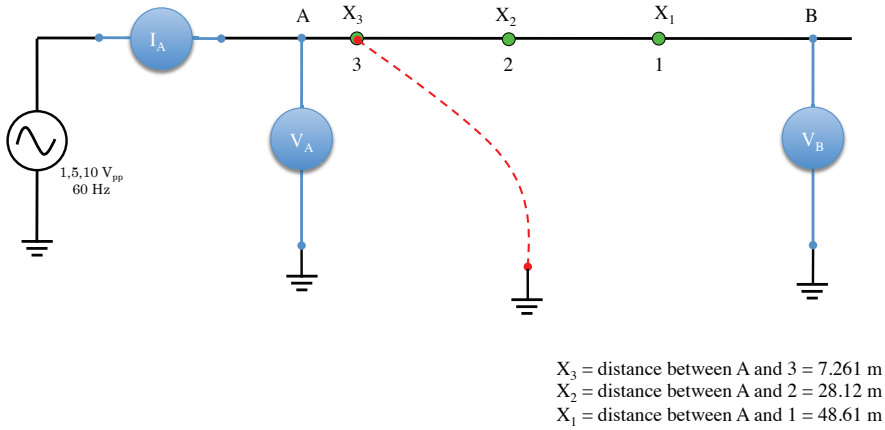

Figure 5.5: Esquematic of the simulated power grid deliver system.

The estimate fault location (calculated distance) applying Equation 5.1 and using the sensor information recorded at point A during different experiments is shown in Table 5.2. As we can observe, using this method the error increases in locations closer to the recorded point A. There is no consistency between experiments performed at the same location. For example an induced

fault at location X_1 (48.6 m) shows an error variation of 13%. Additionally, the closer location (X_3 = 7 m) presents highest deviations, which is the worse case scenario.

Actual Distance x_a [m]	**Calculated Distance** x_e [m]	**Difference** [m]	**Error** %
48.617	56.200	7.58	15.60
48.617	56.291	7.67	15.78
48.617	51.283	2.67	5.48
48617	48.704	0.09	0.18
28.121	31.347	3.23	11.47
28.121	29.278	1.16	4.11
7.261	15.024	7.76	106.91
7.261	10.301	3.04	41.87
7.261	14.879	7.62	104.92
48.617	48.800	0.18	0.38
48617	48.980	0.36	0.75
28.121	29.617	1.50	5.32
28.121	33.370	5.25	18.67
7.261	10.518	3.26	44.86
7.261	10.960	3.70	50.94
48.617	49.647	1.03	2.12
48617	50.050	1.43	2.95
28.121	36.311	8.19	29.12
28.121	29.552	1.43	5.09
7.261	10.683	3.42	47.13
7.261	11.217	3.96	54.48
7.261	12.079	4.82	66.35

Table 5.2: Fault Location and error estimation using the Absolute Value of Impedance Method

We propose a modification of the Absolute Value of Impedance Method by considering the voltage from both sides of the distribution line as well as the resistance of the fault. In order

to estimate the impedance, we include the complex components. Thus the impedance can be calculated as follows:

$$Z_l = R + j(X_L - X_C) \tag{5.3}$$

where Z_l is the complex impedance value, R is the resistance, X_L is the inductive reactance, and X_C is the capacitive reactance. For the present experiment we assume the capacitance effect as negligible. Therefore, equation (5.3) becomes:

$$Z_l = R + jX_L \tag{5.4}$$

Through this approach X_L can be calculated as follows:

$$X_L = \omega L \tag{5.5}$$

where L is the inductance, and ω is the system's frequency. These two parameters depend on the the geometry and the frequency of the source respectively. Therefore, those can be found in the following way: $\omega = 2\pi f$ here, f is frequency of the source. Likewise, the inductance L can be found with the following expression:

$$L = 0.2D\left(\ln\left(\frac{4D}{\phi_w}\right) - 0.75\right)\ [nH] \tag{5.6}$$

where D is length of the wire, and ϕ_w is the diameter of the wire. Finally, the magnitude of the impedance line is found as follows:

$$Z_l = \sqrt{R^2 + X_L^2} \tag{5.7}$$

hence, equation (5.7) can be expressed by

$$z_l = \sqrt{R_l^2 + \left(0.2\omega\left(\ln\left(\frac{4D}{\phi_w}\right) - 0.75\right)10^{-9}\right)^2} \tag{5.8}$$

Where z_l is the line impedance, and R_l is the line resistance. Therefore, the distance to the fault can by calculated by:

$$d = \frac{V_{a_{rms}} - V_{b_{rms}} - \left(\frac{V_{b_{rms}}}{R_B}\right) z_l * D}{i_{a_{rms}} * z_l - \left(\frac{V_{b_{rms}}}{R_B}\right) z_l}$$

Using different configurations at the simulated power source, and changing the physical value of the arc resistance, the modification method reduce significantly the error in the fault distance estimation as shown in Table 5.3

Location Identi.	**Actual Distance** x_a [m]	**Calculated Distance** x_e [m]	**Difference** [m]	**Error** %
X_1A Exp.1	48.62	48.93	-0.31	0.64
X_1A Exp.2	48.62	48.70	-0.08	0.17
X_1A Exp.3	48.62	48.55	0.07	0.14
X_2A Exp.1	28.12	28.14	-0.02	0.08
X_2A Exp.1	28.12	28.13	-0.01	0.03
X_2A Exp.1	28.12	28.11	0.01	0.02
X_3A Exp.1	7.26	7.23	0.03	0.47
X_3A Exp.1	7.26	7.24	0.02	0.25
X_3A Exp.1	7.26	7.21	0.05	0.64
X_1A Exp.1	52.28	52.59	-0.32	0.61
X_1A Exp.1	52.28	52.63	-0.35	0.66
X_1A Exp.1	52.28	52.62	-0.34	0.65
X_1B Exp.1	55.82	56.42	-0.60	1.07
X_1B Exp.1	55.82	56.42	-0.60	1.08
X_1B Exp.1	55.82	56.47	-0.65	1.16

Table 5.3: Fault Location and error estimation using the modified Absolute Value of Impedance Method

5.4 Discussions

Increasing the information from the system reduce significantly the error. Include the value of the impedance of the source does not improve the distance estimation it can be neglected . Using the new model, most of the experiments performed had a distance difference less than 1 meter which give us an error smaller than 2%. In low voltage cases, rms values can be used with high accuracy to perform the fault distance estimation. During the transient, the method applied can not be used. This method required a window sized data analysis. Our model includes the

value of the arc fault resistance which is the most significative effect in low voltage systems.

5.5 Summary

In this chapter, a new Fault Location Method is developed in detail. Data comparison is presented to show the capabilities of the model compare with the previous one. Arcing fault is included in the model in order to reduce the error presented in teh Absolute Value of Impedance Method.

Chapter 6

CONCLUSIONS AND FUTURE WORK

6.1 Conclusions

The monitoring of home electrical systems is very important in order to reduce the permanent hazard of fire due to a serial arcing fault. In this dissertation, straight blades receptacles were studied under arcing fault. As a result, a new model which consider the accumulative degradation of wire and receptacle was presented. This new model can help to develop a different design concept for new generations of electrical outlets.

The permanent technological evolution creates systems with higher degree of nonlinearity, or simply the system becomes more complex. In these situations the signal-based approach is usually adopted. The wavelet transform analysis is used to reduce the redundancy of the sampled signals. The success in the use of the fingerprint analysis using wavelet transform lies in the correct selection of the function used as a mother wavelet. Each application requires extensive try and error approach up to reach the desire objective. FDD using wavelet coefficients, combine with window-sized sampling analysis can be used effectively for serial arcing application in low voltage electrical systems.

Electrical fault location is a relevant matter in power grid systems. The financial cost associated with failures in the electrical delivered system is most of the time huge. Electrical distribution companies permanently try to develop new algorithms and techniques to mitigate this associated effects. During this experiments, a model used in high voltage system was evaluated for a low voltage configuration. A new model for fault location in parallel arcing was developed. Using this model, arcing fault location can be detected within a very low error margin (less than 2%).

Serial arcing fault still is a no well know phenomena. The random nature of arcing, the amount of variables related, and the lack of information available for low voltage systems applica-

tions increases the uncertainly for a practical model. A preliminary signal approach was utilized, combined most of the accepted methods. More understanding of the phenomena is required.

6.2 Future Work

Three areas of future work for the study of arcing faults in residential electric systems are: (1) Further research study on serial arcing, (2) smart devices through sensor integration, and (3) energy monitoring.

There have been several methods developed for arcing fault detection. They are based on examining different characteristics of currents and voltages in time, frequency, and time frequency domains. The time-domain methods analyze such characteristics as the ratio of zero- and positive-sequence currents, half-cycle current asymmetry, and randomness of arcing current behavior. In the frequency domain, the harmonic contents of phase currents or some coefficients measuring waveform distortion are monitored. The timefrequency methods analyze the transient behavior of arcing faults in both time and frequency domain using wavelet transforms. Artificial neural networks were also proposed to discriminate the arcing faults from the normal currents [70].

The time-domain analysis involved calculating effective (rms) values of currents and sensor values voltages over a period of a few seconds and comparing changes in those values during the staged arcing faults against the normal conditions. Figure 6.1 shows a typical signal output of the voltage sensor. An abrupt change in the voltage signal between 1.5 and 2.5 seconds can be noted when arcing appears. The signal from current sensor (rms values) is shown in Figure 6.2.

6.2.1 Sensor fusion and integration

The need for energy efficiency combined with advances in compact sensor network technologies presents an opportunity for a new type of sensor to monitor electricity usage in residential environments. The second topic regards the research investigation on serial arcing fault in electrical home systems is considering more variables involve during the fault. Fault arcs are accompanied with radiation in the form of light, sound, heat and radio waves. Arcing processes represent an essential erosion process and impurity source between surfaces in contact. Unfortunately, the identification, observation, and diagnostic of such arc events during the ongoing discharge proved to be difficult because of transient phenomena, difficult surface geometry, sev-

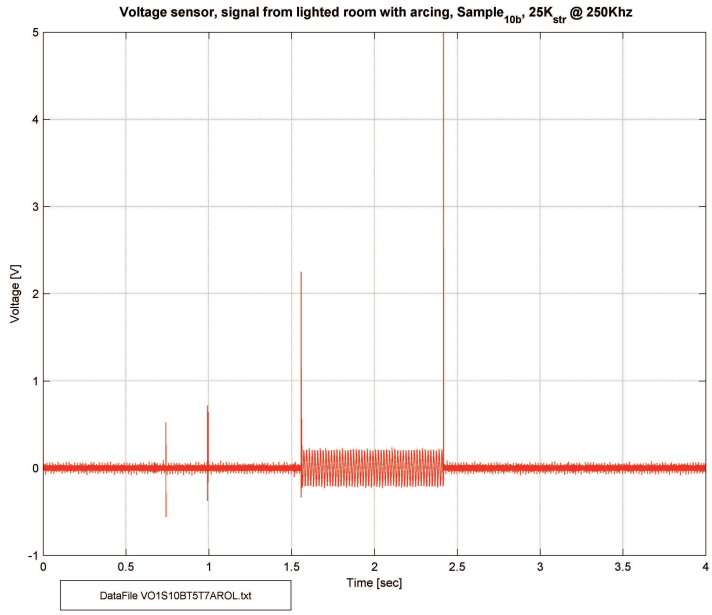

Figure 6.1: Waveform from voltage sensor, receptacle under arcing fault

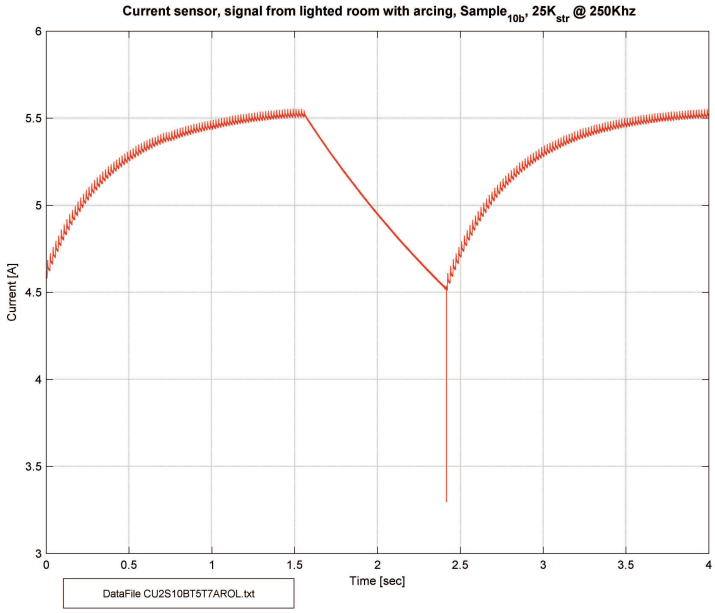

Figure 6.2: Waveform from current sensor, receptacle under arcing fault

eral contact points and numerous other effects. Various system integration can be utilized with audio sensors, light sensors, electromagnetic sensors. For example, loop antenas can be used to

detect the change in the magnetic field due to arcing of electric current. A design is shown in Figure 6.3. Table 6.1 list frequency ranges of some antenna types.

Antenna Type	**Frequency Range**
Loop	20 Hz $\sim$ 30 MHz
Vertical monopole	10 kHz $\sim$ 30 MHz
Radiation monitor probes	300 kHz $\sim$ 26 GHz
Broadband dipoler	30 MHz $\sim$ 20 MHz
Discone	1 GHz $\sim$ 10 GHz
Pyramidal horn	1 GHz $\sim$ 40 GHz
Reflector	1 GHz $\sim$ 10 GHz

Table 6.1: Antenna and probes for various frequency ranges

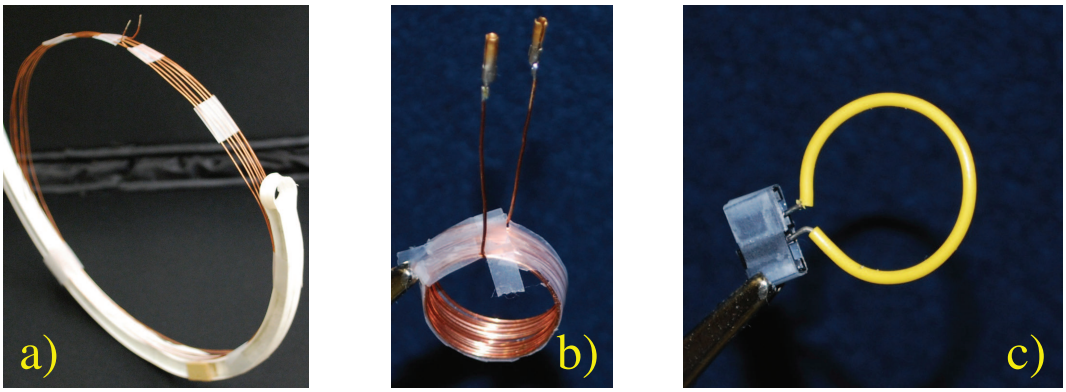

Figure 6.3: Loop antennas use for detecting variations in the electromagnetic field. a) 8 inches diameter (7 turns), b) 0.75 inches diameter (10 turns) and c) 0.75 diameter (1 turn with isolation).

6.2.2 Energy Monitoring

Energy technologies for smart homes exist, but there are still barriers. One of the most important barrier is economics. Consumers cannot be expected to invest on their own in energy monitoring and control technologies unless it delivers economic payback. Smart home technology is a complex market due to fastest change in technology. According to NEMA, some types of monitoring and control technologies that could be adopted in residences include:

- Smart utility meters which track use over time and communicate

- Wired (especially through power line) and wireless network architecture/protocols
- Personal computer/input-output device hub
- Sensors (temperature, flow, current, pressure)
- Progammable and networked cooler and heater devices.

These elements can be combined in different ways to realize systems delivering particular monitoring/control services. Implementing a sensor network to monitor energy consumption of household appliances in a meaningful way requires sophisticated network design. The challenge is how to collect necessary data and store them for producing smart advice on household energy monitoring. One practical approach is to obtain raw data from sensors installed in an intelligent outlet.

Bibliography

[1] Y. Dote, S.J. Ovaska, and X. Gao. Fault detection using rbfn- and ar-based general parameter methods. Systems, Man, and Cybernetics, 2000 IEEE International Conference on, 1:77–80, May 2001.

[2] Y. Zhao, J. Lam, and H. Gao. Fault detection for fuzzy systems with intermittent measurements. Fuzzy Systems, IEEE Transactions on, 17(2):398–410, 2009.

[3] Janos Gertler. Fault detectiona and diagnosis in engineering systems. Marcel Dekker Inc., 1998.

[4] V. Venkatasubramanian, R. Rengaswamy, K. Yin, and S.N. Kavuri. A review of process fault detection and diagnosis part i: Quantitative model-based methods. Computers and Chemical Engineering, 27(3):313–326, 2003.

[5] M Ozbek and D. Soffker. Feature-based fault detection approaches. Mechatronics, 2006 IEEE international conference on, pages 342–347, 2006.

[6] M. Bagajewicz. Process plant intrumentation: Design and upgrade. Techomic publishing company, Inc., 2001.

[7] R. Iserman. Model-based fault-detection and diagnosis status and applications. Annual reviews in controll, vol. 29:71–85, May 2005.

[8] A. S. Willsky. A survey of design methods for failure detection in dynamic systems. Automatica, 12:601–611, 1976.

[9] J. Korbicz, J.M. Kocielny, Z. Kowalczuk, and W Cholewa. Fault Diagnosis. Models, artificial intelligence, applications. Springer-Verlag, 2004.

[10] L.H. Chiang, E.L. Russel, and R.D. Braatz. Fault Detection and Diagnosis in Industrial Systems. Springer, 2001.

[11] C. Combastel, S. Gentil, and J.P. Rognon. A symbolic reasoning approach to fault detection and isolation applied to electrical machines. In Proc. IEEE Int. Conf. on Control Applications, pages 475–479, 1998.

[12] S.V. Kartalopoulos. Understanding neural networks and fuzzy logic: basic concepts and applications. Wiley-IEEE Press, 1995.

[13] L. Kanal. Patterns in pattern recognition: 1968-1974. IEEE Transactions on information theory, 20:697–722, 1974.

[14] Y.F. Chen and N.A. Warsi. A knowledge-based system for multiple pattern recognition paradigms support. In Proc. IEEE Int. Conf. on Systems, man and cybernetics, 1995. Intelligent Systems for the 21st century, pages 269–278, Vancouver,BC, Oct. 22-25 1995.

[15] A.k. Jain, R.P.W. Duin, and J. Mao. Statistical pattern recognition: A review. IEEE Transactions on pattern analysis and machine intelligence, 22(1):4–34, 2000.

[16] S. Xiaochun. Comparison of two modern pattern recognition methods. In Proc. IEEE Int. Conf. on Intelligent information hiding and multimedia signal processing, IIHMSP 2008, pages 351–353, Harbin, China, Aug. 15-17 2008.

[17] Y. Zhang, Y. Liu, X. Wang, and Z. Wang. Fault pattern recognition in power system engineering. In Int. Conf. on Industrial mechatronics and automation, ICIMA 2009, pages 109–112, Chengdu, China, May 15-16 2009.

[18] M. M. Polycarpou and A. T. Vemuri. Learning methodology for failure detection and accommodation. IEEE Control systems magazine, 15(3):16–24, 1995.

[19] M.E El-Hawary. Electric Power Applications of Fuzzy Systems. Wiley-IEEE Press, 1998.

[20] H.C. Tseng and D.W. Teo. Medical expert system with elastic fuzzy logic. In IEEE Conf. on Fuzzy systems, 1994, IEEE world congress on computational intelligence, pages 2067–2071, Orlando, US, June 26-29 1994.

[21] S. Quiang, X.Z. Gao, and X. Zhuang. State-of-the-art in soft computing-based motor fault diagnosis. In IEEE Conf. on Control Applications, CCA 2003, pages 1085–1992, Istanbul, Turkey, June 23-25 2003.

[22] C-M. Cheng and K.A. Loparo. Electric fault detection for vector-controlled induction motors using the discrete wavelet transform. In American Control conference 1998, pages 3297–3301, Philadelphia, PA, June 24-26 1998.

[23] J. Korbicz and M. Kowal. Neuro-fuzzy networks and their application to fault detection of dynamical systems. Engineering applications of artificial intelligence, 20(5):609–617, 2007.

[24] R. Javadpour and G.M Knapp. A fuzzy neural network approach to machine condition monitoring. Computer and industrial engineering, 45:323–330, 2003.

[25] C. Capria and I. Kao. Research project supplement iree: Research in intelligent fault detection and diagnosis (fdd) and fingerprint analysis for intelligent systems and international collaboration. In Conf. on International Research and Education in Engineering (IREE 2007), Lafayette, 2007.

[26] F. Gustafsson. Statistical signal processing approaches to fault detection. Annual reviews in control, 31(1):41–54, 2007.

[27] J. Cusido, A. Jornet, L. Romeral, J.A. Ortega, and A. Gacria. Wavelet and psd as a fault detection techniques. In Int. Conf. on Instrumentation and measurement technology, IMTC 2006, pages 1397–1400, Sorrento, Italy, April 24-27 2006.

[28] A. Widodo, B-S. Yang, D-S Gu, and B-K Choi. Intelligent fault diagnosis of induction motor based on transient current signal. Mechatronics, 19(5):680–689, 2009.

[29] J. Rafiee, P.W. Tse, A. Harifi, and M.H. Sadeghi. A novel technique for selecting mother wavelet function using an intelli gent fault diagnosis system. Expert Systems Applications., 36(3):4862–4875, 2009.

[30] National Fire Protection Association (NFPA). National Electric Code 2008. NFPA, 2007.

[31] R. Isermann. Fault-Diagnosis systems. An introduction from Fault detection to Fault Tolerance. Springer, 2006.

[32] R. Isermann, K.-H. Lachmann, and D. Matko. Adaptative control system. Prentice Hall International UK. London, 1992.

[33] P. Eykhoff. System identification: parameter and state estimation. John Wiley,Chichester, England, 1974.

[34] L. Ljung. System identification - theory for the users. Prentice Hall, Englewood Cliffs, 1987.

[35] D. Fussel. Fault diagnosis with tree-structured neuro-fuzzy systems. VDI Reihe 8., 2002.

[36] Consumer Product Safety Commission. Electrical Receptacles Outlets. CPSC, 2009.

[37] J. J. Shea. Conditions that can cause upper thermal limits on residential wiring to be exceeded. In Proc. Int. Conf. on Fire and Materials, pages 101–114, San Francisco, CA, Jan. 29-31 2007.

[38] US Fire Administration. Fire in the United States 2003-2007. Federal Emergency Management Agency, 2009.

[39] J. R. Hall Jr. Home Electrical Fires. National Fire Protection Association, 2009.

[40] J. Rabban, J. Blair, C. Rosen, and R. Sheridan. Mechanisms of pediatric electrical injury. (new implications for product safety and injury prevention). Archives of pediatrics and adolescent medicine, 151(7):696–700, 1997.

[41] M. Zubair and G. Besner. Pediatric electrical burns: Management strategies. Burns, 23(5):413–420, 1997.

[42] V. Babrauskas. How do electrical wiring faults lead to structure ignitions? In Proc. Conf. on Fire and Materials 200, pages 39–51, London, Oct. 22-25 2001.

[43] J. J. Shea. Glowing contact physics. In Proc. IEEE Holm Conf. on Electrical contacts, 2006, pages 48–57, Montreal,QB, Sep. 25-27 2006.

[44] J. Sletbak, R. Kristensen, H. Sundklakk, G. Navik, and M. Runde. Glowing contact areas in loose copper wire connections. IEEE Transactions on Components, Hybrids and Manufacturing Technology, 15(3):322–327, 1991.

[45] Underwriters Laboratories Inc. UL 1699. Arc-Fault Circuit Interrupters. Underwriters Laboratories Inc., 2008.

[46] R. H. Lee. The other electrical hazard : electric arc blast burns. IEEE Transactions on industry applications, IA-18:246–251, 1982.

[47] J. J. Shea. Conditions for series arcing phenomena in pvc wiring. IEEE Transactions on components and packaging technologies, 30(3):532–539, 2007.

[48] Underwriters Laboratories Inc. UL 498. Attachment Plugs and Receptacles. Underwriters Laboratories Inc., 2007.

[49] National Electrical Manufacturers Association NEMA. Arc fault protection: using advanced technology to reduce electrical fires. NEMA, 2006.

[50] P. G. Slade. Electrical contacts: principles and applications. Marcel Dekker Inc., 1999.

[51] National Electric Manufacturers Association. Arc Fault Breaker Safety. NEMA, 2007.

[52] IEEE. IEEE Guide for Performing Arc-Flash Hazard Calculations. IEEE Standard, 2002.

[53] G. R. Jones. High Pressure Arcs in Industrial Devices: Diagnostic and Monitoring Techniques. Cambridge University Press, 1988.

[54] H. Edels. Properties and theory of the electric arc. a review of progress. Proceedings of the IEE - Part A: Power Engineering, 108(37):55 –69, feb. 1961.

[55] C. J. Buchenauer W. B. Maier, A. Kadish and R. T. Robiscoe. Electrical discharge initiation and a microscopic model for formative time lags. IEEE Trans Plasma Science, 21(6):676–683, 1993.

[56] R. Holm. Electrical contacts: Theory and application. Springer, 1967.

[57] P. G. Slade and M. D. Nahemow. Initial separation of electric contacts carrying high currents. Journal of Applied Physics, 42(9):3290–3297, Aug 1971.

[58] N. H. Wagar. Contact and Connection Technology. In Integrated Deviced and Connection Technology. Prentice Hall, 1971.

[59] J. K. Somerville. The electric Arc. Methuen, 1959.

[60] M. F. Hoyaux. Arc physics. Springer-Verlag, 1968.

[61] T. A. Short. Electric Power Distribution Handbook. CRC Press LLC. New York, 2004.

[62] G. D. Gregory and G. W. Scott. The arc-fault circuit interrupter: an emerging product. IEEE Trans. on Industry Applications, vol. 34:928–933, May 1998.

[63] C. Christopoulos and A. Wright. Electrical Power System Protection. Kluwer Academic Publishers, 1999.

[64] National Instruments. Measurement Fundamentals. National Instruments Inc., 2008.

[65] R. F. Ammerman and P. K. Sen. Dc-arc models and incident-energy calculations. IEEE Trans. on Industry Applications, vol. 46:1810–1819, Sep 2010.

[66] A. Gaudreau A. Hamel and M. Cote. Intermittent arcing faults on underground low-voltage cables. IEEE Trans. on Power Delivered, vol. 19:1862–1868, Oct 2004.

[67] T.E. Brown Jr. The electric arc as a circuit element. Journal of the electrochemical society, vol. 102:27–37, Jan 1955.

[68] D. Cubillos G. Idarraga Ospina and L. Iba nes. Analisys of arcing fault modes. Transmission and Distribution Conference and Exposition: Latin America, 2008 IEEE/PES, pages 1–5, Aug 2008.

[69] J.J. Burke and D.J. Lawrence. Characteristics of fault currents on distribution systems. Power Apparatus and Systems, IEEE Transactions on, 103(1):1–6, 1984.

[70] W. Charytoniuk, W-J. Lee, M-S. Chen, and J. Cultrera. Arcing fault detection in underground distribution networks - feasibility study. IEEE Trans. on Industry Applications, vol. 36:1756–1761, Nov 2000.

[71] I. Daubechies. Ten lectures on Wavelets. Society for Industrial and Applied Mathematics, 1992.

[72] A. Grasp. An introduction to wavelets. Computational Science and Engineering, IEEE, 2(2):50–61, May 1995.

[73] I. Daubechies. Where do wavelets come from? a personal point of view. Proceedings of the IEEE, 84(4):510–513, 1996.

[74] G. Kaiser. A friendly guide to wavelets. Birkhäuser, 1999.

[75] P. S. Addison. The illustrated wavelet transform handbook. Institute of Physics London, 2002.

[76] I. Daubechies and T. Paul. Wavelets - some applications. In Proc. Int. Conf. on Mathematical Physics, pages 675–686, Marseille, France, Apr. 21-24 1987.

[77] J. Liu Y.Y. Tang, L.H. Yang and H. Ma. Wavelet Theory and its application to pattern recognition. World Scientific Publishing Co. Pte. Ltda., 2000.

[78] D.B. Percival and A.T. Walden. Wavelet Methods for Time Series Analysis. Cambridge University Press, 2000.

[79] M. Thuillard. Wavelets in Soft Computing. World Scientific Publishing Co., 2001.

[80] L. Debnath. Wavelet Transforms and Their Applications. Birkhäuser, 2002.

[81] A. Jensen and A. la Cour-Harbo. Ripples in Mathematics. The Discrete Wavelet Transform. Springer Verlag, 2001.

[82] W. Sweldens. The lifting scheme: A custom-design construction of biorthogonal wavelets. SIAM Journal on Mathematical Analysis, 3:186–200, 1996.

[83] W. Sweldens. The lifting scheme: A construction of second generation wavelets. Applied and Computational Harmonic Analysis., 29:511–546, 1997.

Appendix A

DATA FILE IDENTIFICATION

Identification for data files had been created following the next protocol:

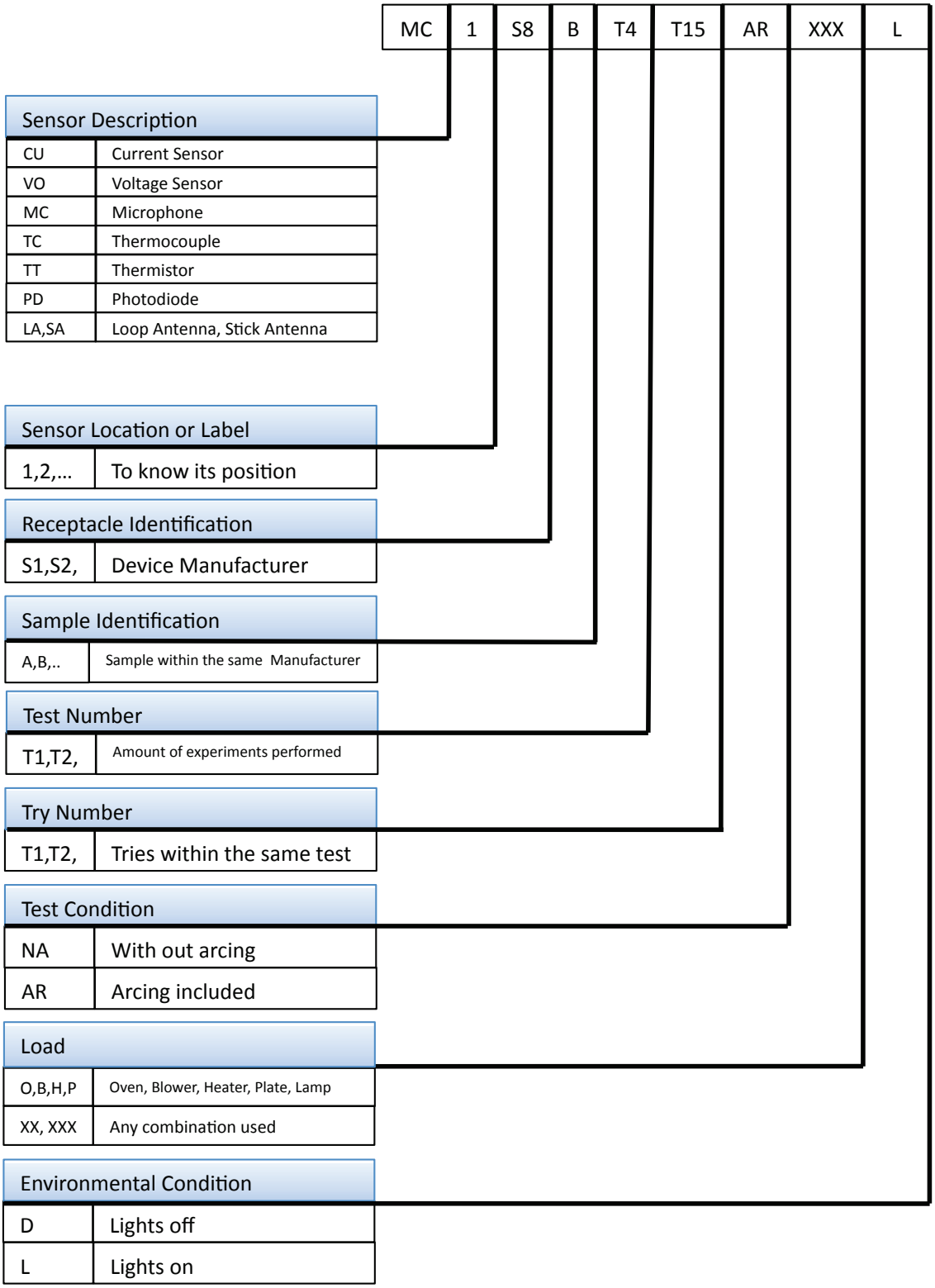

Figure A.1: Parameters used to identification of data files

Appendix B

THERMAL SIMULATION

The following pages present the result of FEM simulation with different heat sources in order to compare a BSafe receptacle against a regular receptacle. A summary of the combination was listed in Table 3.1

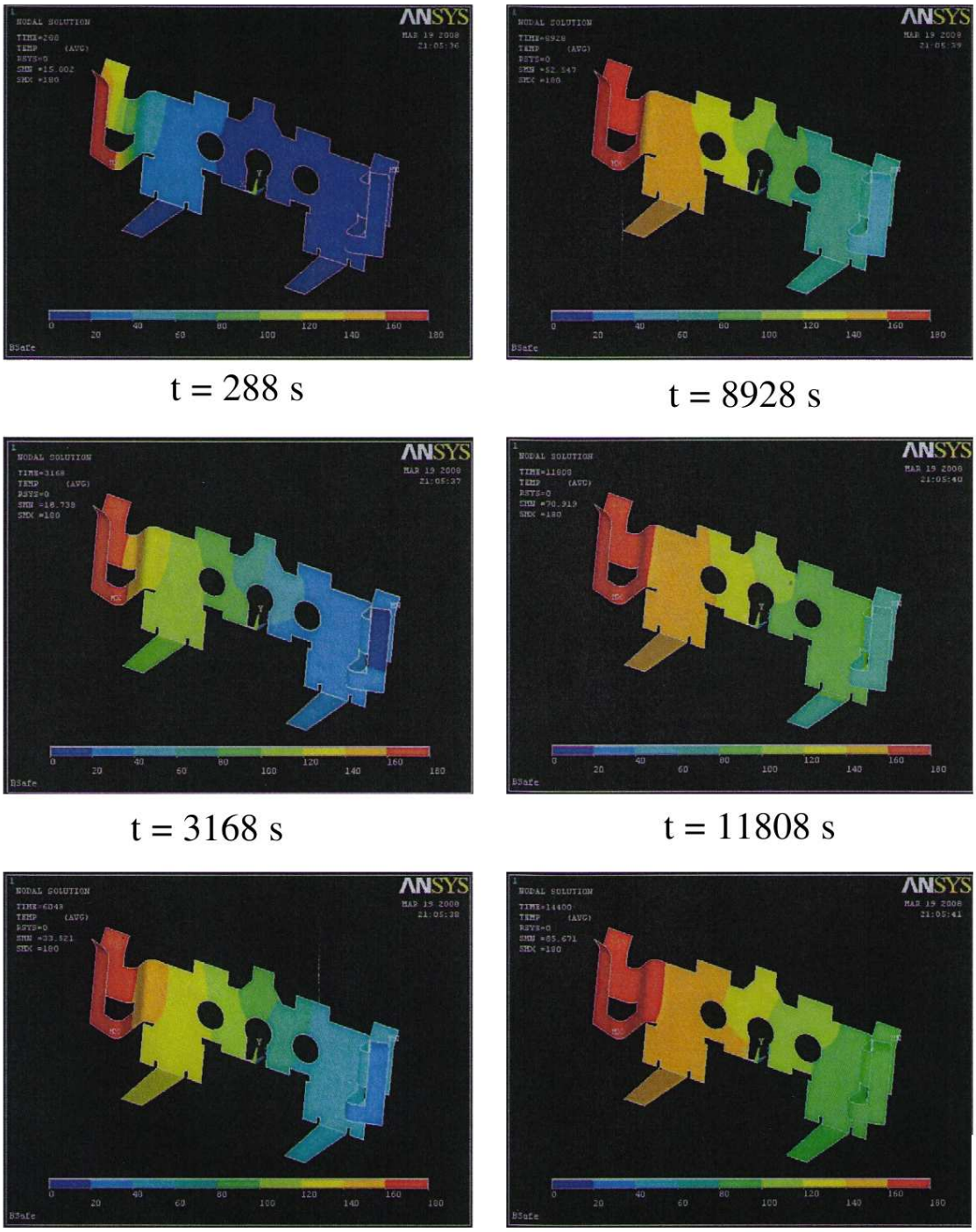

Figure B.1: Thermal simulation of BSafe receptacle with one blade as heat source

t = 288 s

t = 8928 s

t = 3168 s

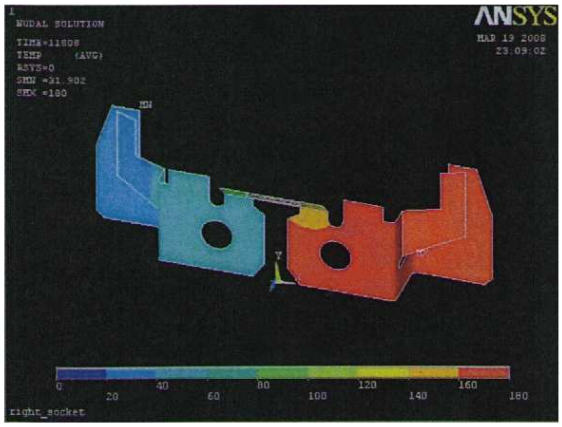

t = 11808 s

t = 6048 s

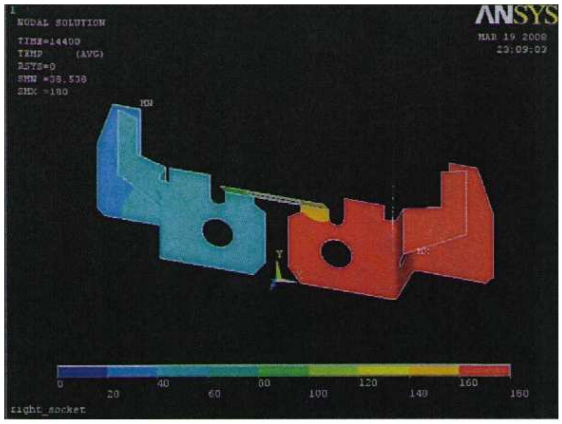

t = 14400 s

Figure B.2: Thermal simulation of regular receptacle with one blade as heat source

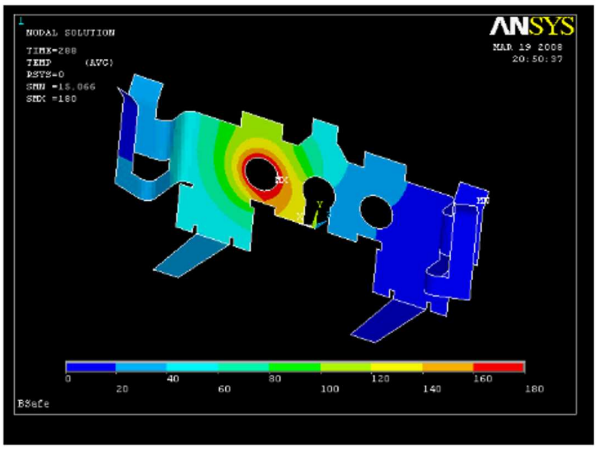

t = 288 s

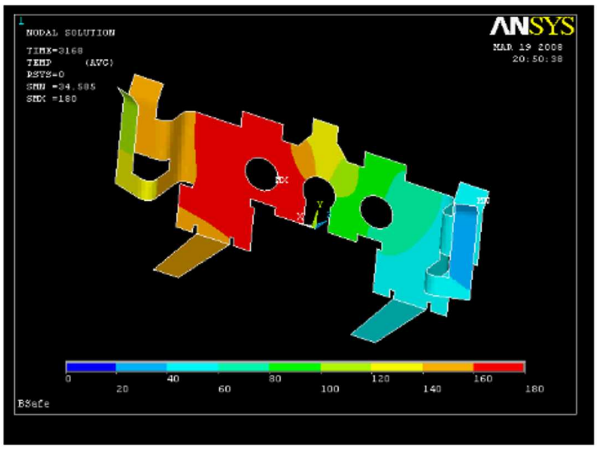

t = 3168 s

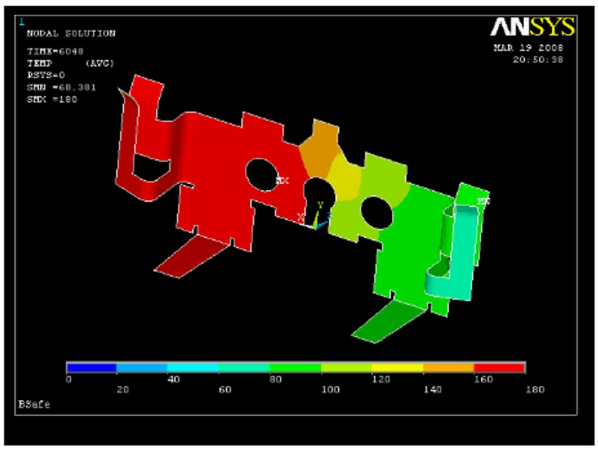

t = 6048 s

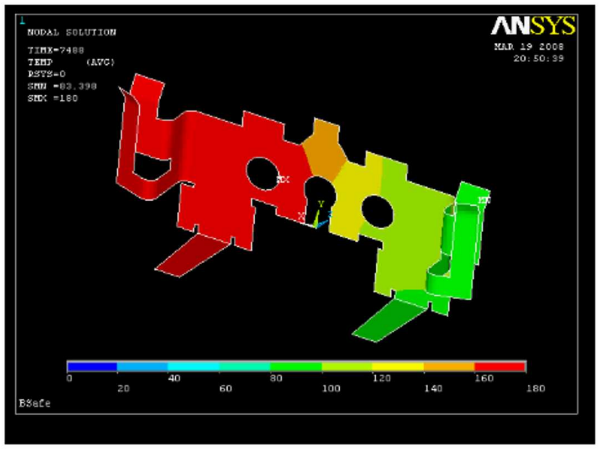

t = 8928 s

t = 11808 s

t = 14400 s

Figure B.3: Thermal simulation of BSafe receptacle with one terminal screw as heat source

t = 288 s

t = 8928 s

t = 3168 s

t = 11808 s

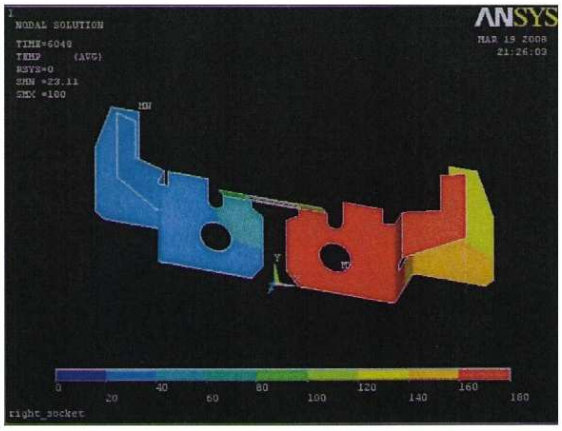

t = 6048 s

t = 14400 s

Figure B.4: Thermal simulation of regular receptacle with one terminal screw as heat source

t = 288 s

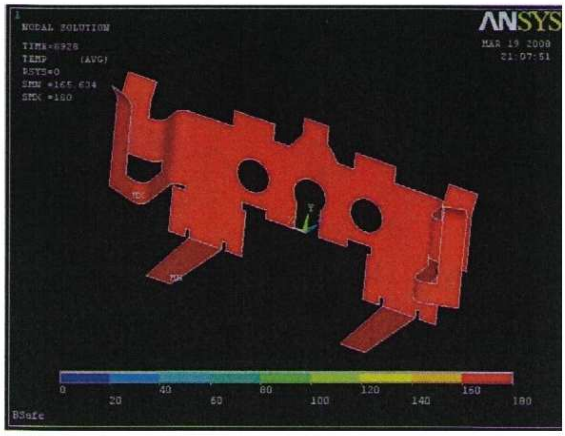

t = 8928 s

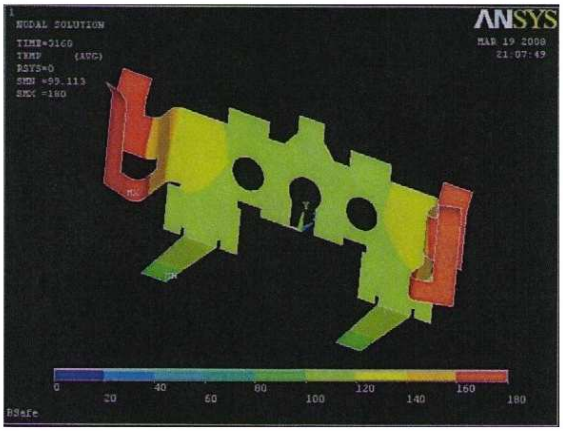

t = 3168 s

t = 11808 s

t = 6048 s

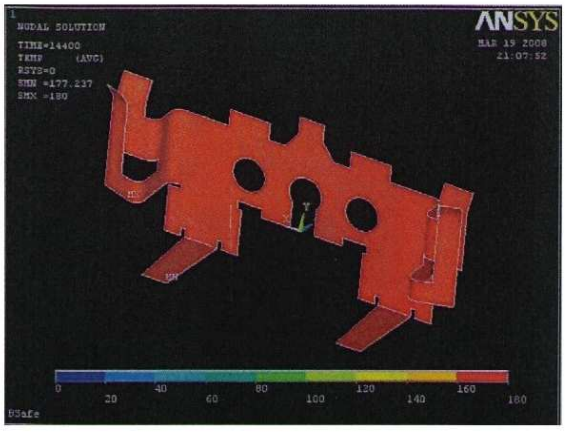

t = 14400 s

Figure B.5: Thermal simulation of BSafe receptacle with two blades as heat sources

t = 288 s

t = 8928 s

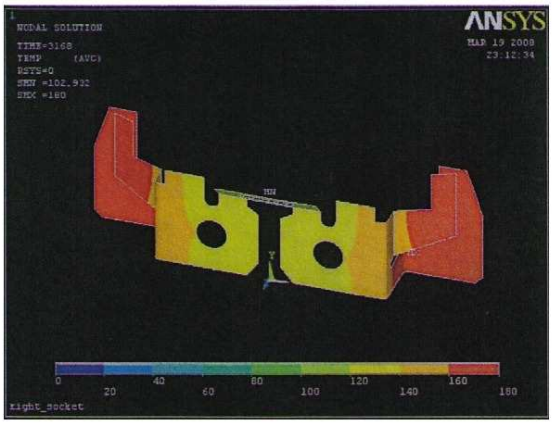

t = 3168 s

t = 11808 s

t = 6048 s

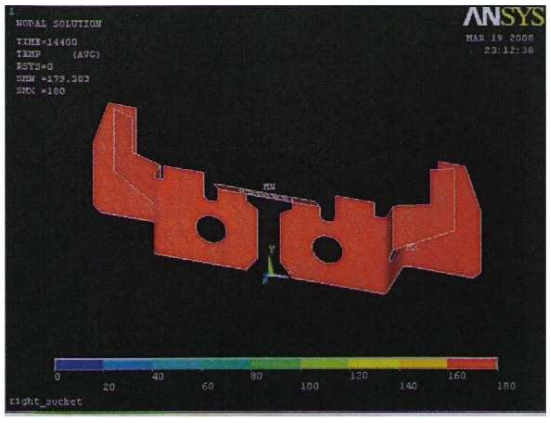

t = 14400 s

Figure B.6: Thermal simulation of regular receptacle with two blades as heat sources

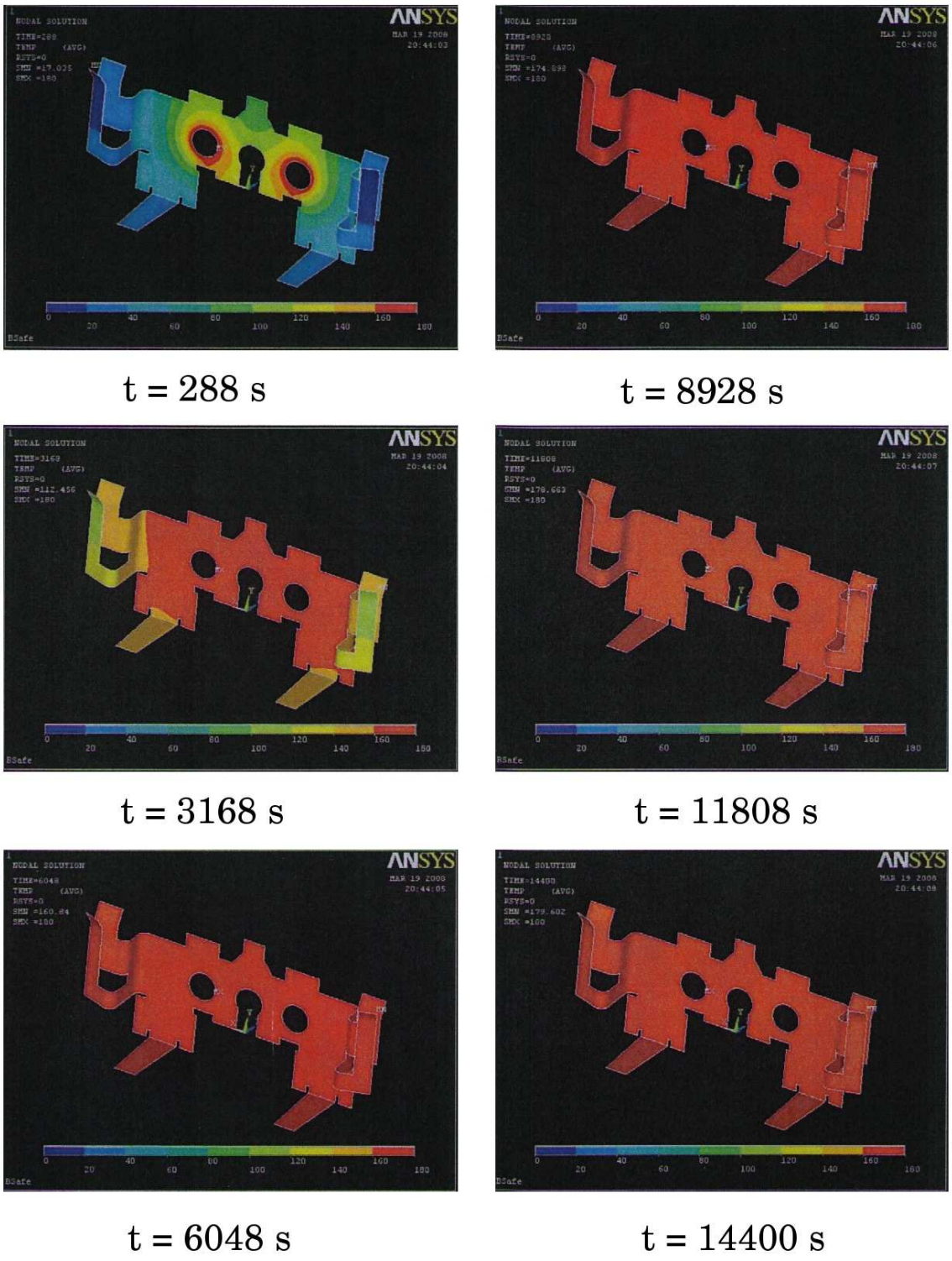

Figure B.7: Thermal simulation of BSafe receptacle with two terminal screw as heat sources

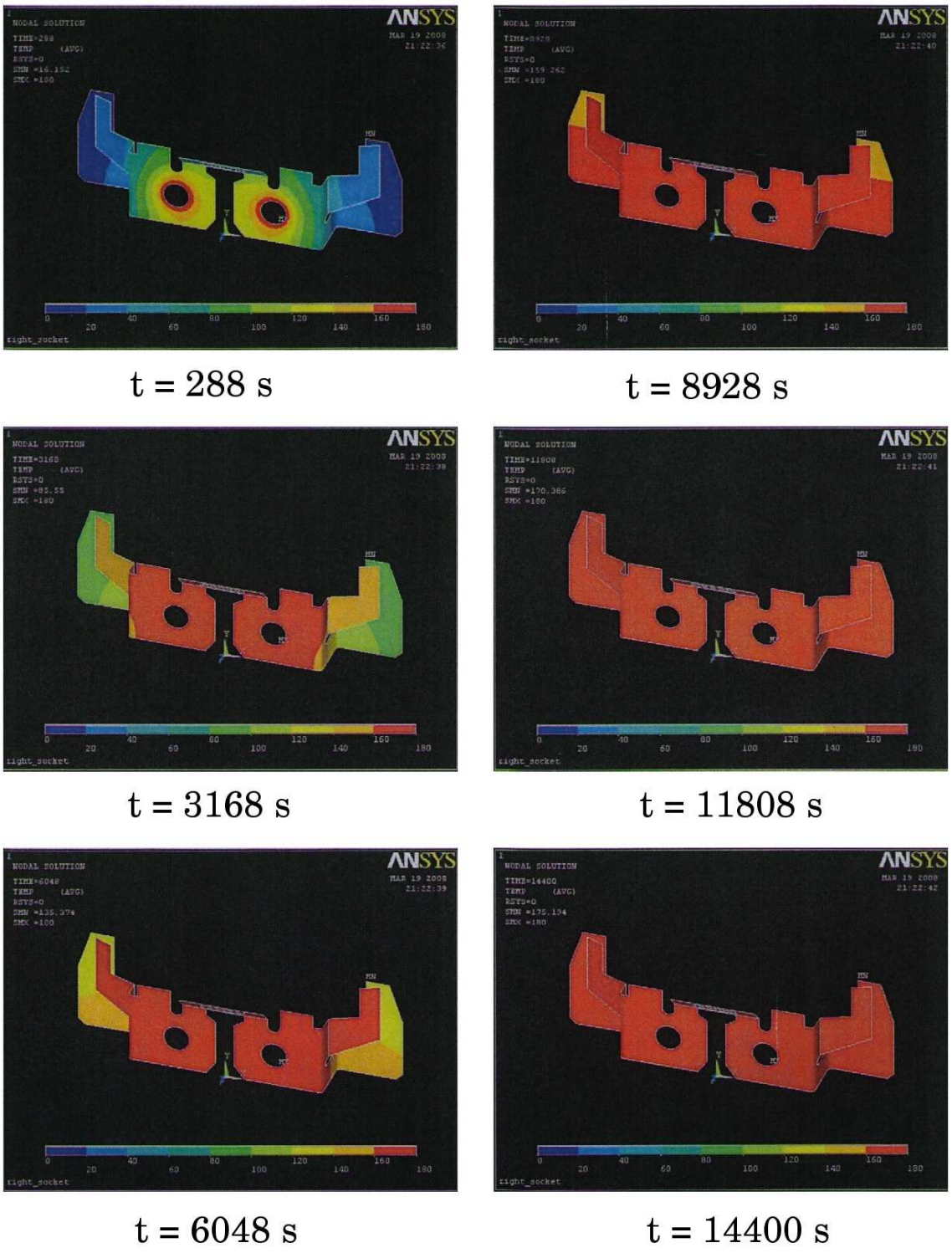

Figure B.8: Thermal simulation of regular receptacle with two terminal screw as heat sources

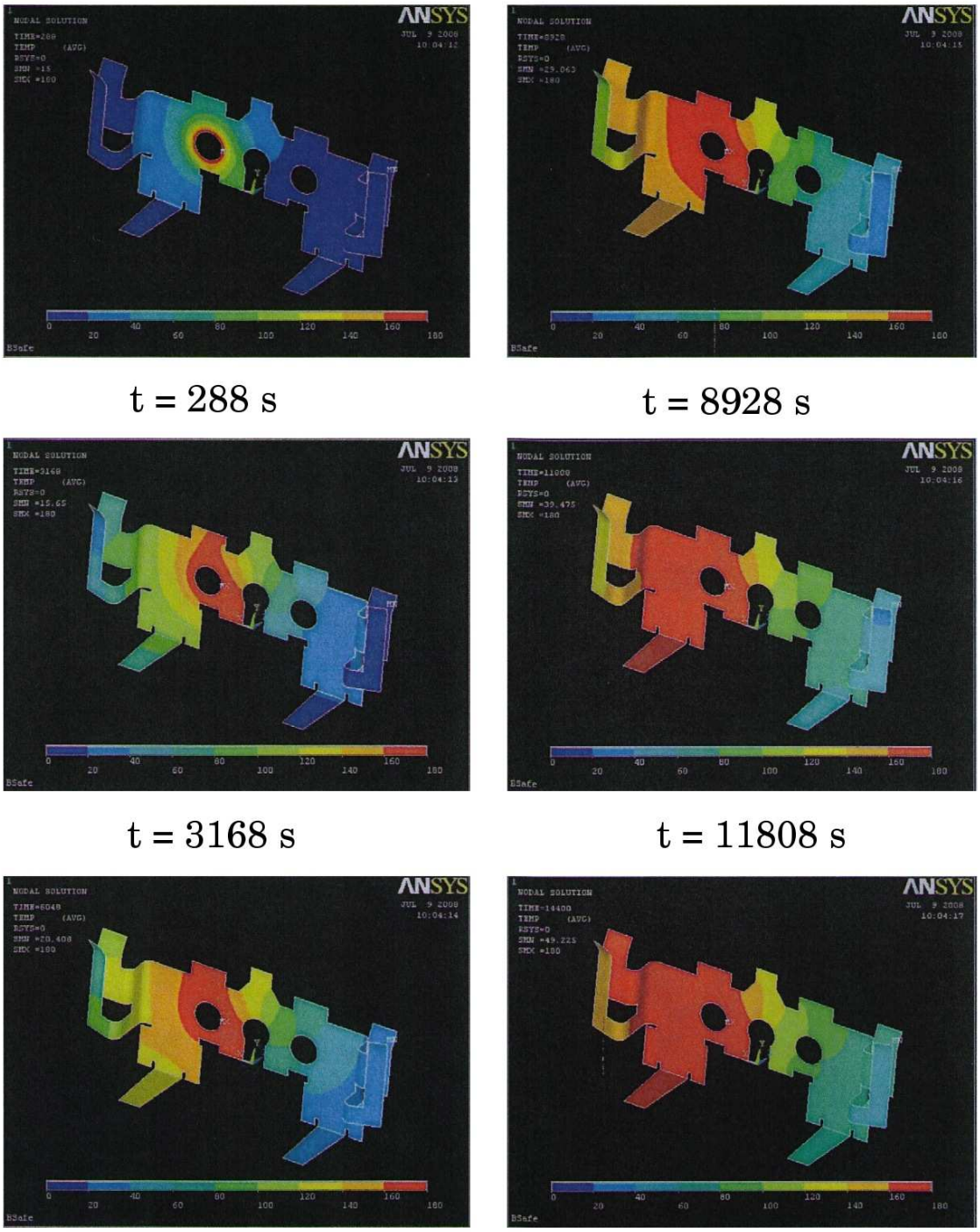

Figure B.9: Thermal simulation of BSafe receptacle with one terminal screw as heat source and considering yellow brass as one component of the bimetalic part

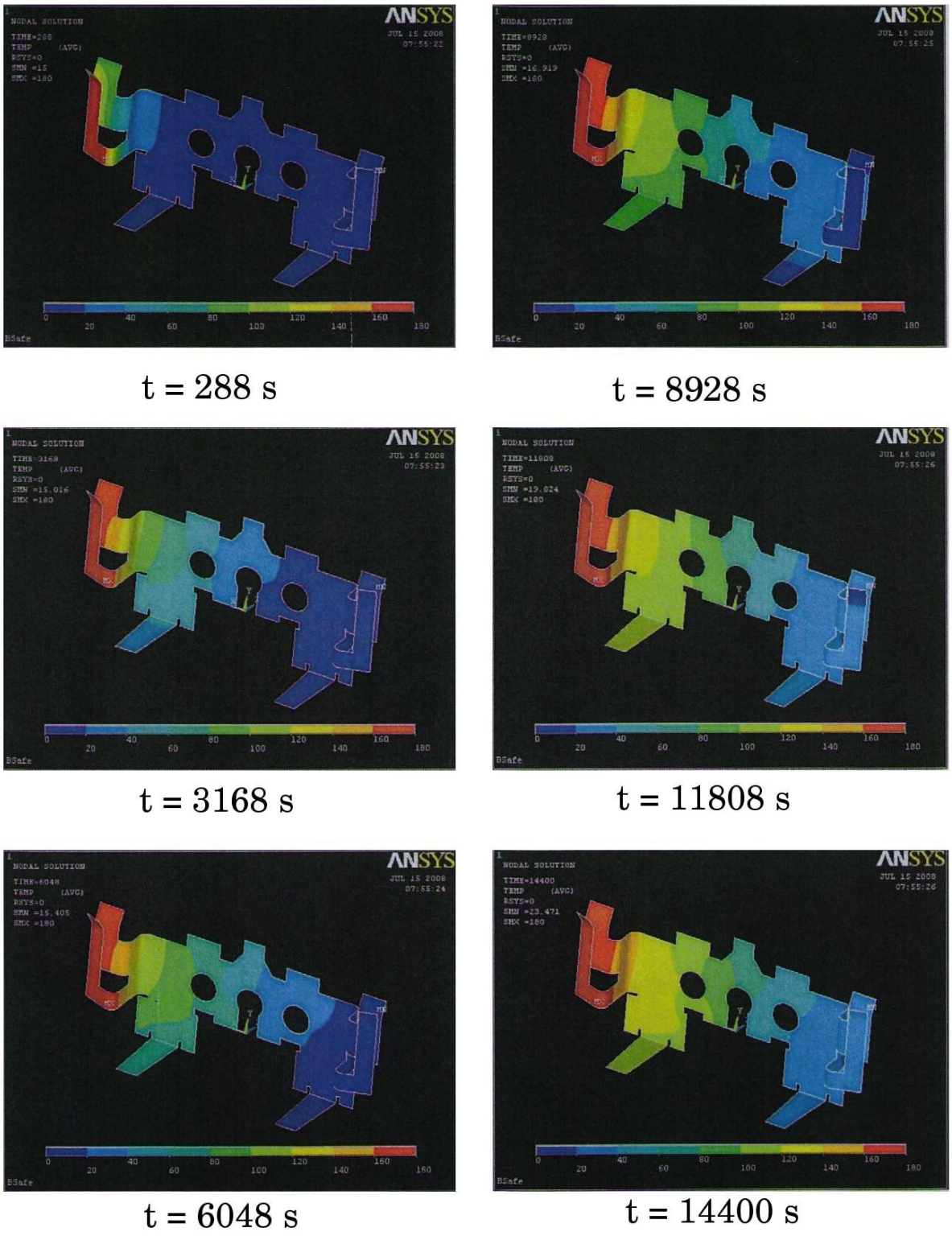

Figure B.10: Thermal simulation of BSafe receptacle with one blade as heat source and considering yellow brass as one component of the bimetalic part

Appendix C

WAVELET TRANSFORM THEORY AND A LITERATURE SURVEY

C.1 Introduction

The idea of representing a function by using superposition was implement by Joseph Fourier in 1800. Fourier superposed sines and cosines to represents other functions. This representation can be also realized by using wavelets. Wavelets are functions which satisfy specific and mathematical requirements. Wavelet transforms are considering a mathematical tool that cuts up data or functions into different frequency components, and then studies each component with a resolution matched to its scale [71]. Using wavelet techniques we divide a complicated function into several simpler ones that can be study independently.

Wavelets are well-suited for approximating data with sharp discontinuities. In contrast, Fourier analysis includes nonlocal functions that do a very poor job in approximating sharp spikes [72]. The general procedure when performing Wavelet Analysis consist of: (1) to adopt a wavelet prototype function, called *mother wavelet* or *analyzing wavelet*, (2) perform time domain analysis using a high-frequency (contracted) version of the prototype function, (3) perform frequency domain analysis using a low-frequency (dilated) version of the same wavelet and (4) create a linear combination of the coefficients founded in the previous steps (wavelet expansion).

C.2 Background on Wavelet Transform

Daubechies *et al.* reviewed the history and evolution of wavelet theory . The subject area of wavelets, developed mostly over the last 20 years, is connected to older ideas in many other fields, including pure and applied mathematics, physics, computer science, and engineering [73]. The evolutions towards wavelets, began with Joseph Fourier and his theory of frequency analysis (1807), now refered to as Fourier synthesis. According to Fourier, any 2π-periodic function $f(x)$

is the sum

$$a_o + \sum_{k=1}^{\infty} (a_k Coskx + b_k Sinkx) \tag{C.1}$$

of its Fourier series, where the coefficients a_o , a_k and b_k are calculated by:

$$a_o = \frac{1}{2\pi}\int_0^{2\pi} f(x)dx \qquad a_k = \frac{1}{\pi}\int_0^{2\pi} f(x)Cos(kx)dx \qquad b_k = \frac{1}{\pi}\int_0^{2\pi} f(x)Sin(kx)dx$$

Mathematicians start to use this innovated tool in order to develop a new functional universe. Some years later, scientific gradually were led from their previous notion of *frequency analysis* to the notion of *scale analysis*. Scale analysis consist basically in find or construct a function, shift it by some amount and change its scale, then apply that structure in approximating a function (or signal). This procedure is repeated until get the desired approximation [72].

In the case of the Fourier Transform (FT), a signal is analyzed in the time domain in order to get its frequency content. The method requires translating a signal (or function) in the time domain into a function in the frequency domain. Because each coefficient of the transformed function represent the contribution of each sine and cosine at each frequency, the frequency content of the signal can be analyzed. The inverse Fourier transform allows to us to transform data from frequency domain into the time domain. The discrete Fourier transform (DFT) allows to obtain the Fourier transform from a finite number of a function's sampled points. The sampled points are supposed to represent most of the behavior of the function at other locations.

If a function f represents a nonperiodic signal, the Fourier series does not accurately represents the signal. One solution to this problem is the windowed Fourier transform (WFT). The WFT can be use to give information about signals simultaneously in the time and the frequency domain. The function f is divided into sections, each section is analyzed for its frequency content separately. Every sharp transition of the function is windowed in order to guarantee a zero-convergence at the end points of the selected window. A weight function is used to emphasized the middle points of the selected interval. The effect of the window is to localize the signal in time [74]. The WFT is also known as short time Fourier Transform (STFT).

A problem associated with the Fourier transform is the amount of operations involves. If n samples are taken to approximate a function, a Fourier integral will need a matrix of the same order. This mathematical process of a n x n matrix by an vector costs on the order of n^2 operations , the problem gets quickly worse as the number of sample points increases. However,

if the samples are uniformly spaced, then the Fourier matrix can be factored into a product of just a few sparse matrices, reducing the operations in a total of order of n log n. This is the so called fast Fourier transform (FFT) [72].

According to Addison, wavelet transform analysis began in the mid-1980s where they were developed to analyze seismic signals. In the last 20 years, an increasing numbers of journal paper in this area had been observed [75]. Wavelets are used to transform the signal under consideration into another representation in a more useful form. The wavelet can be manipulated in two ways: it can be translated (move to another location) and can be stretched or squeezed as is showing in figure C.1.

(a) Typical waveforms of wavelets

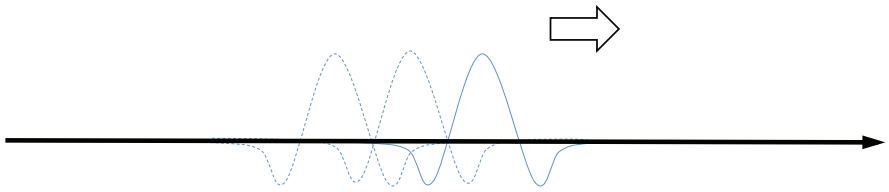

(b) Wavelet Location

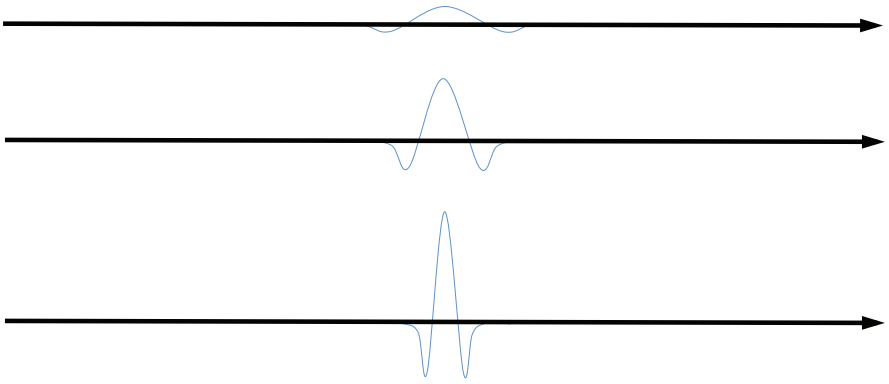

(c) Wavelet Scaling

Figure C.1: Basic representation and operations on wavelets.

The schematic presented in figure C.2 shows how a wavelet transform works [75]. First, a local matching between the signal and the wavelet is required. If the wavelet matches the signal well at a specific scale and location, then a large transform value is obtained. In contrast, when wavelet and signal does not match well, a low transform value is obtained. Second, the value obtained in the previous step is then located in the two-dimensional transform plane. Finally, the transform is computed at various location of the signal and for various scales of the wavelet in order to filling up the transform plane. The last procedure is performed in a smooth continuous fashion for the continuous wavelet transform (CWT) or in discrete steps for the discrete wavelet transform (DWT).

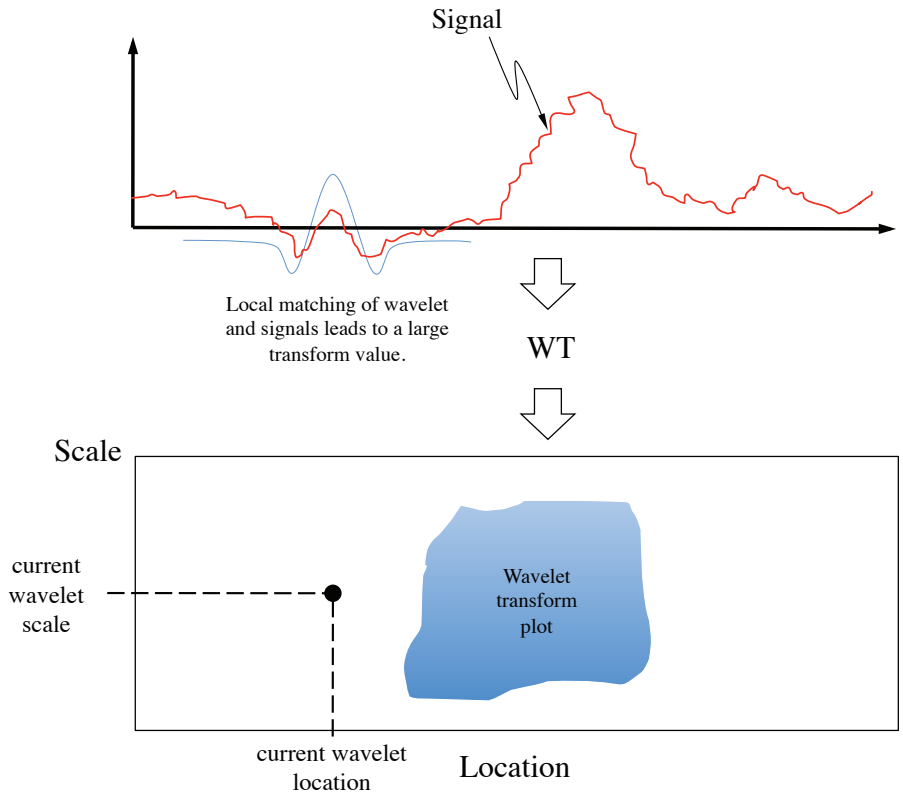

Figure C.2: Schematics of the Wavelet Transform procedure.

Wavelets constitute a family of functions, derived, and indexed by two labels, one for position and one for frequency. More explicitly,

$$h^{(a,b)}(x) = \mid a \mid^{-\frac{1}{2}} h\left(\frac{x-b}{a}\right) \tag{C.2}$$

where h is a square integrable function such that

$$C_h = \int_{-\infty}^{\infty} \mid y \mid^{-1} \mid \hat{h}(y) \mid^2 dy < \infty \tag{C.3}$$

and where $a\ ,\ b\ \in \mathbb{R},\ a \neq 0$. The parameter b in $h^{(a,b)}$ gives the position of the wavelet, while the dilatation parameter a governs its frequency.

If the dilation and translation parameters a and b vary continuously, this transform is called *continuous wavelet transform*. In analogy to the structure associated with the short-time Fourier transform, which can be viewed as a discrete subset of the continuously Fourier Transform, the discrete structure of wavelets can be obtained from the continuous wavelet transform. We choose to discretize the dilation parameter a by taking powers of a fixed dilation step $a_0 > 1, a = a_0^m$ with $m \in \mathbb{Z}$. For different values of m the wavelets will be more or less concentrated, and we adapt the discretized translation steps to the width of the wavelet by choosing $b = n\ b_0\ a_0^m$,with $n \in \mathbb{Z}$. Then a discrete wavelet bases $h_{mn}(x)$ can be formed by

$$h_{mn}(x) = a_0^{-\frac{m}{2}}\ h\left(a_0^{-m} x - n b_0\right) \tag{C.4}$$

Based on the discrete wavelet bases, a *discrete wavelet transform* (DWT) of a finite energy sequence with N samples, $f(x)$, can be computed as:

$$W_{mn} = \frac{1}{a_0^m} \sum_{x=0}^{N-1} h\left(a_0^{-m} x - n b_0\right)\ f(x) \tag{C.5}$$

where W_{mn} are referred to as the DWT coefficients of the sequence $f(x)$. The wavelet transform can be used, like the short-time Fourier transform, for signal analysis purposes. As in the short-time Fourier transform the two integer indices, m and n, control respectively, the frequency range and the time translation steps. There are however some significant differences between the two transforms. Some of these differences may well make the less widely used wavelet transform a better tool for the analysis of some types of signals (e.g., acoustic signals, such as music or speech) than the short-time Fourier transform [76].

One of the DWT and the simplest well-know wavelet is the Haar wavelet, which was presented in 1910 by the Hungarian mathematician Alfréd Haar [77]. The Haar wavelet has bad decay in the frequency domain. But in the time domain it is compactly supported on $[0,1]$. For an input represented by a list of 2^n numbers, the Haar wavelet transform may be considered to

simply pair up input values, storing the difference and passing the sum. This process is repeated recursively, pairing up the sums to provide the next scale: finally resulting in $2^n - 1$ differences and one final sum.

By imposing an appealing set of regularity conditions over the Harr wavelet, the Belgian mathematician Ingrid Daubechies formulated in 1988 a useful class of wavelet filters, all of which yield a DWT. This formulation is based on the use of recurrence relations to generate progressively finer discrete samplings of an implicit mother wavelet function; each resolution is twice that of the previous scale [78].

Other forms of discrete wavelet transform include the non- or undecimated wavelet transform (where downsampling is omitted), the Newland transform (where an orthonormal basis of wavelets is formed from appropriately constructed top-hat filters in frequency space). Wavelet packet transforms are also related to the discrete wavelet transform [77].

To allow fast numerical implementations, the scaling factor a_0 in equation C.5 is varied along the dyadic sequence $(2^j\ ,\ j = 1,2,3,...)$. Thus, the DWT can be estimated using an algorithm called the *fast wavelet transform* (FWT). The FWT, permits the computation of the wavelet transform. At each level, the data are processed through a low-pass and a high-pass filter. The high-pass filtered data are known as the *detail wavelet coefficients* . The low-pass outputs, are used as input data to compute the next level of detail wavelet coefficients, and they are refereed as *wavelet approximation coefficients* [79].

C.3 Multiresolution Analysis and Wavelet Construction

According to Debnath [80], Multiresolution Analysis (MRA) is central to all constructions of wavelet bases. The concept of multiresolution is intuitively related to the study of signals or images at different levels of resolution. The resolution of a signal is a qualitative description associated with its frequency content. The fundamental idea of MRA is to represent a function or signal f as a limit of successive approximations, each of which is a finer version of the function f. One of the most important concept of MRA lies in the definition of nested spaces.

Nested spaces are created during the decomposition of the whole function. The function f is decomposed into individual subspaces $V_n \subset V_{n+1}$ so that the space V_{n+1} consists of all rescale functions in V_n. These subspaces contain an individual component of the original function f. The components can describe a finer and finer versions of f. Figure C.3 shows an example of a nested space, together with a representation of the complementary spaces W_0 and W_{-1}. In

this case, $V_{n-1} \subset V_0 \subset V_{n+1}$, the space W_{-1} is the complementary space of V_{-1} with $W_{-1} \oplus V_{-1}$ ($\oplus$ represents the orthogonal sum). Similarly we have $V_1 = W_0 \oplus V_0$.

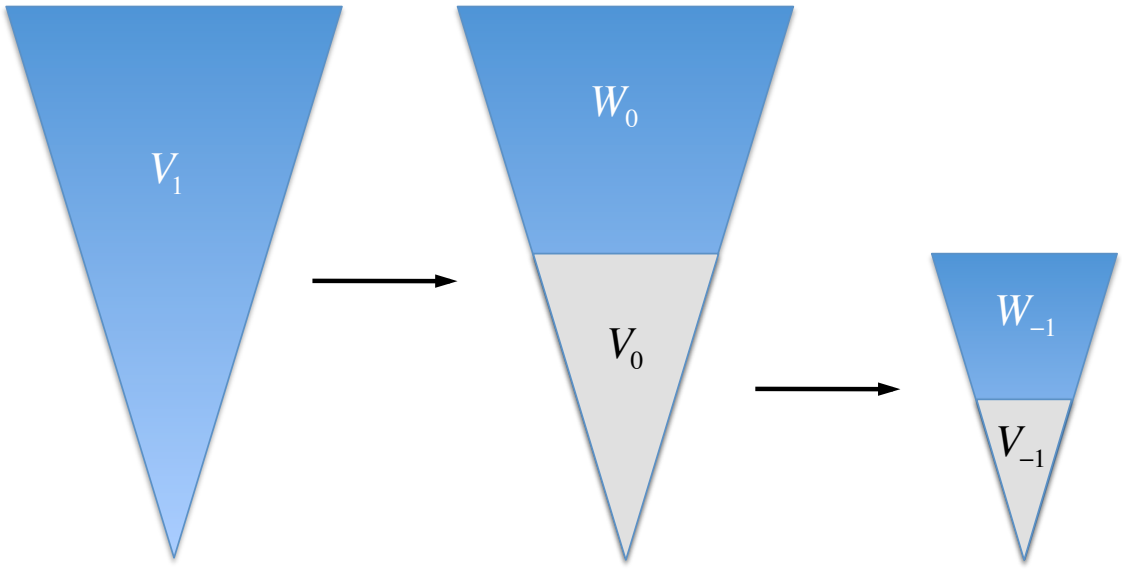

Figure C.3: Schematic representation of nested spaces

In general, let ϕ a function that we use to generate nested spaces by linear combinations. We define V_1 as the space generated by $\phi(2x)$ and its integer translates, then $V_1 : \{\phi(2x-n)\}$. Let us consider a second space V_0, generated by the $2x$ dilated function $\phi(x)$ and its translates : $V_0 : \{\phi(x-n)\}$. As we can see in Figure C.3 $V_0 \subset V_1$, therefore, any function in V_0 can be written as a linear combination of the functions generating V_1

$$\phi(x) = \sum_n g_n \cdot \phi(2x-n) \tag{C.6}$$

Now under the same line of though, the space W_0 which is the complement space of V_0 follows $W_0 \subset V_1$ consequently, any function ψ in W_0 can be written as a linear combination of the basis function in V_1

$$\psi(x) = \sum_n h_n \cdot \phi(2x-n) \tag{C.7}$$

equations C.6 and C.7 are called dilation equations or two-scales relations and they are the core of the multiresolution analysis.

The other fundamental concept of MRA is called decomposition and reconstruction. Since $V_1 = W_0 \oplus V_0$, a function V_1 can be expressed as the weighted sum of the basis functions of V_0 and W_0. The relation is called the decomposition relation and can be written by:

$$\phi(2x-k) = \sum_k p_{k-2n} \cdot \phi(x-n) + q_{k-2n} \cdot \psi(x-n) \quad \therefore \quad k \in \mathbb{Z} \tag{C.8}$$

The function ϕ is called the scaling function, while the function ψ is the mother wavelet. Using the decomposition relation we get the decomposition algorithm, hence we obtain:

$$c_{m-1,n} = \sum_k p_{k-2n} \cdot c_{m,k} \tag{C.9}$$

and

$$d_{m-1,n} = \sum_k q_{k-2n} \cdot c_{m,k} \tag{C.10}$$

The decomposition algorithm can be used iteratively in a cascade of filters, so that a function f may be decomposed into the sum;

$$f = g_0 + g_{-1} + g_{-2} + \cdots + g_{-N} + f_{-N} \quad \therefore \quad g_{-j} \in W_{-j} \tag{C.11}$$

Figure C.4 shows a representation of a decomposition algorithm where we can see the filter bank we referred in previous lines.

Working in the similar way, the reconstruction algorithm is given by:

$$c_{m,n} = \sum_k g_{n-2k} \cdot c_{m-1,k} + h_{n-2k} \cdot d_{m-1,k} \tag{C.12}$$

The decomposition algorithm is invertible and the function (or signal) can be reconstructed iteratively from the detailed coefficients together with the last level of coefficients of the low-pass filter as shown in Figure C.5. The coefficients g and h are defined by the two-scales relation.

C.4 Time-Frequency Domain, Scale and Resolution

The wavelet transform performs the MRA with the varying scale factor a. However, in the time domain the wavelet must oscillate to have a zero mean. The wavelet must be a small wave that oscillates and vanishes very fast. This means that wavelets are localized in the time domain.

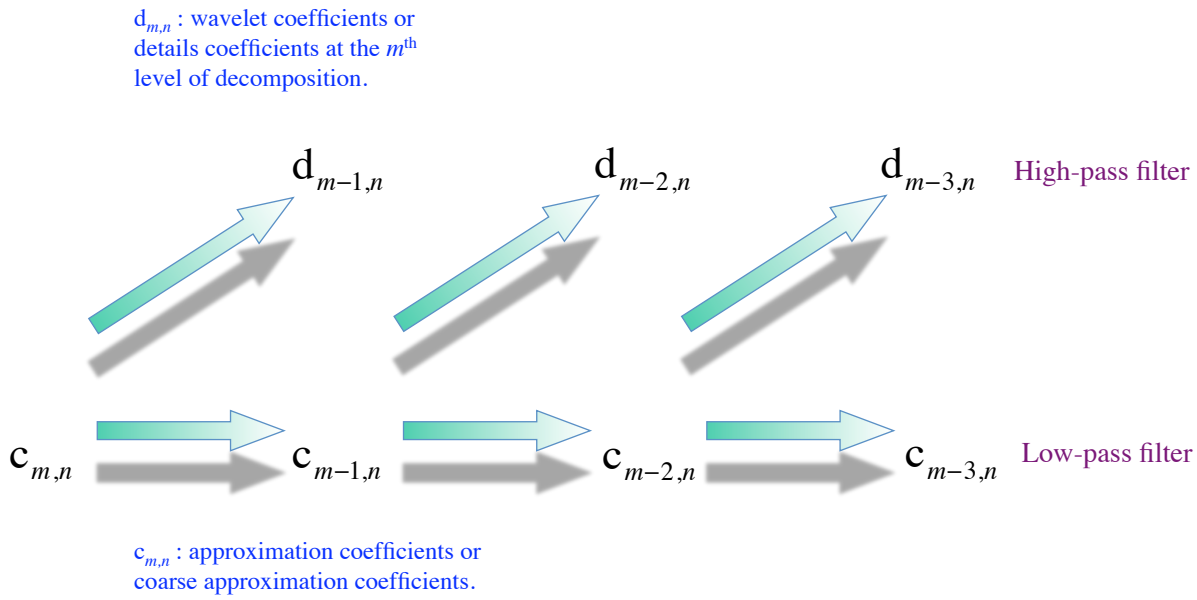

Figure C.4: Schematic representation of the decomposition algorithm

When the scales a decreases, the wavelet $H(a\omega)$ in the frequency domain is dilated to caver a large frequency band of the signal Fourier spectrum. In other words, the Fourier transform of the wavelet must decay fast with the frequency ω, which means that the wavelet is localized in frequency domain.

The scale is related to the windows size of the wavelet, The wavelet transform of a large scale performs an analysis of global view, and that of a small scale performs an analysis of detailed view. The resolution is related to the frequency of the wavelet oscillation. For a given function, reducing the scale will reduce the window size and increase the resolution in the same time.

C.5 Improving The Wavelet Transform

The Haar wavelet is the simplest algorithm that shows perfect reconstruction. However, Haar wavelets can miss detail and do not always represent change at all resolution scales [81]. In contrast, the Daubechies D4 algorithm shows better multi-scale resolution, at the cost of a more complex algorithm. To overcome this disadvantages, Wim Sweldens [82], [83] showed how Haar wavelets could be expressed in Lifting Scheme form and extended to provide accurate multiscale resolution. The Lifting Scheme provides a simpler view of many wavelet algorithms.

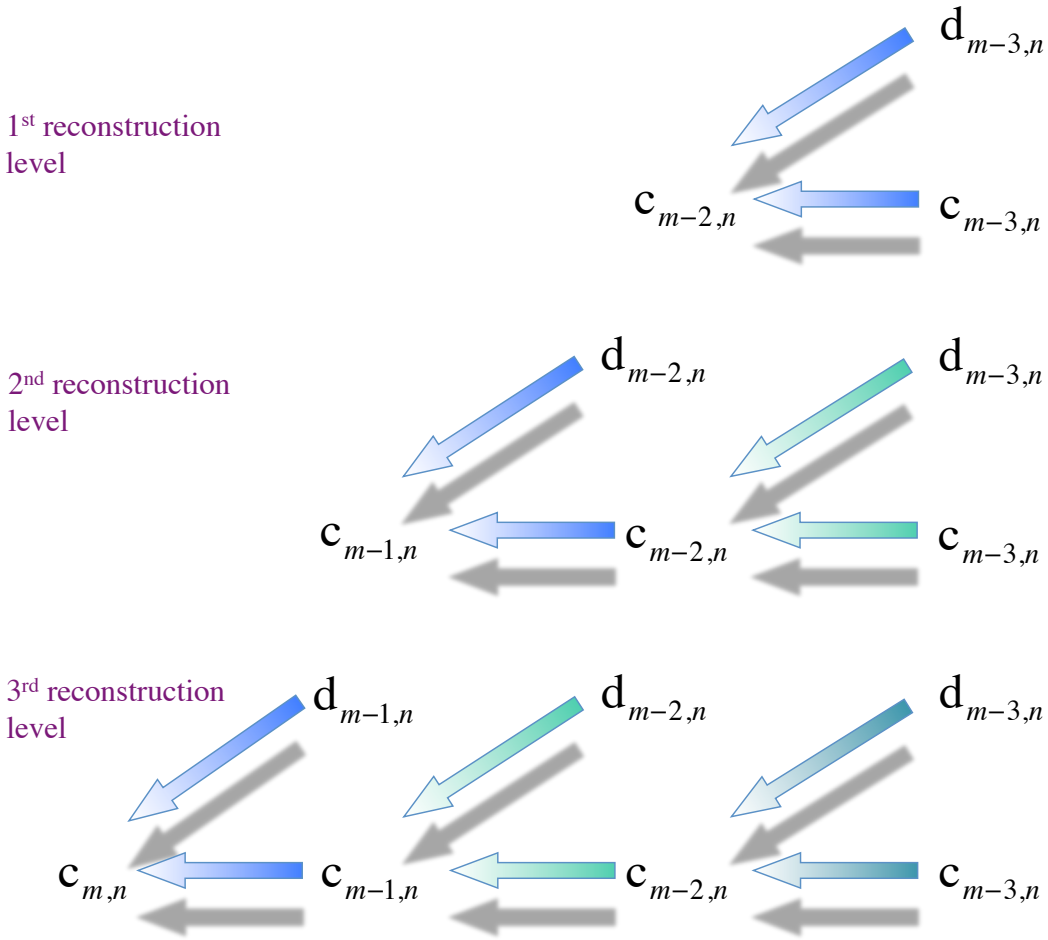

Figure C.5: Schematic representation of the reconstruction algorithm

The wavelet Lifting Scheme is a method for decomposing wavelet transforms into a set of stages. Lifting scheme algorithms have the advantage that they do not require temporary arrays in the calculation steps. A basic representation of the Lifting Scheme is shown in Figure C.6.

The Lifting Scheme starts with a split step, which divides the data set into odd and even elements. The predict step uses a function that approximates the data set. The difference between the approximation and the actual data replaces the odd elements of the data set. The even elements are left unchanged and become the input for the next step in the transform. The predict step, where the odd value is ”predicted” from the even value is described by the equation

$$odd_{j+1,i} = odd_{j,i} - P(even_{j,i}) \tag{C.13}$$

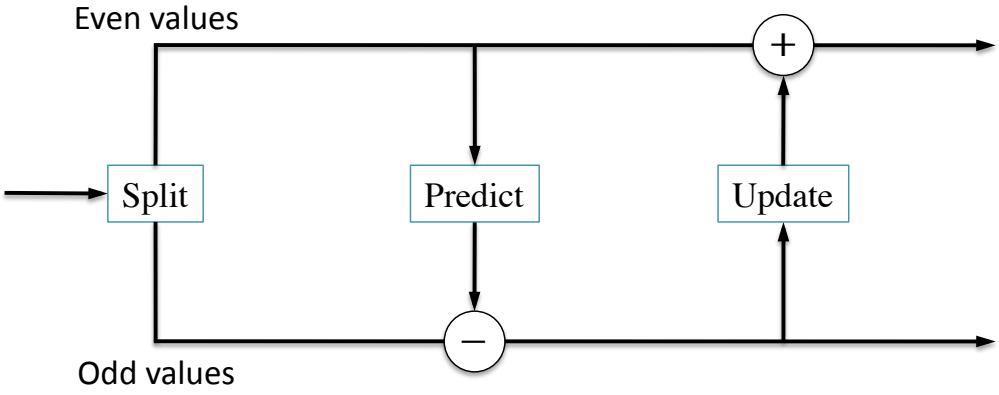

Figure C.6: Lifting scheme forward wavelet transform

The even elements that are used to ”predict” the odd elements result from sampling the original data set by powers of two. Viewed from a compression point of view this can result in large changes in the differences stored in the odd elements (and less compression). The update step replaces the even elements with an average. This results in a smoother input for the next step of the next step of the wavelet transform. The update phase follows the predict phase. The original value of the odd elements has been overwritten by the difference between the odd element and its even ”predictor”, thus:

$$even_{j+1,i} = even_{j,i} + U(odd_{j+1,i}) \tag{C.14}$$

Jensen *et al.* consider the predict and update steps as filters. Digital signal processing deals with filters that can remove selected parts of the signal. A high pass filter allows high frequency components to pass through, suppressing low frequency components. A low pass filter does this opposit: it allows the low frequency parts of the signal to pass through while removing the high frequency components. Based on this argument, The predict step replaces the odd elements with the difference between the odd elements and the predict function. The differences that replace the odd elements will reflect high frequency components of the signal. This can be viewed as a high pass filter. In the other hand, the update step replaces the even elements with a local average. The result will be an approximation of the signal that is smoother than the signal at the previous level. This can be viewed as a low pass filter, since the smoother signals contains fewer high frequency components.

Daubechies *et al.* develops its own language to referring the Wavelet Transform. The Lift-

ing Scheme was developed fifteen years or so after wavelet mathematics started to be developed as a recognized area of applied mathematics. So there is small body of wavelet terminology that predates the Lifting Scheme. The wavelet literature refers to a wavelet function. Mapped into the lifting scheme, this is the function used in the predict phase. The wavelet function is used to calculate the differences, or wavelet coefficients, and acts as the high pass filter for the odd half of the data set. Similarly, in the wavelet literature the partner to the wavelet function is the scaling function. The scaling function results in a smoother representation of the even half of the input data set. The scaling function acts as a low pass filter.

C.6 Summary

In this appendix, we present the basic concepts about wavelet transform. Our start point was the Fourier Transform. To overcome some disadvantages when applying Fourier Analysis, mathematicians developed a new class of functions to perform the Continuous Wavelet Transform. After that, we described the fundamentals on Multiresolution Analysis (MRA) and the Discrete Wavelet Transform. Finally, we showed how the Fast Wavelet Transform can be modify to increase the computational speed through the new concept called Lifting Scheme. The wavelet Transform will be use in the present document as a tool for feature selection.